Multiple hazards and paths to eruptions: A review of the volcanic system of Vulcano (Aeolian Islands, Italy)

J. Selva[a,*], C. Bonadonna[b], S. Branca[c], G. De Astis[d], S. Gambino[c], A. Paonita[e], M. Pistolesi[f], T. Ricci[d], R. Sulpizio[a,g,j], A. Tibaldi[h], A. Ricciardi[i]

[a] Istituto Nazionale di Geofisica e Vulcanologia, Sezione di Bologna, Bologna, Italy
[b] Université de Genève, Département des sciences de la Terre, Geneva, Switzerland
[c] Istituto Nazionale di Geofisica e Vulcanologia, Osservatorio Etneo, Catania, Italy
[d] Istituto Nazionale di Geofisica e Vulcanologia, Sezione Roma 1, Rome, Italy
[e] Istituto Nazionale di Geofisica e Vulcanologia, Sezione di Palermo, Palermo, Italy
[f] Università di Pisa, Dipartimento di Scienze della Terra, Pisa, Italy
[g] Università di Bari, Dipartimento di Scienze della Terra e Geoambientali, Bari, Italy
[h] Università di Milano Bicocca, Dipartimento di Scienze dell'Ambiente e della Terra, Milan, Italy
[i] Dipartimento della Protezione Civile, Rome, Italy
[j] IGAG-CNR, Milano, Italy

ARTICLE INFO

ABSTRACT

Vulcano is one of the 7 volcanic islands and 6 seamounts forming the Aeolian volcanic district (Italy). Vulcano has a long eruptive record, and its last eruption (1888–90 AD) originated the definition of the Vulcanian eruptive style. Like most volcanic islands, Vulcano generates many potentially interconnected hazards, determining a potentially high risk. Here, we review the state of knowledge on its geology, eruptive activity, historical accounts, structural setting, geophysical and geochemical surveillance, and available hazard assessment, in order to have an updated picture of the state knowledge on volcanic hazard. We follow a prototypal reviewing scheme, based on three standardized steps: i) review of the volcanic system; ii) review of available eruptive and non-eruptive hazard quantifications; iii) development of a conceptual interpretative model. We find that, while a rather vast literature is dedicated to the volcanic system of Vulcano and the reconstruction of past events, few quantitative hazard assessments exist. In addition, the range of natural variability considered for each hazard is potentially underestimated (e.g. limited range of considered eruption magnitude and style and of vent position), as it is the potential effect of multi-hazard impact. The developed conceptual model for the feeding system provides a synthetic picture of the present knowledge about the system, as emerged from the review. In addition, it allows for the identification of potential paths-to-eruption and provides a first order link among the main hazards. This review provides an up-to-date snapshot of existing knowledge on volcanic hazard at Vulcano on which to build future hazard quantifications as well as to support present and future decision making.

1. Introduction and methods

The island of Vulcano is the southernmost emerged volcanic edifice of the Aeolian archipelago. Vulcano generated many eruptions in historical times, the most recent of which occurred between 1888 and 1890 AD. Even if the island is lightly populated (fewer than 1,000 permanent residents), the population can reach 15,000 during tourist season (Galderisi et al., 2013). Given the small size of the island (~ 21 km^2), the tourist interest in volcano-related phenomena (hot muds, fumaroles, etc.), and the high exposure of inhabited areas, the volcanic risk at Vulcano is high, even for small events (Galderisi et al., 2013).

Extensive scientific literature exists on the geology and the eruptive dynamics of Vulcano (e.g., Mercalli and Silvestri, 1891; De Fiore, 1922; Keller, 1980; Fiorillo and Wilson, 2004; Dellino et al., 2011; De Astis et al., 2013a, 2013b; Di Traglia et al., 2013; see Section 2 and references therein). Several studies describe past secondary (e.g., landslides or tsunami; Frazzetta et al., 1980; Pareschi and Ranci, 1997; Tinti et al., 1999; Tommasi et al., 2007, 2016; Marsella et al., 2013; see Sections 3.2.4 and 3.2.5 and references therein) and primary (e.g., gas dispersal, lava flows, pyroclastic density currents, ballistic blocks, tephra

---

accumulation; Granieri et al., 2014; Piochi et al., 2009; Dellino et al., 2011; Gurioli et al., 2012; Doronzo et al., 2016; see Sections 3.1.3, 3.1.4, 3.1.5 and 3.2.2 and references therein) hazards, in some cases also proposing quantitative hazard assessments (Biass et al., 2016b, 2016c; see Sections 3.1.3 and 3.1.4 and references therein).

The aim of this paper is to provide an overview of the state of the art about hazard quantification for Vulcano, starting from the existing vast but dispersed literature. Being volcanoes intrinsically multi-hazard systems, we extend to all the potential hazards generated by the Vulcano system, including eruptive and non-eruptive phenomena. By eruptive and non-eruptive phenomena, we distinguish between the phenomena prevalently generated during eruptions from the ones that may occur at any time. The final goal is the identification of strengths and weaknesses in the state of knowledge about hazards for Vulcano, extracting established knowledge, existing debated issues, as well as scientific gaps with impact on the quantification of the hazards.

The identification of strengths and weaknesses in hazards quantifications for Vulcano is twofold. On the one side, this will help identify required future research activities to strengthen future hazard quantifications. On the other side, it provides decision-makers a comprehensive global picture about the present day knowledge about hazards and existing uncertainties, increasing the awareness of decision making.

To this end, we follow a prototypal standardized review scheme, developed for reviewing the state of knowledge on hazards in the islands of Vulcano (this paper) and Ischia (Selva et al., 2019). This review scheme may represent a prototype scheme for establishing the state of the art about hazard quantifications at any volcano. This scheme is based on the development of 3 temporally consecutive review steps.

STEPs 1 and 2 are dedicated to reviewing the general knowledge about the volcanic system (STEP 1), and the available phenomenological and hazard studies (STEP 2), extending to all the potential hazardous phenomena associated with a volcanic system. STEP 3 is instead focused on developing a (subjective) reference interpretative model, providing a synthetic picture of the knowledge that emerged during STEPs 1 and 2.

These steps have specific goals in the process of establishing the state of knowledge about the hazards. STEP 1 defines the available knowledge on the geological context and the available data. For hazard quantification, its primary goal is the definition of a reference period for hazards and a reference catalogue of unrest and eruption episodes (and related phenomena). These definitions are the starting points for any hazard quantification and thus provide the basis for a critical analysis of the scientific ground of available hazard studies. STEP 2 provides a homogeneous review of hazard quantifications available in literature. Its specific goals are to discuss the coherence of these analyses with the generic context emerged in STEP 1, to evaluate their capability in exploring the effective natural variability of the phenomena (beyond the observed one), and to identify significant gaps in hazard quantifications, both in terms of methodological gaps in existing analyses and in terms of hazards not yet assessed in literature. STEP 3 has the goal of providing a reference conceptual model that future studies may either adopt for developing coherent hazard quantifications, or challenge with new data or evidence for triggering new research lines.

Noteworthy, STEPs 2 and 3 provide a basic multi-hazard picture, which is especially relevant for volcanic islands, where multiple hazards may affect small areas. While complete multi-hazard risk analyses should deepen into all the interdependencies among the hazards and the consequent risks (e.g., Marzocchi et al., 2012a; Selva, 2013; Mignan et al., 2014; Liu et al., 2015), here we stop at a very first order analysis by providing, in STEP 2, an homogeneous parallel view of all hazards and their potential role in multi-hazard and, in STEP 3, hints about their actual interconnections within the general behaviour of the volcano. In absence of any multi-hazard risk analysis, this represents a very first step toward multi-hazard.

In all STEPs, it is of primary importance to expose the emerging epistemic uncertainty, by carefully analysing the full spectrum of

Table 1
Acronyms and other abbreviations or symbols.

CEU	Commenda Eruptive Unit
DEM	Digital Elevation Model
DPC	Italian Department of Civil Protection, http://www.protezionecivile.gov.it
EDM	Electronic Distance Measurement
EE	Eruptive Epoch
ERS	Eruption Range Scenario
ERT	Electric Resistivity Tomography
Fs	Factor of safety for landslides
GC	Gran Cratere formations
GCEC	Gran Cratere Eruptive Cluster
GP	Grotta dei Palizzi formations
GPS	Global Positioning System
IAEA	International Atomic Energy
INGV	Istituto Nazionale di Geofisica e Vulcanologia, www.ingv.it
LFC	La Fossa Caldera
LVVC	Lipari-Vulcano Volcanic Complex
MCS	Mercalli-Cancani-Sieberg scale
OES	One Eruption Scenario
PC	Pietre Cotte formation
PDC	Pyroclastic Density Current
PEU	Palizzi Eruptive Unit
PCEC	Palizzi-Commenda Eruptive Cluster
PGA	Peak Ground Acceleration
PN	Punte Nere formation
TGR	Tuffs of Grotta dei Rossi
TLF	Tindari–Letojanni Fault system
UBT	Upper Brown Tuffs
VEI	Volcanic Explosivity Index
VT	Volcano-Tectonic seismic events

scientific opinions retrieved from literature (as in SSHAC, 1997). While seeking for the existence of evidence in favour of either interpretation, when this is not possible we leave controversies as open questions, highlighting their potential impact in hazard quantification. This process is fundamental as controversies are the main drivers of epistemic uncertainty to be reduced with future research efforts.

In this paper, we dedicate one section to each one of the 3 STEPs briefly described above, reporting STEPs 1, 2 and 3 in Sections 2, 3, and 4, respectively. In Section 5, we distil some conclusions and final remarks, also identifying potential specific research topics that could improve the future understanding and the characterization of hazards for Vulcano.

To help the reader, we report in Table 1 the main acronyms, symbols and abbreviations that appear within the paper.

2. STEP 1: State of knowledge on the volcanic system

STEP 1 is dedicated to summarize available data (geological, historical and geophysical data) and their interpretations, to reconstruct the state of the art of the volcanic system. For hazard quantification, the main goals of STEP 1 are: i) the definition of the reference period, and ii) the definition and characterization in terms of types and frequency of the various physical states of the volcano (rest/unrest/eruption). The main result of STEP 1 consists of the definition of a reference catalogue for hazard assessments. This information is critical for the evaluation of existing hazard quantifications (STEP 2). It represents also the fundamental base for future hazard quantifications, being at the the base of all volcanic hazard quantification techniques (e.g., with probability trees: Newhall and Hoblitt, 2002; Marzocchi et al., 2008; Selva et al., 2014; Newhall and Pallister, 2015; with Bayesian Belief Networks, see Aspinall et al., 2003; Hincks et al., 2014; Tierz et al., 2017; with conditional hazards: Selva et al., 2010, 2018; Jenkins et al., 2012; Biass and Bonadonna, 2012), as well as for the evaluation of the potential strategies for risk management (e.g., Marzocchi et al., 2012b; Winson et al., 2014; Woo, 2015; Papale, 2017; Pallister et al., 2019)

2.1. Structural setting and tectonics

Geophysical, volcanological, structural and compositional data indicate that the Aeolian Volcanic District is defined by 3 main sectors (e.g., Ventura, 2013; Fig. 1A): a western sector (Alicudi, Filicudi and older part of Salina), a central sector (Vulcano, Lipari, younger Salina) and an eastern sector (Panarea, Stromboli). Vulcano is the southernmost Island of the central sector (Fig. 1B) where the NNE striking and dextral strike-slip Tindari–Letojanni Fault (TLF) system dominates the tectonics. Stromboli and Vulcano are the youngest volcanic edifices in the Aeolian archipelago, whose subaerial products range in age between 0.43 Ma and the Present Time (see Section 2.2).

2.1.1. Field data

Although the Aeolian Archipelago has a general arc shape in plan view, the alignment of the Lipari and Vulcano edifices highlights a NNW-SSE trend normal to the arc elongation (Fig. 2A). This trend is interpreted as the effect of the NNW-striking regional Tindari–Letojanni Fault (TLF, Ghisetti and Vezzani, 1982; Barberi et al., 1994; Ventura et al., 1999; De Astis et al., 2003). This is a right-lateral strike-slip fault that trends southward from the center of the Aeolian arc to the Sicily coast. The TLF has also been interpreted as the continuation of the Malta escarpment, which is a lithospheric transtensional active fault (Continisio et al., 1997; Lanzafame and Bousquet, 1997). Billi et al. (2006) argued that the TLF is not linked with the Malta escarpment to the south, whereas it is also difficult to confirm a direct linkage between the NNW-SSE faults on Vulcano to the TLF.

On Vulcano, the first structural investigations pointed out the widespread presence of NW-SE to NNW-SSE structures, interpreted to represent the expression of the TLF system, accompanied by the presence also of N-S- to NE-SW-striking normal faults (Frazzetta et al., 1983; Mazzuoli et al., 1995). Some authors also recognized the presence of NNW-SSE to NW-SE grabens (Gabbianelli et al., 1991; Barberi et al., 1994; Ventura, 1994). More recently, Argnani et al. (2007), based on oceanographic surveys, showed the presence of compressional structures around the Aeolian Arc, proving the dominant compressive tectonic regime in the area.

More in detail, Ventura (1994) showed that the NE-SW fractures guided magma upwelling in the interior of the island, as also suggested by the migration of the eruptive vents of La Fossa and Vulcanello, and controlled the shape of the calderas. The eruptive centers of the western part of the island (Quadrara, Spiaggia Lunga, Saraceno, Alighieri), as well as the main volcanoes of the island (Sud Vulcano, La Fossa, Lentia and Vulcanello), are linked to N-S fractures (Keller, 1980). More recent field surveys showed the presence on the island of NW-SE, NE-SW, N-S

and E-W fractures in decreasing order of frequency (De Astis et al., 2013b; Fig. 2C). The NW-SE faults show normal kinematics with right-lateral or left-lateral strike-slip components. These observations are consistent with offshore data by Favalli et al. (2005) that show the presence of steep ENE-WSW and NW-SE scarps around the island that should be the morphological expression of faults. Barreca et al. (2014) showed the presence in the island of dominant normal faults striking mainly NNE-SSW and NNW–SSE, and only one strike-slip fault. They thus suggest that the island is affected by transtension, whereas, based on seismic data, the area between the islands of Lipari and Vulcano, comprising Vulcanello, is under transpression.

Ruch et al. (2016) showed that, at Vulcano and Lipari, normal faults, mainly striking NNW-SSE and N-S, dominate in the last about 55 ka (Fig. 2A). Subordinate right-lateral and left-lateral components are present. The location of the volcanic centers has been largely controlled by these two structural sets. In particular, the most recent periods of volcanic activity (8 ka and < 2 ka, Fig. 2A) were characterized by magma upwelling only along N-S fractures (Ruch et al., 2016). These structures were produced by a combination of deep and shallow stresses; magmatic overpressure at depth generated by the intrusive system produced a stress field where magmatic stresses (pressures) dominated over tectonic ones. At shallower level, gravitational instability linked to the eastward deepening of the sea bottom also favoured the formation of the N-S faults. Following Ruch et al. (2016), the faults of the TLF system did not exert control on volcanism during recent times and at the shallowest level.

2.1.2. Shallow structure of La Fossa cone

La Fossa cone, the most recent center of activity together with Vulcanello, is characterized by the presence of at least five distinct crater rims and by a strong, diffuse alteration of the outcropping rocks due to a very active hydrothermal system (Section 2.5; De Astis et al., 2013a). The complexity of the volcanic edifice is increased by the proximity and overlapping of eruptive centers active in different epochs. The significant hydrothermal fluid flow along the main structural features (crater boundaries and volcano-tectonic lineaments) is also shown by thermal and degassing anomalies (Revil et al., 2008, 2010; Barde-Cabusson et al., 2009; Schöpa et al., 2011). The widespread hydrothermal alteration produces effects at both microscopic and macroscopic scale, ranging from the alteration of minerals to the weakening of the volcanic edifice (Fulignati et al., 1998, 1999; Boyce et al., 2007; Tommasi et al., 2016). These weakness planes allow the infiltration of meteoric waters and the rise of hydrothermal fluids.

High-resolution electrical resistivity tomography (ERT), coupled with self-potential, temperature, and CO_2 diffuse degassing measurements, permitted the imaging of the inner structure of La Fossa cone and modelling of its hydrothermal circulation (Revil et al., 2008, 2010; Barde-Cabusson et al., 2009). These surveys identified the main geological structures and the characteristics of the central hydrothermal system. The latter is enclosed within the most recent active craters, where an upward migration of hydrothermal fluids is evident (Fig. 2B). In the periphery, the hydrothermal circulation is influenced by the structure of the edifice and is visible along structural boundaries of older crater rims. The simulation of the hydrothermal circulation pattern along an E-W section of La Fossa cone using self-potential data (Revil et al., 2008) is consistent with the position of the deformation source inferred by Gambino and Guglielmino (2008) for the subsidence of the Fossa edifice that occurred during the period 1990–1996.

Crater boundaries are characterized by clear horizontal variations in electrical resistivity that can be interpreted as sharp lithological transitions marking subvertical resistive structures.

The central sector of La Fossa edifice is characterized by the presence of a resistive body identified at approximately 70 m depth below the bottom of the youngest crater area and interpreted as a low-porosity body or dry steam present in the hydrothermal system (Revil et al., 2008). A conductive region is instead evidenced below the highest-
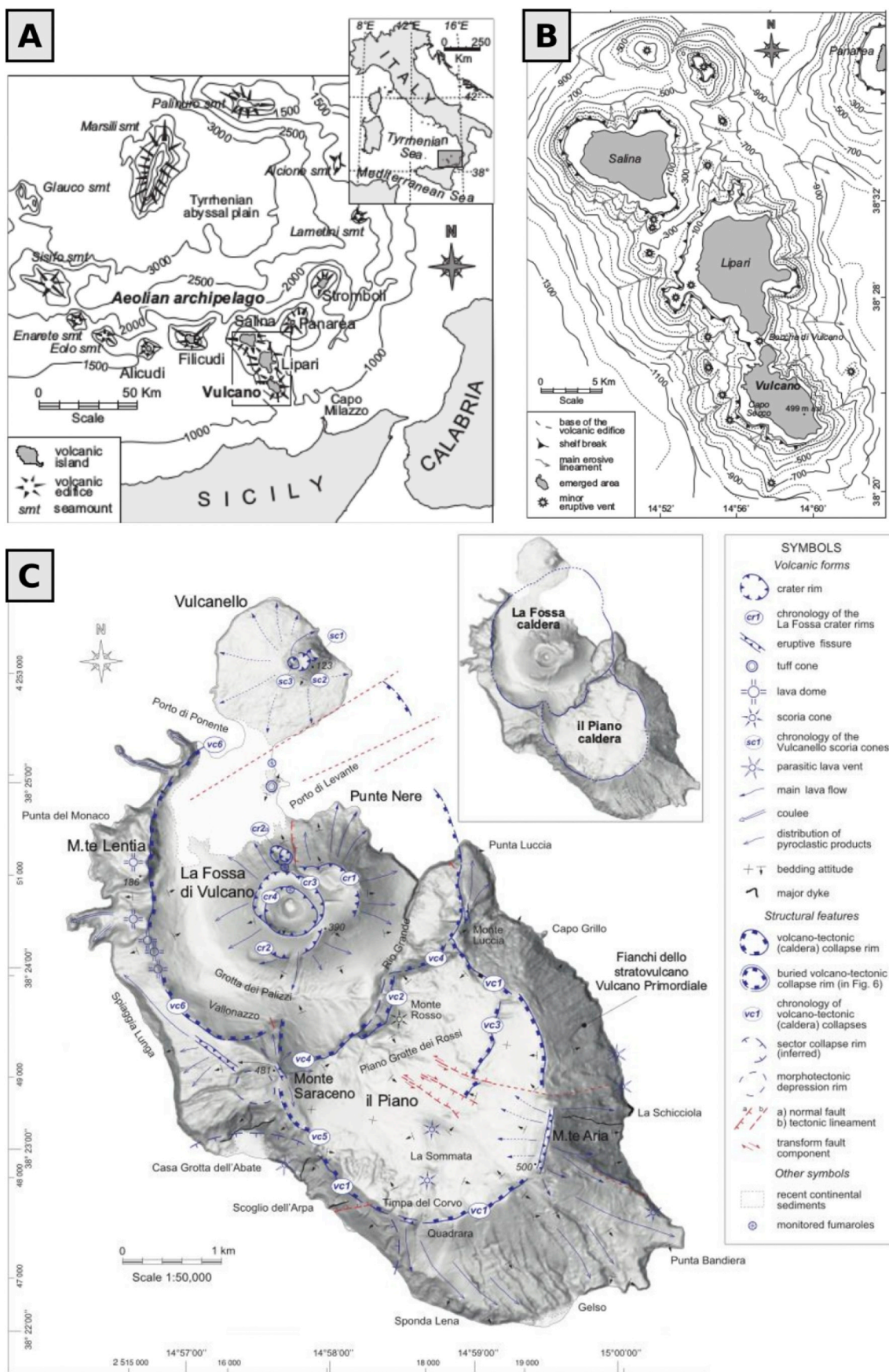
Fig. 1. Regional settings of Aeolian islands. A) The Southern Tyrrhenian Sea, with the Aeolian archipelago and associated seamounts; B) the Aeolian archipelago central sector with morphobathimetry, showing the presence of submerged volcanic centers along the Vulcano-Lipari-Salina ridge. C) morpho-structural map of Vulcano (from De Astis et al., 2013b).
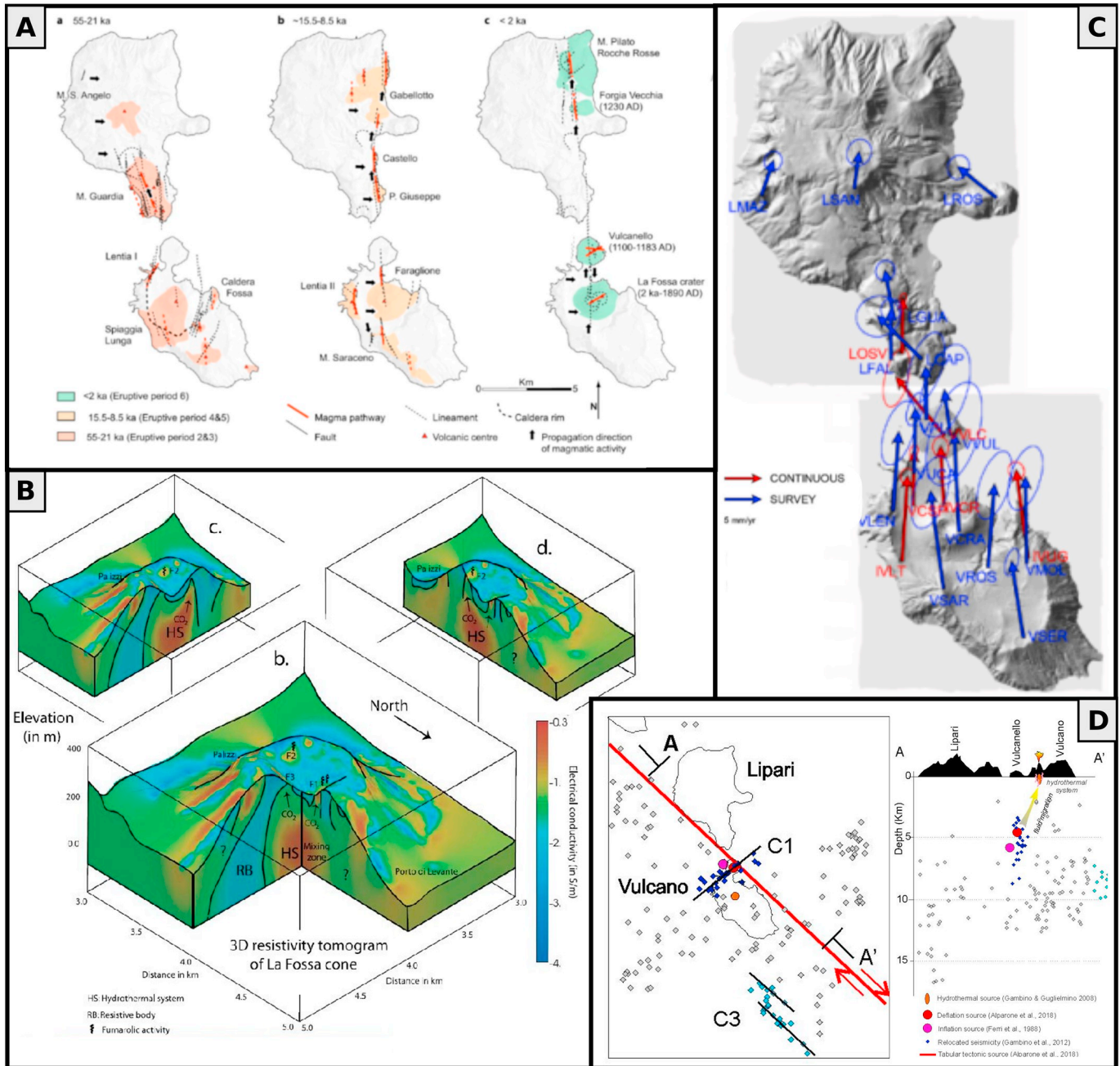
Fig. 2. Structural features and deformation field. A) Main structural features and eruptive centers active during the various phases of evolution of the Lipari-Vulcano complex (after Ruch et al., 2016). B) Resistivity tomogram and its interpretation. Craters: PN (Punte Nere); FV (Forgia Vecchia); PC (Pietre Cotte); GC (Gran Cratere); Fumaroles F1, F2, and F3 (from Revil et al., 2010). C) the horizontal velocity field from the GPS survey style networks of Lipari-Vulcano (after Esposito et al., 2015). D) Map and A-A' section showing the magmatic/hydrothermal sources obtained from ground deformation data inversions. Seismic events (and related C1 and C3 clusters) are redraw from Gambino et al. (2012).

temperature fumarolic field and can be extended to a depth of 200 m. This area is probably related to the presence of alteration products combined with the presence of liquid-dominated hydrothermal circulation occurring in this zone.

In the eastern sector of La Fossa, a buried resistive body was identified and its electrical resistivity values are in the range of the ones expected for a lava flow pile or intrusive rocks (Revil et al., 2008). Barde-Cabusson et al. (2009) interpreted this body, truncated to the west by the Pietre Cotte crater (1739 AD activity), as an intrusion or a dome contemporary with the Punte Nere activity (5.3 ka–3.8 ka). The existence of this resistive structure was already highlighted by previous aeromagnetic investigations (Supper et al., 2001, 2004; Okuma et al.,

2006; De Ritis et al., 2007; Blanco-Montenegro et al., 2007) and by a high-resolution magnetic survey (Napoli and Currenti, 2016). Blanco-Montenegro et al. (2007) interpreted the magnetic anomaly related to the resistive body as a pile of tephritic lavas emplaced in an early phase of activity of La Fossa cone. This result confirms the shallow high-velocity body evidenced through seismic tomographic data identified in the same area by Chiarabba et al. (2004). This resistive body was interpreted by Rosi et al. (2018) as a buried lava body formed during the effusive activity immediately before the Breccia di Commenda eruptive event (1230 AD, see Section 2.2).

The buried structures beneath and around the Fossa cone, characterized by null or low magnetization, can be ascribed to the presence

of pyroclastic and hyaloclastic rocks, as well as to a large volume of hydrothermally altered materials. This suggests that the hydrothermal system affected a larger area in the past (Blanco-Montenegro et al., 2007). Presently, the presence of a magnetized body inside the Fossa cone implies that high temperatures characterising the fumarolic fields must be contained in very limited spaces mainly restricted to fumarolic conduits and vents. In fact, while the magnetization in the volcanic rocks of Vulcano is mainly due to low-Ti titanomagnetite (Curie temperature 550 ± 30 °C; Zanella and Lanza, 1994), high temperature fumaroles (>300 °C; up to 690 °C in May 1993, Chiodini et al., 1995) currently develop only on the rim of the northern sector of La Fossa cone with an average temperature of 317 °C in February 2020 (INGV-BullVulcanoFeb20, 2020).

Geophysical evidences of preferential hydrothermal circulation is also present at the base of the north-western flank of La Fossa cone (Barde-Cabusson et al., 2009) in the Grotte dei Palizzi area, probably due to the existence of volcano-tectonic features (Barberi et al., 1994).

A high-resolution seismic survey carried out by Bruno and Castiello (2009), partially overlapping one of the ERT profiles realized by Revil et al. (2008) at the bottom of the western flank of La Fossa cone, permitted the location of a parasitic vent, or hyaloclastite mound, buried at the western base of La Fossa cone.

2.2. Geological and historical knowledge

Entirely made of volcanic rocks, Vulcano is formed through a complex geological history - characterized by the progressive shifting of volcanic activities from SSE to NNW. For this reason, Vulcano shows several edifices and morpho-tectonic lineaments revealing that magnitude and intensities of eruptions were variable and repeated caldera collapses occurred. Fig. 1C summarizes the main volcanic landforms and structural features of the island (Keller, 1980; Gioncada and Sbrana, 1991; Ventura, 1994; Mazzuoli et al., 1995; De Astis et al., 1997a,b, 2006, 2013a,b; Ventura et al., 1999)

2.2.1. Volcanic history

De Astis et al. (2013b) produced the most recent geological map of Vulcano, accompanied by accurate explanatory notes. We used it as benchmark for the stratigraphy, geology and eruptive history of Vulcano.

The volcanic activity of Vulcano has been the subject of many scientific works since the 19th century (e.g., Cortese and Sabatini, 1892; Bergeat, 1899; De Fiore, 1922, 1925a, 1925b, 1926; Keller, 1980; Frazzetta et al., 1983, 1984, 1985; De Astis et al., 1989, 1997a,b, 2006, 2013a,b; Gioncada and Sbrana, 1991; Clocchiatti et al., 1994; Dellino and La Volpe, 1997; Del Moro et al., 1998; Gioncada et al., 1998; Arrighi et al., 2006; Peccerillo et al., 2006; Davì et al., 2009; Dellino et al., 2011; Gurioli et al., 2012; Di Traglia et al., 2013; Fusillo et al., 2015).

The whole eruptive history was split into eight Eruptive Epochs (EE, summarized in Table 2), starting from ~127 ka up to 1888-90 AD (the last eruption). We focus here on the most recent eruptive period (8th EE).

Several studies (Mazzuoli et al., 1995; De Astis et al., 2013a, 2013b; Ruch et al., 2016) agree in identifying the N-S and NE–SW tectonic lineaments as those driving the 8th EE. Evidence of these preferential directions are: i) N-S alignment of lava domes and coulées in the Mt. Lentia area and the N-S Mt. Saraceno eruptive fissure (Fig. 1C); and, ii) overlapping of both La Fossa and Vulcanello craters along NE–SW direction.

Normal faults (E-W extension) dominate the recent tectonic setting, and form a N-S, 10 km-long and 2 km-wide tectonic depression (including the central-southern sector of Lipari), which favours the magma rise to the surface (Ruch et al., 2016). Although the transition between the 7th and the 8th Eruptive Epochs is not precisely dated, the available chronostratigraphic data (Dellino et al., 2011; De Astis et al., 2013a)

places it at around 10-11 ka.

During the 8th EE, four main sources were active (central or fissural vents; Table 2 and Fig. 3A): a) La Fossa Caldera (LFC), with vents located along the caldera borders or unidentified; b) La Fossa tuff-cone; c) Faraglione, a largely dismantled small tuff-cone of unknown age; d) Vulcanello, formed by a lava platform and 3 small overlapping cones.

The main eruptive activities that occurred during the 8th EE, reported in Table 3 and Fig. 3, are briefly summarized here. Details and age references are also reported in Table 3.

The La Fossa cone (Gran Cratere di La Fossa lithosome) consists of pyroclastic rocks and a few lava flows. According to De Astis et al. (2013a), the activity and formation of this cone (Fig. 2A) comprises three phases: i) early eruptive activity (La Fossa older products), ii) intermediate activity (ca. 2.2 ka – 776 AD), and, iii) a final phase (XVIII-XIX centuries, until 1888-90 AD).

The early La Fossa activity ($\approx$5.5/5.3-2.9 ka) includes two formations (Table 3): Punte Nere (PN) and Grotta dei Palizzi 1 (GP1), largely made of pyroclastic deposits, the first of which erupted from a still visible crater and built most of the present La Fossa Cone up to 250-300 m (Fig. 1C). It is worth noting for hazards evaluation that the PN lava age is still a matter of debate (age = $3.8 \pm 0.9/-0.8$ by Soligo et al., 2000; age = 1170 ± 20 AD by Arrighi et al., 2006). Based on Arrighi et al.'s (2006) framework and stratigraphic evidence, Di Traglia et al. (2013) encompass the PN and Campo Sportivo lava flows within a single eruptive unit (Palizzi Eruptive Unit, PEU), which also includes the Palizzi lava, thus considering all these flows erupted in the time interval from 1170 to 1250 AD. Beyond this different age attribution, submarine geological studies (Casalbore et al., 2018) evidence two distinct phases of PN delta formation with a progradation along the NE flank of La Fossa cone, since some deeper/lower lava lobes result to be cut by a shore platform whereas some overlying and younger overlap the formation of that erosive platform.

A dominantly phreatomagmatic activity resumed after a quiescence of a few centuries, emplacing the GP1 formation (2.9 ka; Voltaggio et al., 1995; Table 3) from a new crater (cr2 in Fig. 1C), probably with multiple eruptive phases

Eruptive activity (Grotta di Palizzi 2 and 3, GP2-3, or Palizzi eruptive unit, PEU) renewed at around 2.2 ka (or 1200 AD according to Di Traglia et al., 2013) mainly producing dilute PDCs and occurring from two different, intersecting craters (cr2, cr3; Fig. 1C). Two fallout deposits and two lava flows are also present. This intermediate period of activity is completed by the Caruggi formation as described by De Astis et al. (2013a), named Commenda eruptive unit (CEU) in Di Traglia et al. (2013) (Fig. 1C). Whatever the age, (all) stratigraphic evidence place the sequences of Palizzi and Commenda as younger than the Punte Nere lavas and the Vulcanello lava platform. Some of the deposits emplaced during this period (i.e. GP2a, see Dellino et al., 2011) show the greatest thickness and dispersal in the La Fossa sequence.

Field studies (Rosi, pers. comm.) and historical chronicles concur in indicating the occurrence of a phreatic event from La Forgia crater during upper Middle Age (conventionally 476 to 1453 AD). The activity, dated February 5, 1444 AD by Fazello (1558), is attributed to La Forgia Vecchia crater by Rosi (pers. comm.) and to La Fossa by Barbano et al. (2017). Based on Fazello's chronicle, the latter authors set the formation of La Fossa-Vulcanello isthmus between 1525 and 1550 AD, from accumulation of ash erupted from La Fossa.

The most recent phase of La Fossa activity occurred between 1727 and 1890 AD through various (discrete) eruptive pulses, which produced a volcanic succession that is subdivided into Pietre Cotte (PC) and Gran Cratere (GC1 and GC2) formations (Table 3). Eruptive activity was prevalently Vulcanian, and most of the products are distributed around the summit area of the cone, consisting in successions of dilute PDCs alternating to fallout deposits. A lava flow was emplaced in 1739 AD (Pietre Cotte, PC), as discussed in historical chronicles and in agreement with archeo-magnetic datings (Arrighi et al., 2006). It marks the last effusive activity from La Fossa cone (De Fiore, 1922; Keller,

Table 2
Summary of Eruptive Epochs reconstructed for Vulcano Island eruptive history according to De Astis et al. (2013a) (1 = detailed age references reported in De Astis et al., 2013b; 2 = Lucchi et al., 2008).

| Eruptive Epoch	Synthem	AGE (Time Span)	Active Volcanic centers (lithosomes)	Synthetic Description
Eruptive Epoch 1	Paleovulcano (informal unit)	127-113 ka ca.(1)	Capo Secco (small shield volcano)	Effusive eruptions
Eruptive Epoch 2	Casa Grotta dell'Abate	117-101 ka ca.(1)	Primordial Vulcano (Serro di Punta Lunga stratovolcano)	Effusive to subordinate Strombolian activity, with minor phreatomagmatic eruptions
Eruptive Epoch 3	Scoglio dell'Arpa	99.5-94 ka ca. (1)	Scoglio Conigliara Caldera ring faults	Mainly effusive activity and subordinate phreatomagmatic eruptions (PDC)
Eruptive Epoch 4	Rio Grande	83-78 ka ca. (1)	Monte Aria and Timpa del Corvo fissures (mostly located along the rims of Piano Caldera); Casa Petrulla scoria cone	Effusive activity producing lava piles; phreatomagmatic dilute PDCs interlayered with Strombolian fallout deposits.
Eruptive Epoch 5	Il Piano	70-42 ka ca. (1)	Il Cardo, Monte Rosso, Punta Luccia, La Sommata (tuff-cones or scoria cones)	Dilute PDC activity alternated to minor Strombolian fallout; effusive and/or pure Hawaiian to Strombolian activity
Eruptive Epoch 6	Serra delle Felicicchie	28-21 ka ca. (1)	Monte Lentia dome field ("Lentia group", Keller, 1980; "Lentia complex", De Astis et al., 1997b) and other vents, originating various: P.Sciarra del Monte, Sc. Capo Secco, P.ta Bandiera, Faro vecchio	Various effusive and explosive (Quadrara Fm.) western border activities generating lava domes and coulees, scoriae/pumices blankets, lava flow
Eruptive Epoch 7	Vallonazzo (Menichedda sub-synthem)	< 21 ca. to 10 ka ca. (1)	La Fossa caldera (LFC) borders and inner vents, Punta Roja, Monte Lentia	Medium to high-energy PDC (Piano Grotte dei Rossi Fm. = Upper Brown Tuffs (2)); effusive activity (domes, lava flows)
Eruptive Epoch 8	Vallonazzo (Porto di Levante sub-synthem)	from 9-8 ka to the last eruption (1888-1890 AD) (1)	Mt. Saraceno, LFC western (small domes and lava flow), La Fossa tuff-cone, Vulcanello cone(s)	Frequent phreatomagmatic eruptions with both Vulcanian style (low energy PDC and fallout) or PDC dominated (La Fossa cone and inside LFC: i.e. final units of Upper Brown Tuffs). Strombolian to Hawaiian and effusive activity (Mt. Saraceno, Vulcanello, La Fossa) Dome-type activity (LFC border)
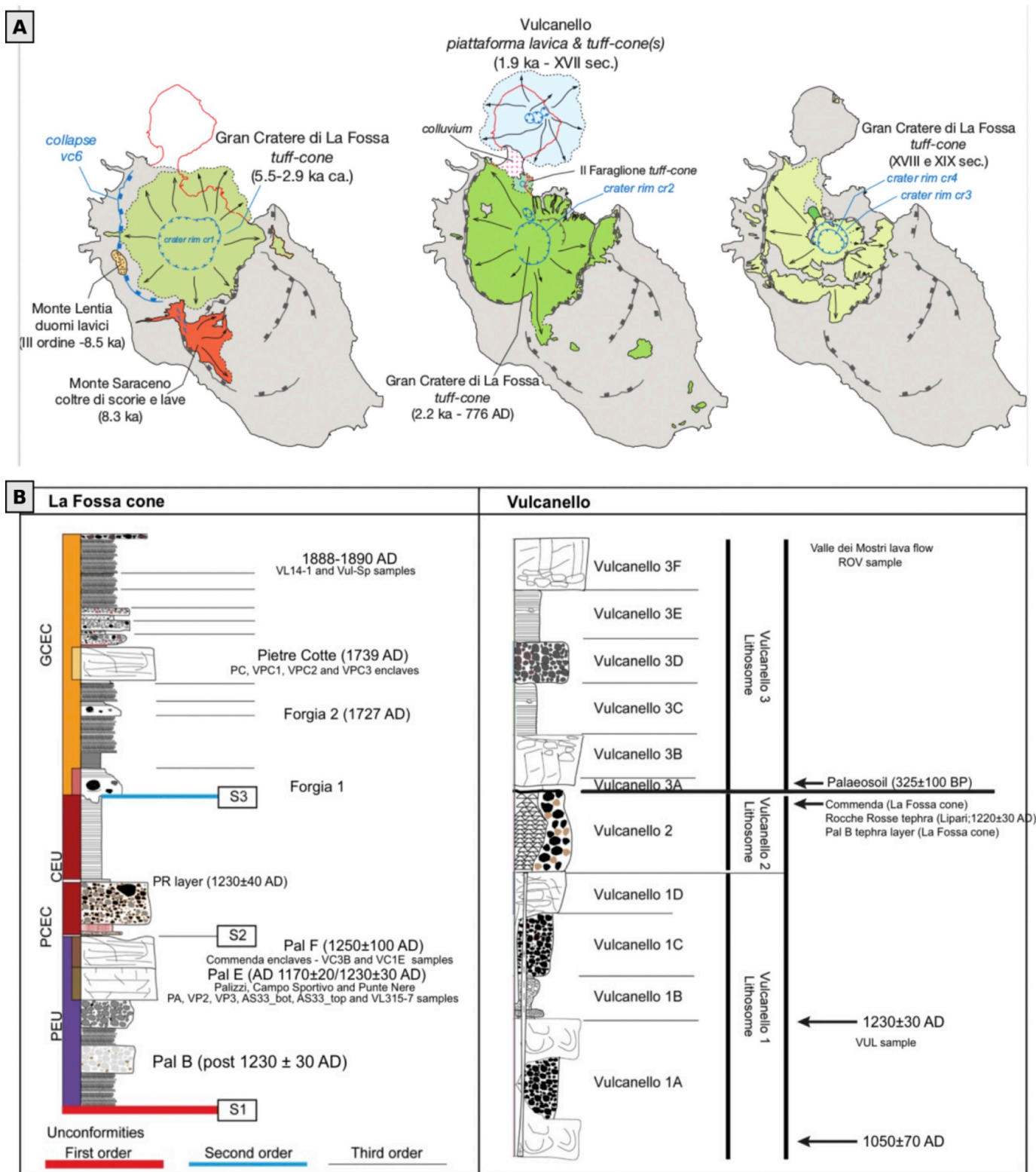
Fig. 3. Geology of Vulcano and eruptive epochs. A) 8th Eruptive Epoch - Schematic reconstruction of volcanic activity occurred at Vulcano in the last 10 ka ca. Different vents erupted either along the LFC boundaries (Mt. Lentia, Mt Saraceno, Vulcanello) or within it (i.e. La Fossa tuff-cone, Faraglione). (left) Volcanism between about 8.5 and 2.9 ka old, including La Fossa lower portion (older products); (center) La Fossa intermediate portion and Vulcanello activities (about 2.2 ka to 1600AD); (right) La Fossa upper portion (volcanic products erupted in the last 300 yr of activity). B) La Fossa cone (partial) stratigraphy according to Di Traglia et al. (2013) compared with Vulcanello stratigraphy according to Fusillo et al. (2015), based on Arrighi et al. (2006) data. Both activities are included in the last about 1000 years.

Table 3

Reconstruction of La Fossa and Vulcanello activities according to De Astis et al., 2013a) and Di Traglia et al. (2013). (A = De Astis et al., 2013b and references therein; B = Di Traglia et al. (2013) and references therein; C = Mercalli and Silvestri, 1891). The green shadowed boxes roughly correspond to the PCEC (Palizzi-Commenda Eruptive Cluster) units, whereas the light blue boxes roughly to those forming the GCEC (Gran Cratere Eruptive Cluster) ones, as reported in Di Traglia et al. (2013); P.t.* is referred to Mt. Pilato activity in Lipari forming a regional marker-bed differently dated in the Aeolian archipelago (see A for further details). The column "Eruption Type" reports the type of eruption following the classification discussed in Section 2.7.2.

Eruptive center (lithosome)	Formation	Eruptive style and deposits	Age Range	Eruptive Type
La Fossa (older activity)	Piano Grotte dei Rossi	PDC-forming explosive activity and minor fallout beds originated from eruptive vent(s) located within the La Fossa caldera (14). They are considered the proximal counterparts of the Upper Brown Tuffs (UBT) recognized in several Aeolian Islands.	10-8 ka (8.5±0.08 ka) (A) UBTs have an age range between 24 to 8 ka	**Type 4**
La Fossa (older activity)	Punte Nere (3 members) Crater 1 (Fig....)	PDC-forming explosive phreatomagmatic activity interbedded with recurrent Strombolian fallout beds, Final "Punte Nere" lava flow.	≈ 6 – 3.8 ka (A) 1170±20 AD (B, lava flow)	**Types 1, 2b**
La Fossa (older activity)	Grotta dei Palizzi 1 Crater 2 (coalescent with cr1)	Strombolian fallout bed (scoriaceous bombs) followed by PDC-forming explosive phreatomagmatic activity.	2.9±0.35 ka (A)	**Types 1, 2b**
Il Faraglione 56-m-high stack	Faraglione	Difficult recognition due to strongly hydrothermally altered and locally hardened deposits. Probably from dilute PDCs and associated ballistic deposition.	Undefined	**Types 2a**
Vulcanello cone (crater1 and lava plateau)	Vulcanello 1 (2 members)	Strombolian fallout with sporadic dilute PDC generation, and multiple phases of lava effusion forming the plateau.	1.9÷2.0 (A); 1050±70 to 1230±30 AD(B)	**Type 1**
Vulcanello cone (crater2)	Vulcanello 2 (2 members)	Strombolian fallout beds (scoriaceous lapilli and bombs sequence, max 8m-thick).		**Type 1**
La Fossa (interm. activity)	Grotta dei Palizzi 2 (2 members) Crater 2 (coalescent with cr1, Fig. 1)	PDC-forming explosive phreatomagmatic activity and minor fallout beds. Late effusive activity generated the Commenda obsidian lava flow.	≤ 2.2-2.1 ka (A) Younger than 1050 AD (B) 1250±100 AD(lava; B)	**Types 1, 2b, 3**
La Fossa (interm. activity)	Grotta dei Palizzi 3 (2 members) Crater 2 (Fig. 1)	PDC-forming explosive phreatomagmatic and late effusive activity of emplacing the Palizzi trachytic lava flow.	1.6±1.0(A); 1.5±0.2(A) 1170±20 AD(B)	**Types 1, 2b**
La Fossa (interm. activity)	Caruggi (2 members) Crater 3 (Fig. 1)	PDC-forming explosive phreatomagmatic activity. Lithic rich massive, concentrate PDCs crop out on southern slopes of La Fossa cone.	Due to P.t.* interbedding: VIII century AD (A) 1230 AD (B)	**Type 0**
La Fossa	Forgia Vecchia	Lahar deposits (A). Vulcanian activity (PDCs and fallout beds) interbedded with lahar deposits (B).	Undefined (A) 1444 AD (B)	**Types 2a and various remobilization**
Vulcanello cone (crater3)	Vulcanello 3 (2 members)	Repeated effusive activity followed by or associated with Strombolian fallout beds (and minor dilute PDCs).	0.397±0.097(A)	**Type 1 and rare 2b**
La Fossa	Pietre Cotte (2 members) Crater 3 (Fig...)	PDC-forming explosive phreatomagmatic activity alternating with Vulcanian activity (PDCs and fallout beds). Late effusive activity produced the *Pietre Cotte* rhyolitic lava flow.	1739 AD; 1720±30 AD (B)	**Types 2a to 2b**
La Fossa	Gran Cratere 1 Crater 4 (Fig. 1)	Succession of several, intermittent (i.e. quiescence periods of years or tens of years), Vulcanian eruptions, characterized by emplacement of multiple, dilute PDCs alternating with fallout beds.	1739 to 1888 AD	**Types 2a to 2b**
La Fossa (last eruption)	Gran Cratere 2 Crater 4 (Fig. 1)	Succession of several Vulcanian eruptions, characterized by emplacement of multiple, dilute PDCs alternating with fallout beds.	1888-1890 AD (C)	**Types 2a to 2b**

1970b; Frazzetta et al., 1983). The eruptive activity between 1739 AD and the last eruption (1888-1890 AD) were also characterized by Vulcanian activity, with the emplacement of bread-crust bombs widely dispersed in the summit area of La Fossa cone.

The activity of Vulcanello (Fig. 1C) – nowadays visible as a lava plateau topped by a Strombolian cone with three inactive and coalescent craters - started with a submarine lava effusion, probably observed during Roman times (II century BC, Ciucciarelli, pers. comm., also reported in Stothers and Rampino, 1983). Therefore, the Vulcanello plateau is the upper part of a larger submarine structure, progressively grown through the accumulation of basaltic pillow and tube lavas (Gamberi and Marani, 1997) covered by a thin veneer of sediments as indicated by Romagnoli et al. (2013). The oldest age attributed to Vulcanello subaerial portion is still debated (2.1-1.9 ka in De Astis et al., 1997, 2013a; or 1020-1050 AD in Arrighi et al., 2006, accepted by Di Traglia et al., 2013). There is no evidence that eruptive activities were continuous from the submarine phase (observed by the Romans) to the emerged one, whose products have been dated (with different methods). The most conservative hypothesis places the onset of the subaerial activity in a period between 0-1000 AD, with final phases occurred around XVI century.

The early phases of subaerial volcanism from Vulcanello 1 were Strombolian and produced near-vent scoria fall deposits (Table 3, vu1 formation), with some spatter and a limited amount of deposits from diluted PDCs. The explosive phases alternated with the effusion of some aa- to pahoehoe-type lava flows. An erosive unconformity and re-worked material mark a period of quiescence between this activity and the overlying products of Vulcanello 2 formation (Table 3). A paleosol dated at 0.397 ± 0.097 ka (Keller, 1980) separates Vulcanello 2 from Vulcanello 3 products (Table 3). The Vu3 formation comprises both dilute PDC and Strombolian deposits, and ends with an effusive phase (Punta del Roveto lava flow). Some tephra layers overlie this lava flow (Fusillo et al., 2015), and are topped by another lava flow (Valle dei Mostri).

Whatever the age attributed to Vulcanello, all stratigraphic evidence indicates that Vulcanello eruptions partially overlapped with those from La Fossa and from Lipari, because their products are interfingered in the stratigraphy (Fusillo et al., 2015). In fact, thin fallout beds originated from La Fossa activity (GP2 or PEU; De Astis et al., 2013a; Fusillo et al., 2015 and references therein) outcrop on Vulcanello platform as well as the Pilato tephra layer (i.e. Sciarra dell'Arena Formation; Forni et al., 2013). Therefore, all the published studies converge in highlighting that, during the Middle Age, near contemporaneous eruptions occurred at Lipari (Mt. Pilato from AD 776 to 1230; Table 3), La Fossa and Vulcanello, with the ash marker bed from Mt. Pilato activity interbedded with both the Vulcanello and La Fossa deposits.

It is worth noting that, while maintaining almost the same stratigraphic succession, the scientific literature slightly diverges on chronostratigraphy and on the relations among La Fossa and Vulcanello activity. Some of these discrepancies can be however reconciled by considering longer and/or multiple events characterizing the eruptive activity. For Vulcanello, difference arises for the onset of the activity (2.1-1.9 ka in De Astis et al., 2013a; or 1020-1050 AD in Arrighi et al., 2006 and Di Traglia et al., 2013). However, early eruptions of Vulcanello may have occurred below sea level with sporadic emissions during Roman age, as reported in historical chronicles, and the subaerial part of Vulcanello (XI Century as obtained by archemagnetic datings) could be considered as the final part of a submarine growth process as suggested in Fusillo et al. (2015). The same applies to the Punte Nere products (age = $3.8 \pm 0.9/-0.8$ by Soligo et al., 2000; age = 1170 ± 20 AD by Arrighi et al., 2006) which can be interpreted as a multi-phase period of activity, as recently shown by submarine geological studies (Casalbore et al., 2018). The most important consequence of these uncertainties is that the reconstruction by De Astis et al. (2013a) implies a quiescence interval of almost 1 ka between the emplacement of

Caruggi and Pietre Cotte formations (see Table 3). The interval of quiescence between Caruggi/Commenda and Pietre Cotte is far smaller following the reconstruction of Di Traglia et al. (2013), who consider most of this activity to have occurred between XI and XIII centuries. These discrepancies in chronostratigraphy will be hopefully solved in the future.

2.2.2. Historical accounts of La Fossa eruptions

The present state of knowledge of the historical eruptive activity of Vulcano (starting from V-VI century BC) lacks systematic studies comparing written historical sources with volcanological studies.

The available volcanological studies date back to the late XIX-early XX centuries and were primarily carried out by two scientists: Giuseppe Mercalli (1891) and Ottorino De Fiore (1922). The catalogues of historical eruptions published in these works represented the reference data cited in the modern volcanological literature (e.g. Keller, 1970, 1980; Frazzetta et al., 1983; De Astis et al., 2013a, 2013b and reference therein) and they are merged into the catalogue of Siebert et al. (2010).

The historical studies are collections of historical accounts of natural events not only related to the island of Vulcano, but also to the entire Mediterranean area in the classical period (Panessa, 1991) or in the Middle Age, with particular reference to the Sicilian area (Agnello, 1992). Surprisingly, the volcanological literature analysing the historical accounts did not take into account the important work of Stothers and Rampino (1983), which deals with the eruptive phenomena of the Mediterranean area in ancient times up to 630 AD. This work contains a few records regarding ancient eruptions at Vulcano, which are worth to be evaluated in future historiographic works. Beyond the reference to Vulcanello formation in II century, our review has not found there information able to re-define the already know stratigraphy. However, the analyses of the information requires specific historiographic research that is out of the scope of this paper. Recently, Barbano et al. (2017) published a catalogue of Vulcano/Stromboli eruptions and earthquakes in the Aeolian Islands and NE Sicily from 15th to 19th centuries, based on historical researches. In particular, for the Vulcano eruptions, Barbano et al. (2017) provide an update of the original sources, but the study lacks a volcanological interpretation of the phenomena. In the catalogue of Barbano et al. (2017), two eruptions should be mentioned, since they had a significant impact on the island: the 1444 AD activity (uncertain attribution to La Forgia or La Fossa craters) and the 1525/1550 AD activity, the one that gave rise to the isthmus joining Vulcanello and La Fossa cones, which Barbano et al. (2017) indicate to have occurred from La Fossa (according to Fazello, 1558).

The period of time carefully analysed here for the reconstruction of the historical eruptive activity of Vulcano starts from 1739, since only from this year there is an almost continuous record of the activity and a homogeneous description of the phenomena, which allows the reconstruction of the eruptive style and the state of the volcano. For this analysis, we have used the chronicles reported in Mercalli (1883), Mercalli and Silvestri (1891), De Fiore (1922) and Barbano et al. (2017). In Fig. 4 and Table 4 are summarized the description of the activity for the investigated period.

One important observation is that, after the end of the eruptive activity of 1739 AD, the crater of La Fossa alternated repose periods, characterized by degassing activity, with short periods of Vulcanian activity (Table 4). The periods of quiescence had a duration of 30, 10, 3 and 86 years (with a period between 1822 and 1823 AD, lasting only few months). Starting from 1873 AD La Fossa was characterized by explosive events separated by periods of intense degassing. The periods of intense degassing were sometimes accompanied by weak seismicity, felt in the crater area, associated with ground deformations and the formation of fracture systems.

This eruptive period culminated with the eruption of 1888-90 AD, which was not preceded by significant seismic activity (at least none reported by the inhabitants of the island). According to the chronicles
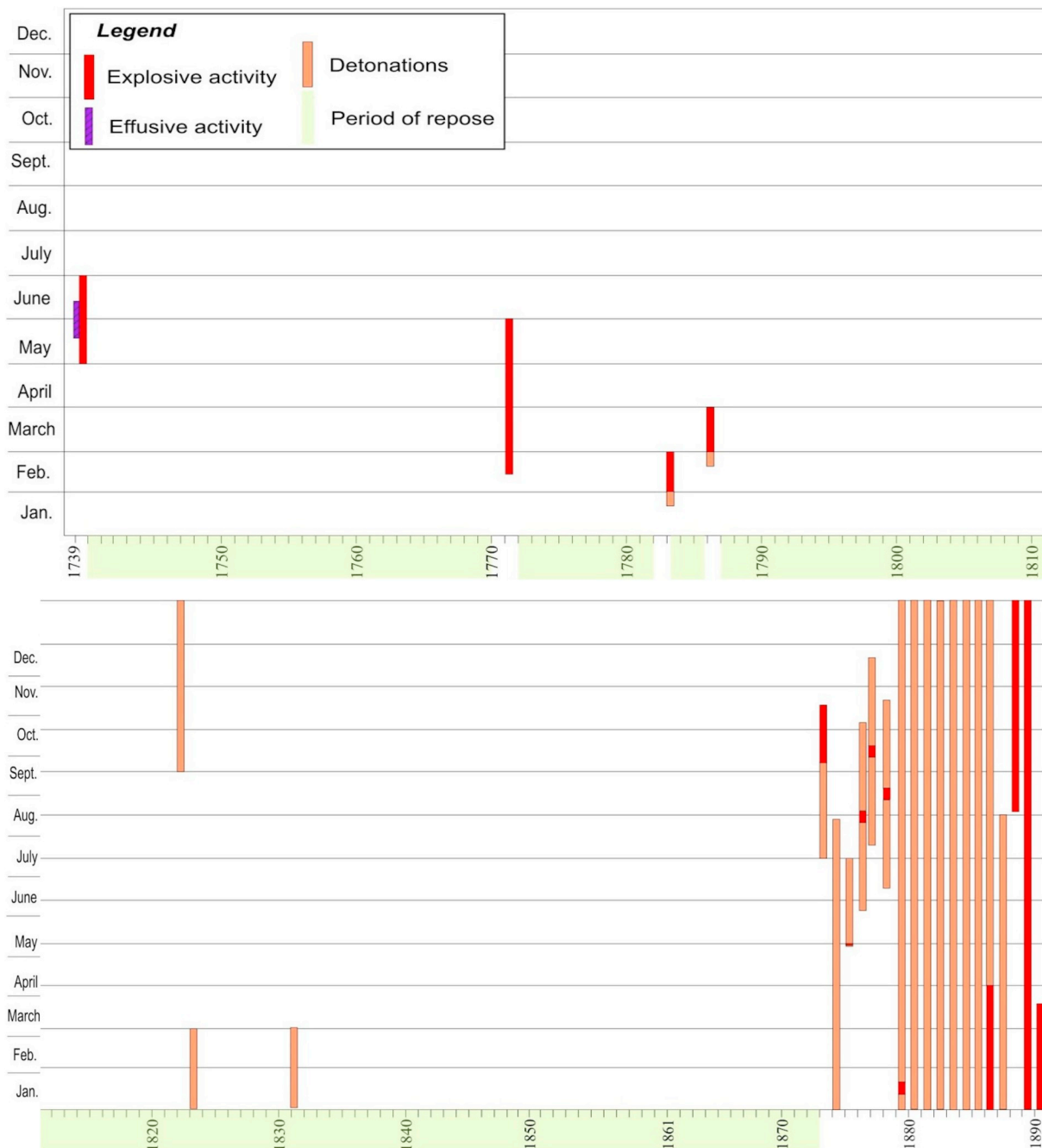
Fig. 4. Synoptic diagram of Vulcano eruptive activity from 1739 to 1890 AD, according to the different types of recognized activity.

(Mercalli, 1891; De Fiore, 1922), after the eruption of 1887, Vulcano appeared calm and characterized by a variable fumarolic activity. On the night of August 3, 1888, a strong roar accompanied by soil tremors was heard by the lighthouse of Gelso in Vulcano, and the volcano crater began to emit dense smoke lit by electric bursts with ballistic boulders. The explosions, with varying intervals, followed until August 4, 1888, with less intensity, and they completely ceased in the night between 5 and 6 August. On 18 August 1888, Vulcano resumed its activity with even more violent explosions at intervals of 30-40 minutes, with the emission of ash and the launch of boulders with maximum diameters from 0.3 to 0.7 m (Mercalli, 1891) and the formation of convective columns to heights of 3-4 km. The intermittent eruptions at variable intervals were associated with abundant gas and steam emissions, coarse solid material and absence of lava or PDCs emissions, and the intensity of the explosions decreased with the rest interval separating

them (size-predictable behaviour). The period lasted about 2 years with substantially repetitive behaviour, with inter-eruptive stasis intervals between explosions (Mercalli, 1891) and changes in the composition of magma (Clocchiatti et al., 1994).

At the end of the 1888-90 AD eruption, a period of repose began, to date 126 years, in which the crater of La Fossa is obstructed and characterized only by degassing activity.

As a whole, the historical analyses have evidenced that: i) after the end of the 1739 AD eruption, Vulcano was characterized by an open conduit system during which short Vulcanian-type explosive eruptions, separated by periods of repose of highly variable duration, occurred; ii) the eruptive phenomena of this open-conduit phase, which will ended with the 1888-90 AD eruption, were generally not preceded by seismic activity perceived by the inhabitants of the island; and iii) after the end of the 1888-90 AD eruption, Vulcano entered a phase of closed conduit

Table 4
Description of the activity and related eruptive types since 1739 AD.

Date	Type of activity State of the volcano	Activity description
29 March-5 June 1739 AD	Vulcanian eruption (La Fossa crater)	Intense and discontinuous explosive activity with formation of ash columns and ash fallout in the Aeolian islands. Two sources report the fall of large bombs along the Tyrrhenian coast of Sicily close to the village of Brolo ("*a fiery cloud ... He passed over the land of Pilaino, where in the nearby river he threw a large stone of about 9 'rotoli' (about 8 kg)*" from Mongitore, 1743). According to De Fiore (1922) the Pietre Cotte lava flow was emitted during this eruption based on the observation performed by Le Duc in 1757 AD. Barbano et al. (2017) confirm this hypothesis.
1740-1770 AD	period of repose Open-conduit	About 30 years characterized by degassing activity from a vent located on the crater bottom of La Fossa.
17 February-May 1771 AD	Vulcanian eruption (La Fossa crater)	Discontinuous explosive activity with the formation of ash columns, bombs and ash fall in Lipari with accumulations of several centimetres. According to Mercalli (1891) the Pietre Cotte lava flow was generated during this eruption.
1772-1782 AD	period of repose, open-conduit	About 10 years characterized by degassing activity from a vent located on the crater bottom of La Fossa. Barbano et al. (2017) report an eruptive event in 1780 AD of uncertain attribution.
February 1783 AD	Vulcanian eruption (La Fossa crater)	Detonations and explosive activity with the formation of ash columns.
1783-1786 AD	period of repose, open-conduit	About 3 years characterized by degassing activity from the fumaroles systems located along the crater rims of La Fossa.
March 1786 AD	Vulcanian eruption (La Fossa crater)	Detonations before the eruption onset characterized by explosive activity with the formation of ash columns that produced bombs and ash fallout.
1787-1873 AD	period of repose, open-conduit, obstructed-conduit from 1832 to 1873 AD	About 86 years characterized by degassing activity from a vent located on the crater bottom of La Fossa and by fumaroles systems. From September 1822 to the beginning of 1823 AD detonations heard up to the north coast of Sicily. In 1831 Hoffmann observed the presence of a small scoria cone in the crater bottom characterized by an intense degassing associated with detonations. During the nights the glow of the vent was observed due to the high temperature of the gases. From 1832 to 1873 AD the crater of La Fossa was obstructed and the degassing were associated only to the fumarole systems. From 22 July to the beginning of September 1873 AD detonations heard in the area of La Fossa crater and increasing of fumarolic activity.
7 September 1873 AD	Vulcanian eruption (La Fossa crater)	Short (hours) explosive activity with the formation of ash columns and bombs fallout from the La Fossa crater. This activity continues discontinuously until 18 October. From October 19th to 26th only detonations of decreasing intensity are reported. Before the beginning of the eruption no seismic activity was warned by the inhabitants.
27 October 1873-half of January 1874 AD	period of repose, open conduit	Degassing activity, a few days before January 22nd, 1874 AD the detonations resume and on January 23rd night a new vent was formed inside the crater and the fumarolic activity increases. In the following months the detonations continue and the degassing of fumaroles increased until July 27, 1874 AD then no phenomenon until April 30, 1875 AD when the detonations resumed and an impulsive ash emission occurred. May-June 1875 AD detonations associated with seismic activity recognized in the crater area, increased fumarolic activity and fracture formation.
29 July 1876 AD	Vulcanian eruption (La Fossa crater)	Impulsive explosive activity with the formation of ash column and bombs fallout in the crater area and ash fallout in Lipari and Salina islands. This activity occurred also in September 1877, August 1878 and January 1879 AD. In the intra-eruptive periods, detonations in the crater area were heard.
February 1879-1865 AD	period of repose, open conduit	About 6 years characterized by detonations and intense fumarolic activity.
January-March 1886 AD	Vulcanian eruption (La Fossa crater)	Discontinuous explosive activity with the formation of ash column and lithic clasts fallout in the crater area and ash fall in Lipari.
April 1886-July 1887 AD	period of repose, open conduit	Detonations heard up to Lipari, activity of degassing from two vents located in the crater bottom and intense fumarolic activity.
August 1887-July 1888 AD	period of repose, obstructed conduit	Further increase of degassing at the fumaroles systems. The two vents in the crater bottom were obstructed.
3 August 1888- 22 March 1890 AD	Vulcanian eruption (La Fossa crater)	Discontinuous explosive activity of variable intensity. The most intense explosions produced the fallout of bombs and blocks in the area of Vulcano port and in the sea in front of the Levante port, causing damage to houses located about 1.3-1.4 km away from the crater. The fall of centimetric size lapilli up to Lipari occurred. During this eruptive period the distal fallout of ash from the eruptive column affected the southern Calabria, the northern coast of Sicily up to Palermo and the east coast of Sicily up to Catania and Siracusa.
April 1890 AD-today	period of repose, obstructed conduit	Degassing activity of variable intensity from several fumarolic systems located mainly in the area of La Fossa crater

only affected by a degassing linked to the fumarole systems.

2.3. The plumbing system

Some multidisciplinary studies based on fluid inclusions and gas geochemistry, geophysics, mineral chemistry and petrology, have proposed models for the Vulcano plumbing system that are substantially convergent (i.e., Clocchiatti et al., 1994; De Astis et al., 1997a; De Astis et al., 2013a; Zanon et al., 2003; Peccerillo et al., 2006; Paonita et al., 2013; Fusillo et al., 2015; Mandarano et al., 2016; Nicotra et al., 2018). It is a polybaric system with several magmatic ponding zones that changed over time, showing a progressive shallowing. The different approaches converge in indicating magma storage at about 20-21 km of depth (Moho limit), 13–8 km, 5.5–2.8 km, and a very shallow storage zone at 1–2 km beneath La Fossa cone. More details on the time and space evolution of the Vulcano plumbing system can be found in De Astis et al. (2013a) and references therein or Nicotra et al. (2018 and references therein).

In general terms, the magma differentiation processes are variable, and changed with the evolution of the plumbing system. The early epochs (see Table 2 and Section 2.2) are characterized by a stable feeding system, consisting of a deeper reservoir dominated by fractional crystallization, continental crust assimilation and magma mixing processes. EE 6 (Table 2) marks the establishment of a shallow reservoir(s) system confined between 5.5 km and 2.8 km of depth, related to or fed by deeper reservoirs located in the lower and in the upper crust and at the Moho limit (data from Vulcanello shoshonites).

EE8 shows eruptive activities from different vents (Mt. Saraceno, La Fossa, Vulcanello, see Table 2) fed by quite different magmas, ranging from shoshonites to rhyolites. In historical times, La Fossa and Vulcanello vents erupted almost simultaneously when the shoshonitic products from Vulcanello followed in short time by the trachytic and rhyolitic magmas of Palizzi and Commenda erupted from La Fossa and then again by latites from Vulcanello.

In compositional terms, La Fossa volcanic successions contain the most evolved products in the Vulcano eruptive history, which also show high alkali contents and the highest radiogenic Sr ratio, probably due to (low amounts of) upper crust assimilation by small volumes of rhyolitic magmas. By contrast, the Vulcanello products represent the most mafic magmas erupted on the island in the last 6 ka, characterized by isotopic features close to those recorded for most of the more evolved magmas erupted from La Fossa (De Astis et al., 2013a), despite their deeper origin. By comparing the volcanic rocks and deposits from La Fossa and Vulcanello, we obtain a rather complex history of different magma compositions erupting over the last 6 ka from a plumbing system made up of distinct magma batches with both deep and shallow accumulation zones.

The documented and recurrent mingling and mixing processes observed also in sin-eruptive phases (De Fino et al., 1991; Clocchiatti et al., 1994; De Astis et al., 1997; Bullock et al., 2019; Costa et al., 2020; and references therein), together with the decreasing of the erupted volumes in the last millennia, provides a robust support for the proposed model of the Vulcano plumbing system reported above (and fully explained in Section 4).

As an example that further support the proposed model, the Vulcanian-type eruptions that occurred from La Fossa from 1739 to 1888–1890 AD, with their transient dynamics characterized by alternating eruptions and quiescence periods, provide a strong evidence that stratigraphy reflects the complexity of magma feeding system. Indeed, their pyroclastic deposits contain both lati-trachytic bread-crust bombs and rhyolitic pumice in coexistence; the rhyolitic Pietre Cotte lava contain latitic enclaves showing from plastic to solid behaviour within the host. Therefore, it seems beyond doubt that the shallow system is dominated by a network of dykes and sills at different states of crystallization that can be remobilized and can interact, erupting, through the arrival of fresh and hotter magma into the system. Note that recent

experimental studies on the viscosity of Vulcanello shoshonitic lavas have proposed possible ascent times (from 20 km of depth) on the order of hours to a few days (Vetere et al., 2007).

2.4. Seismicity and ground deformation

Seismic and ground deformation monitoring began at Vulcano in the mid-1970s. EDM/GPS, levelling and tilt time-series revealed processes at different scales ranging from regional tectonics involving the Lipari-Vulcano Volcanic Complex (LVVC) to the volcanic and hydrothermal activity at Vulcano (e.g. Alparone et al., 2019; Harris et al., 2012).

Eighteen years of GPS data show an overall northward trend of the ground motion and an active N-S shortening with a maximum between La Fossa caldera and Vulcanello (Esposito et al., 2015; Fig. 4C), while vertical velocities and levelling show a diffuse northward tilt of the Vulcano main island (Esposito et al., 2015; Alparone et al., 2019). This strain field is in agreement with transpressive kinematics of the NNW–SSE prolongation of the TLF (Bonaccorso, 2002; Bonforte and Guglielmino, 2008; Mattia et al., 2008). The seismicity of LVVC shows depths of the crust comprized between 5 and 20 km and prevailing strike-slip (and subordinately reverse faulting) focal solutions (Barreca et al., 2014).

In the last 50 years, seismic strain release shows a roughly constant background rate (Alparone et al., 2019) interrupted by a few abrupt strong releases due to strong earthquakes as on April 15, 1978 (M = 5.5) and August 16, 2010 (M = 4.6). On Vulcano, seismicity with double-couple sources typically occurs in swarm-like sequences of low magnitude (M ≤ 2.6) at at shallow depth (1-8 km). In particular, a seismogenic structure beneath Vulcanello has been recognized (C1 in Fig. 3D; Gambino et al., 2012). Locally, La Fossa Cone is also affected by a microseismicity composed of long-period, monochromatic and high-frequency events. They have been attributed to the resonance of cracks (or conduits) filled with hydrothermal fluid or to rock-fracturing processes driven by hydrothermal fluid dynamics (Alparone et al., 2010; Cannata et al., 2012).

The Vulcano kinematics can be disrupted by local strong earthquakes that temporarily change the local stress field, such as on April 15, 1978, when a M = 5.5 event caused evident anomalous horizontal and vertical deformation. Levelling measurements showed a significant uplift between September 1978 and March 1980 of the central region surrounding La Fossa, which was explained by Ferri et al. (1988) and Bonafede (1995) as a large increase of the mean stress within a magma chamber at 6.5 km depth close to Vulcanello (Fig. 4D).

For what concerns the sources of ground deformation, a modelling of 1999-2013 GPS and levelling data shows as Vulcano, during quiescence phases, is affected by the action of a tectonic tabular source (TLF) coupled with a deflating magmatic Mogi source 4.7 km b.s.l. under Vulcanello (Fig. 4D; Alparone et al., 2019).

The transition of the volcanic system from a stability phase to unrest induces the heating and expansion of shallow hydrothermal fluids that cause measurable ground deformation on La Fossa cone. Gambino and Guglielmino (2008) inverted the 1990-1996 EDM and levelling data, showing a deflating ellipsoidal source, centered under La Fossa Crater at about sea level depth (Fig. 4D). The subsidence recorded at La Fossa Cone in that period has been explained as the fluid loss from the geothermal reservoir in agreement with the strong increase of steam emission and temperature at crater fumaroles (Italiano et al., 1998).

2.5. Hydrothermal and fumarolic system

Since the last eruption occurred in 1888-1890 AD, Vulcano is in a state of solfataric fumarolic activity. The main fumarolic field is located at the crater of the Fossa volcanic cone, with gas emissions that currently reach temperatures around 400 °C (Fig. 5A). A second exhalative area at a lower temperature (< 100 °C) is located at Baia di Levante
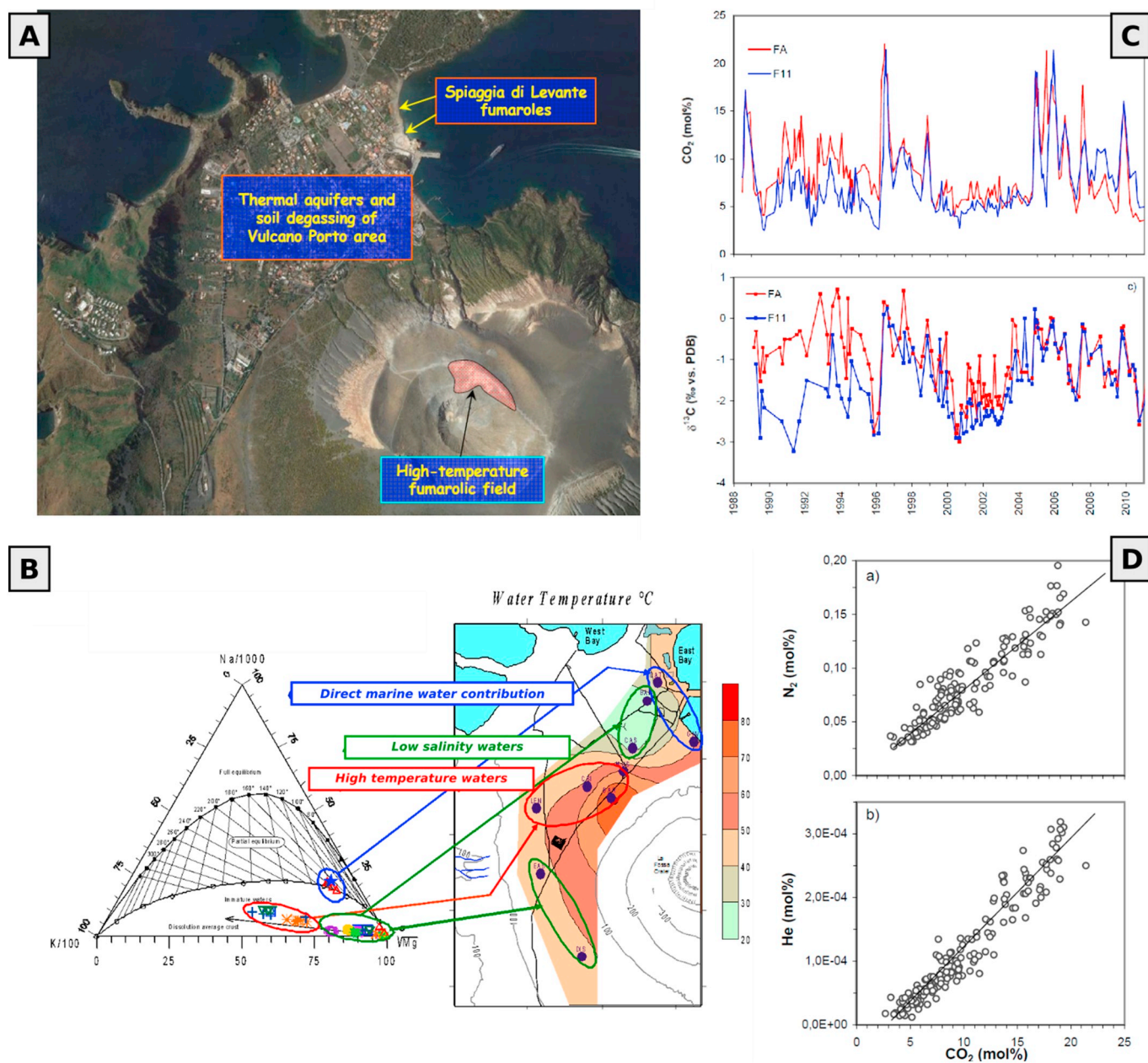
Fig. 5. Hydrothermal and fumarolic system. A) Main degassing and thermal areas. B) Thermal wells in the area of Vulcano Porto, relative distribution of aquifer temperature, and classification of water-rock interaction processes (courtesy by G. Capasso). C) Temporal variations of CO_2 and $\delta^{13}C_{CO2}$ in two crateric fumaroles. D) He-N_2-CO_2 correlation in fumarolic gases.

area, and in particular on the beach of the isthmus, in the area immediately offshore, and near the so-called "Vasca degli Ippopotami". A diffuse degassing of CO_2 develops from the soil in the whole area of the inhabited center of Vulcano Porto and from the non-fumarolic areas of the Fossa cone. Several hot wells in the area of Vulcano Porto bear witness to the existence of a vast thermal aquifer (Fig. 5A and B).

As concerns low-temperature Baia di Levante fumaroles, the genesis of the emitted fluids can be found in two vaporiferous levels existing at depth below this area. In the 1950s, drilled wells by AGIP-Vulcano in the area of Vasca degli Ippopotami at Baia di Levante, revealed the existence of two boiling aquifers at depths of 90 and 200 m b.s.l., respectively, at temperatures of 135°C and 194°C (Sommaruga, 1984). Among the fumaroles of the area, we find 1) gaseous emissions at temperatures close to water boiling at local atmospheric baric conditions, which consist of 80-90 mol% H_2O, with complementary CO_2, H_2S

and N_2 (Paonita et al., 2013, and references therein); 2) emissions with lower temperatures, largely dominated by CO_2 (> 95 mole%), which practically consist of the incondensable species of the first group. Applying geothermo-barometric approaches in the CO-CO_2-CH_4-H_2-H_2O system and assuming boiling conditions in the genesis of the emitted gases, equilibrium temperatures around 195 °C and vapour pressures close to 1.3 MPa can be estimated (Chiodini et al., 1991, 1995). The consistency between the temperatures and pressures estimated by the gases and those measured in the wells confirms the genesis of the fumarolic fluids of Baia di Levante in the underlying geothermal systems. Secondary condensation processes subsequently modify the composition of low-temperature emissions.

Chiodini et al. (1991) showed that increased inputs of high-temperature fluids at the crater were positively correlated with increases in geotemperature and geopressure estimated for Baia di Levante

hydrothermal system. These episodes, therefore, represent moments of pressurization of the geothermal system, which necessarily approaches instability conditions in which the risk of ground explosions increases.

The systematic monitoring of the thermal aquifer in the Vulcano Porto area started in 1977, aimed at the chemical analysis of water and stable H and O isotopes (δD and $\delta 18O$; Martini and Piccardi, 1979; Carapezza et al., 1983). The large set of data obtained since then allows the characterizations of the superficial water table and the identification of the area mainly affected by fumarolic vapour contributions (Fig. 4B; Carapezza et al., 1983, Dongarrà et al., 1988; Capasso et al., 1992). The superficial water is a very immature meteoric water system, permanently fluxed by gases from underlying boiling aquifers (Bolognesi and D'Amore, 1993; Cortecci et al., 2001). Waters can be further distinguished between steam-heated groundwater in Baia di Levante area, and waters most directly fed by deep fluids rich in Cl-SO$_4$ or condensing from the fumarole area along the flanks of the Fossa cone (Bolognesi and d'Amore, 1993; Chiodini et al., 1996; Fulignati et al., 1996; Capasso and Inguaggiato, 1998; Aiuppa et al., 2000; Capasso et al., 1997a, 1997b, 2000, 2001). A general model that describes this process of condensation of steam and related boiling was proposed by Federico et al. (2010). Some variations found during the increased degassing of 1988-1990 can be accordingly explained by a different composition of the fumarolic fluid entering the aquifer, togheter with a higher proportion of this fluid (rich in CO_2, HCl and S) with respect to the superficial meteoric term. According to Capasso et al. (2014), the thermal aquifer chemistry would be significantly modified by the entry of deep fluids only when the hydraulically conductive fractures are opened due to deep pressurization during increased degassing periods. In the La Fossa area, meteoric waters would intercept the rising hydrothermal fluids along vertical volcano-tectonic faults, while the condensed steam could flow horizontally towards the Vulcano Porto aquifer, along volcano-stratigraphic discontinuities (Madonia et al., 2015).

Coupled to the results from the study of the thermal waters, key clues on the existence of a deep hydrothermal system that would feed the widespread thermal manifestations within the La Fossa caldera come from the survey of the high-temperature fumaroles at La Fossa crater (Fig. 5C). The main feature that emerges from the vast geochemical dataset on these fumaroles is the correlation between CO_2 concentration and other geochemical parameters, such as He, N$_2$ (Fig. 5D), $\delta^{13}C_{CO2}$, partly HCl and S, which was interpreted as a result of a mixing process between magmatic and hydrothermal fluids (Chiodini et al., 1993, 1995, 2000; Tedesco, 1995; Capasso et al., 1997a; Nuccio et al., 1999; Di Liberto et al., 2002; Leeman et al., 2005; Taran, 2011). Based on these correlations, it was concluded that the magmatic fluid would be richer in CO_2, He, N$_2$, ^{13}C (i.e., high $\delta^{13}C_{CO2}$) and Ar, and poorer in H_2O, HCl, S and ^2H (i.e., low δD_{H2O}) with respect to hydrothermal vapours (Bolognesi and D'Amore, 1993; Tedesco, 1995; Tedesco and Scarsi, 1999; Capasso et al., 1997a, 2001; Chiodini et al., 1993, 1995, 2000; Nuccio et al., 1999; Di Liberto et al., 2002; Paonita et al., 2002).

Two main points of view in the literature debate the state of the deep hydrothermal systems. According to a "dry" model, the hydrothermal end-member derives from seawater that is completely vaporized when it infiltrates under the La Fossa edifice due to contact with hot igneous rocks (Cioni and D'Amore, 1984; Chiodini et al., 1993, 1995, 2000). Vaporization zones at different temperatures, which produce fluids rich in H_2O with different contents of HCl, HF, H_2S and SO_2, can be recognized when comparing the concentrations of these species in fumarolic fluids with the predicted fluid compositions in equilibrium with various paragenesis of hydrothermal minerals (Chiodini et al., 1993). In contrast, the "wet" model of Carapezza et al. (1981) consists of a two-phase hydrothermal vapour-liquid system at a depth of 1-2 km. Nuccio et al. (1999) reconciled the two models by comparing the compositions of 1970 with the composition of hydrothermal fluid extrapolated from the 1988 fumarolic data, which showed

a decrease in CO_2 and an increase in NaCl. They concluded that the wet model would work until the late 1970s, with the boiling of the hydrothermal system at around 330 °C and 15 MPa. An increase in the magmatic contribution caused the increasing volcanic activity in the second half of the 1980s and the total vaporization of the central part of the hydrothermal system, resulting in a single-phase central column surrounded by a two-phase system with higher temperature and pressure than the 1970 conditions (390 °C and 20 MPa).

It is noteworthy that the value of δD_{H2O} of the source fluid feeding the deep hydrothermal system, recomputed by taking into account a number of secondary processes, is very close to that of local seawater (Chiodini et al., 1995, 2000; Paonita et al., 2002). Seawater in fact undergoes a series of processes while it infiltrates through hot rocks (for example, water-rock and boiling interactions) that modify the isotopic composition of O, B (Chiodini et al., 1995, 2000; Paonita et al., 2002; Leeman et al., 2005) and partly H (Paonita et al., 2002). Na-Ca chemical exchanges between water and local rocks control the pH conditions of this fluid (Di Liberto et al., 2002). According to Taran (2011), hydrothermal fluids would carry a generalized crustal component that may be associated with contributions from both the subduction lithosphere and the crust beneath the volcano.

2.6. Monitoring system

The analysis of the state of activity of Vulcano is based on the use of advanced monitoring systems, which measure geochemical and geophysical parameters through periodic campaigns and permanent instrumental networks (Fig. 6A).

2.6.1. Geochemical monitoring

The gas and water emissions on Vulcano are monitored by one of the most densely distributed and complete observation systems in existence (see Inguaggiato et al., 2018 for a review). The geochemical surveillance network has been implemented since 1984 to monitor the evolving volcanic activity subsequent to the unrest of the end of the 1970s. Monitoring activities include periodic field measurements and sampling collection of thermal waters, high-temperature fumarole gases of La Fossa crater and widespread flows of carbon dioxide from the soils in the area of Vulcano Porto and Spiaggia di Levante. The surveys are performed every two months and provide on-field physical-chemical data of thermal waters (water table level, temperature, pH, Eh, conductibility), emissions temperature of selected fumaroles and diffuse CO_2 fluxes from soils. The collected samples are analysed for measurement of i) chemical composition of hydrogen, helium, oxygen, nitrogen, carbon monoxide, methane, argon and carbon dioxide in fumarolic gases and dissolved in thermal groundwater; ii) chemical composition of the major elements in thermal groundwater; and iii) isotopic composition of hydrogen, helium, argon, oxygen, nitrogen, carbon in fumarolic gases and dissolved in groundwater.

In addition, continuous measurements are produced by permanent instruments installed at both crater and Vulcano village areas (see Inguaggiato et al., 2018; Fig. 6B). Near-real-time heat release has been monitored since 1984 by two temperature-monitoring stations in the main fumarole area of the crater, while three heat-flux monitoring stations have been more recently added in steam-heated soil zones. A network of permanent stations continuously acquires data of temperature, level and conductivity in four thermal wells, and diffuse CO_2 fluxes in several key degassing sites of Vulcano village. Finally, SO_2 output through the crater plume is continuously surveyed by UV scanner fixed station.

2.6.2. Geophysical monitoring

Geophysical monitoring at Vulcano consists of discrete (EDM/GPS, levelling, gravimetric) and continuous (seismic, GPS and tilt networks) measurements (Fig. 6A).

The first EDM network, consisting of 13 benchmarks and 39
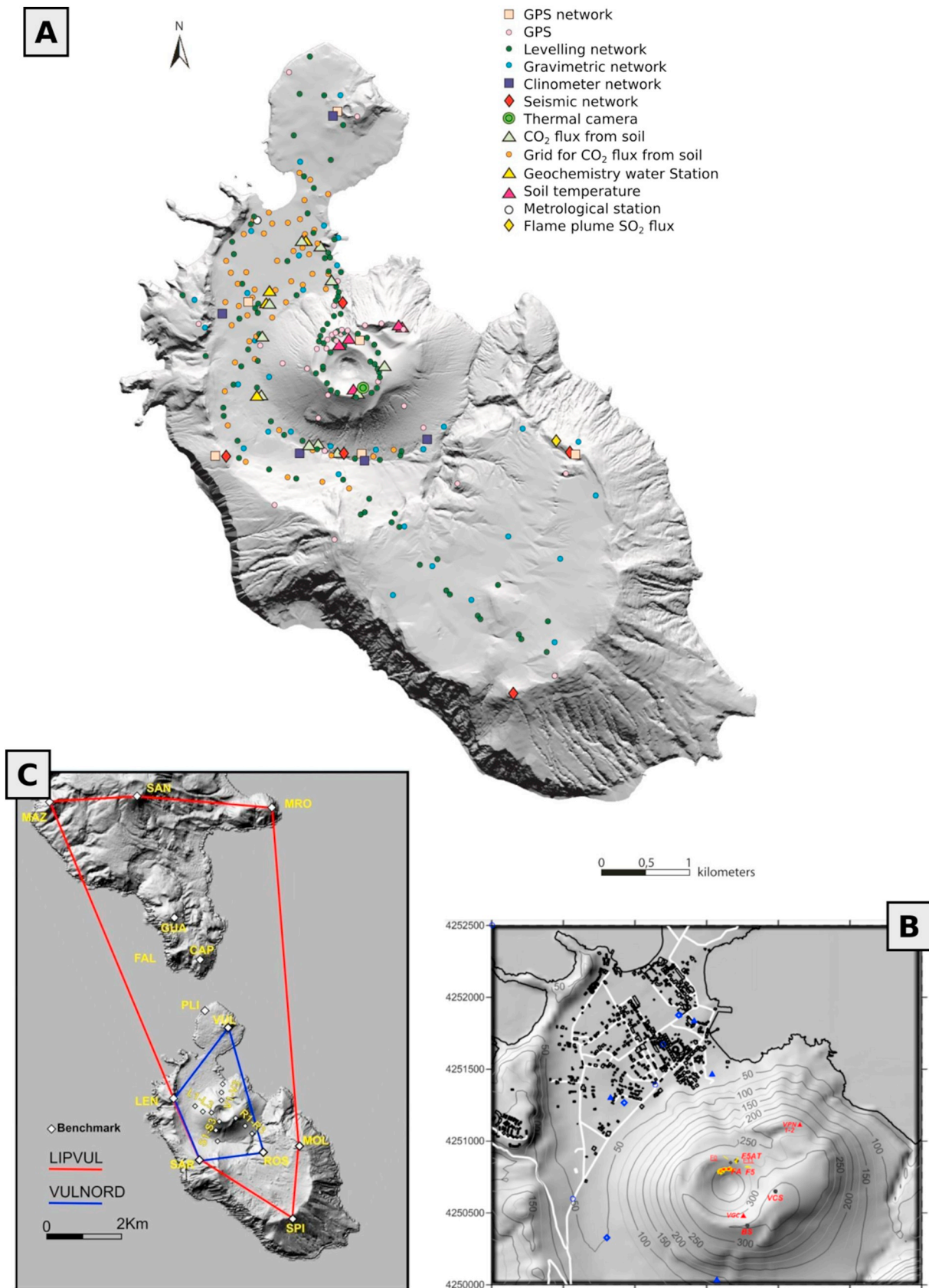
Fig. 6. Vulcano monitoring networks. A) Location of all the networks of the monitoring system in Vulcano. B) Geochemical network for fumaroles, soil degassing and aquifers monitoring; in black: summit stations; in blue: base stations; in yellow: areas with high temperature fumaroles (from Diliberto, 2013); in red: temperature monitoring in vertical profiles (from Ricci et al., 2015). C) EDM/GPS discrete networks (LIPVUL and VULNORD).
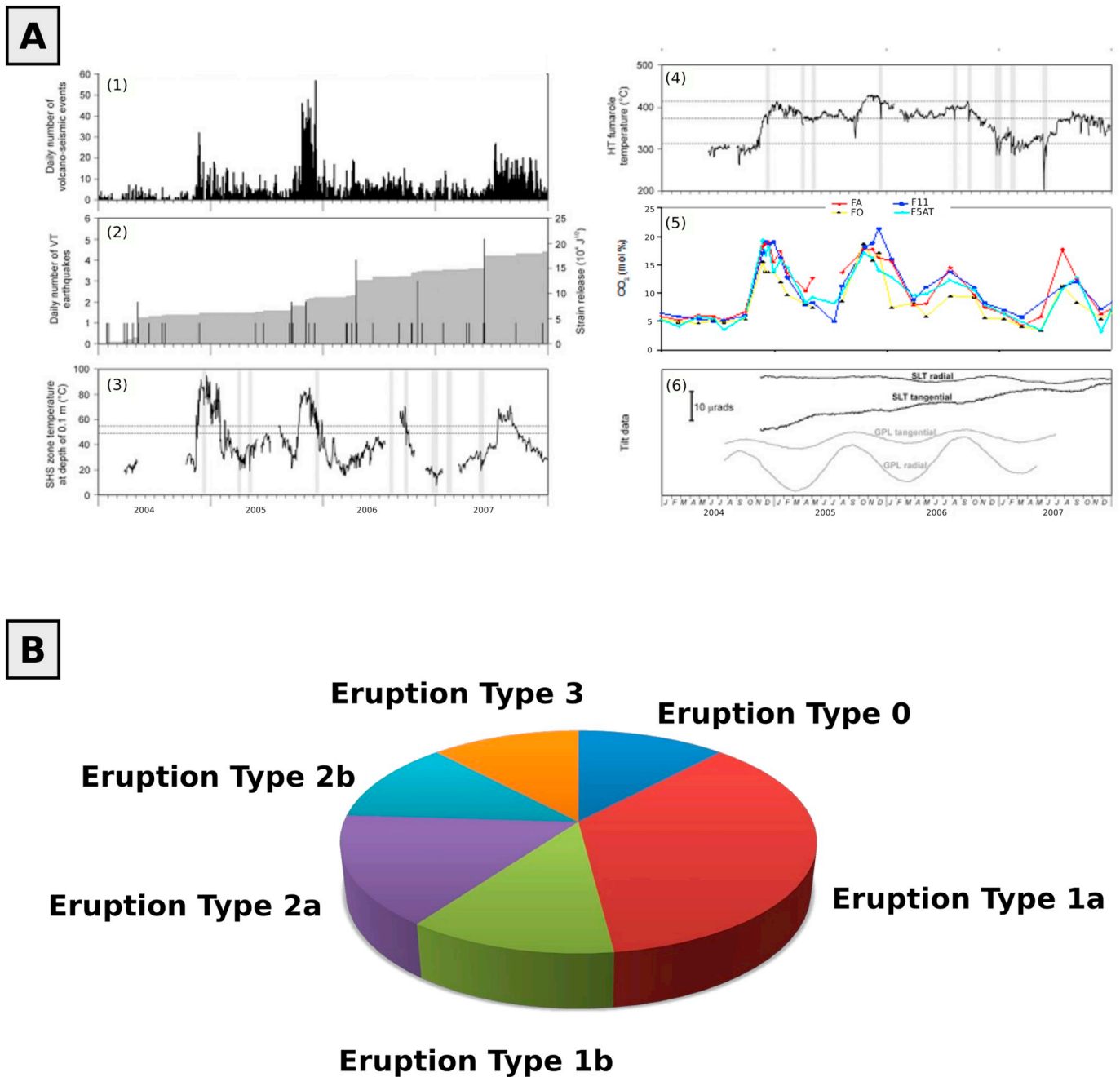
Fig. 7. Volcanic states at Vulcano: A) Unrest phase - A set of monitored parameters, including daily number of seismo-volcanic and seismo-tectonic (1, 2), soil temperature at the bottom of the crater, far from fumaroles (3), temperature of F5AT fumarole on the crater rim (4), CO_2 concentration in fumarolic gas (5), and tilt-components (6) at SLT (Lentia) and GPL (Grotta Palizzi) stations (modified from Cannata et al., 2012); B) Piechart of eruptive events in the last 2000 years by each defined Eruption Types (Type 0: Phreatic eruptions; Type 1: effusive and Strombolian activity; Type 2: Vulcanian eruptions; Type 3: short-lived explosive sustained eruptions; see Section 2.7.2).

baselines, was set up in 1975 and covers the whole island of Vulcano and central-southern part of Lipari (LIPVUL in Fig. 6C). In 1987, a smaller and denser network was set up on the northern part of Vulcano with the aim of monitoring La Fossa cone (VULNORD in Fig. 6C). Since 1996, these two networks are surveyed by using GPS technique (Bonaccorso et al., 2010; Esposito et al., 2015).

The levelling network is currently made up of 100 benchmarks distributed over a length of about 25 km, with a very high density in the center-northern sector of the island. The operating network has been expanded and made denser several times since 1976, the year of installation (e.g., Obrizzo, 2000). Gravimetric measurements started in 1982 and involve a network composed of 26 benchmarks (Di Maio and

Berrino, 2016).

Since the late 1970s, continuous seismic monitoring in the Aeolian Archipelago was performed by a permanent network made up of a few analogue stations. Since 2007, the Aeolian permanent seismic network consists of 12 (4 of which on Vulcano) broadband (40s) three-component digital stations (e.g., Gambino et al., 2012).

A permanent tilt network currently comprises five borehole stations equipped with bi-axial instruments, four of which installed at a depth of 8-10 m (Gambino et al., 2007). A permanent GPS network is active since the end of the 1990s and at present 7 stations cover the Lipari–Vulcano area (Barreca et al., 2014).

2.7. Reference period and states of the volcano

The definition of the reference period is rooted in indentifying a period of time that can be considered representative of the phenomena we want to analyse (the present day volcanic system and its associated hazard, in our case). This period must be long enough to satisfactory represent different eruptive dynamics and vent opening in a volcanic setting comparable to the present day one.

Most of the structural studies converge on identifying a significant structural change around 10 ka, with a change from a NW-SE shear to present E-W extensional regime. During this time period, Vulcano experienced the last sector collapse of LFC, the fissural eruption of Mt. Saraceno, the effusion of small rhyolitic domes and thin lava flows along a N-S alignment, the emplacement of youngest intracaldera PDC units associated with the Piano Grotte dei Rossi formation, and the La Fossa-Faraglione-Vulcanello activity. The intracaldera phreatomagmatic activity associated to the Piano Grotte dei Rossi, occurred approximately 8 ka, is the youngest in a series of large scale eruptions occurred between ca. 80 ka and 8 ka, which means most of them occurred before the structural change in the tectonic regime.

Chrono-stratigraphic reconstructions indicate that most of the activity during the last ≈ 5 ka occurred at La Fossa and Vulcanello. In this period, both the geomorphologic context and the tectonic regime of the volcano have been comparable to present day situation, corresponding to a rather stable pattern of eruption dynamics. Activity between 10 ka and 5 ka occurred in a geomorphological context completely different from present day situation, and with eruptive dynamics (fissural eruptions, dome emplacement, large PDCs) not recognized in the last 5 ka.

The present repose time is the one of the longest among the repose times recorded in the reference period (depending on dating, see Section 2.2). However, it is far too short (< 150 yr) to suggest a significant change in the volcanic feeding system. In addition, historical records, as well as field and monitoring data since last eruption, do not show any event that may suggest a specific change in the volcanic system or in the tectonic regime. Therefore, we do not think that 130 years of repose time can herald a major change in volcano eruptive behaviour.

For these reasons, we consider that limiting the reference period to the last 5 ka is appropriate, at least for the hazards with ordinary mean annual frequencies (> 10^{-4} -10^{-5} yr^{-1}, Connor, 2011). The eruptive patterns observed in this period can be surely expected in the future. Eruptive styles not represented in this period, but that occurred in the same tectonic context (that is, in the period 10 to 5 ka), cannot be completely ruled out. However, they appear unlikely and they should be, at least, contextualized in present day geomorphology of La Fossa caldera (LFC).

In the following, the quantitative characterization of unrest and eruptive periods is discussed considering the reference period of 5 ka.

2.7.1. Characterization of unrest phases

In the last 30 years, the unrest phases at Vulcano were always characterized by variations in the degassing pattern, abundance and composition, sometimes accompanied by an increase in seismicity but not by ground deformation. At least 4 main episodes of unrest have been observed (1987-90, 1996-98, 2004-05, and 2009), as well as the several other minor unrest episodes up to 2017 (Fig. 7A; Paonita et al., 2013). All these episodes have been characterized by an increase of magmatic species (CO_2, He, N_2) in crater fumaroles, accompanied by a generalized increase of the fumaroles' temperature, and an increase of CO_2 and SO_2 fluxes. Note that, as it will be better explained in Section 4, these unrest periods have been named as "crises" in literature and, hereinafter, the word "crisis" can be considered synonymous of unrest.

During the 1988-90 episode and, to a lesser extent also during the 1996 episode, important anomalies occurred outside the crater area, including the Vulcano Porto area (Capasso et al., 1999), which also modified the chemical and physical parameters of the aquifers, with a

pH decrease and an increase in Cl and SO_2 contents. Again, in Vulcano Porto, a significant increase of CO_2 flux was observed (Diliberto et al., 2002), while a progressive appearance of low-temperature fumaroles (hereinafter, mofette) was observed in the southern portion of Vulcano Porto (area of Camping Sicilia). Since 2004, the involvement of these peripheral areas was much less significant, with the exception of the degassing areas of Faraglione and Grotta di Palizzi. The progressive decrease in the intensity of the anomalies (in terms of fluxes and temperatures) seems to indicate a decrease in the involvement of deep sources.

The geochemical anomalies are accompanied by a significant increase in the volcano seismicity, with peaks corresponding to the increase of CO_2 and temperature of fumaroles. This microseismicity has been associated with variations in the hydrothermal system located 0.5-1.5 km below La Fossa (Alparone et al., 2010; Milluzzo et al., 2010; Cannata et al., 2012). On the other hand, neither an increase of volcano-tectonic events nor significant deformation have been observed.

The poor record of unrest episodes and, in particular, the lack of records of unrest preceding eruptions prevent the quantitative definition of different types of unrest episodes or linking them to their causative phenomena and potential outcomes. This can be done only through a subjective interpretative framework of the observations summarized above, as discussed within the conceptual model of Section 4. This lack also prevents a satisfactory description of the potential variability of non-eruptive sources during all periods of intensification of the activity, which not only may help in eruption forecasting, but also are hazards for the population. For Vulcano, the only possibility to quantify these hazards is to model their impact characterizing sources with reference to the activity in other volcanoes, from which, for example, it can be derived a quantitative definition of the variability in size sources.

2.7.2. Characterization of eruptive phases

Based on the geological-stratigraphic reconstruction of the last 5 ka of activity integrated with information obtained through the analysis of historical sources available for the last 2 ka, we identified four main eruptive categories: Strombolian and effusive activities, Vulcanian eruptions, explosive sustained eruptions, and phreatomagmatic eruptions. To these eruptive categories, we also add as fifth eruptive type large phreatic explosions involving massively the deep hydrothermal system. These events have shown in the past all the characteristics of a magmatic-driven eruption, that is they may be accompanied by typically eruptive phenomena like ballistic clasts and PDCs. Thus, hereinafter we refer to these large phreatic explosions as phreatic eruptions.

This classification is aimed at hazard quantification, and it is based on the size of the potential impact area, grouping together distinct activities (such as Strombolian and effusive activity) that are characterized by a comparable areal impact.

The main characteristics of each eruptive category are described in the following. For each category, a reference representative event is described (best observed/studied in the past). In addition to the main features, a possible sequence of pre-, inter- and post-eruptive events that combine to define a possible timeline of the eruptive event itself are briefly presented.

Type 0 includes phreatic eruptions. Phreatic eruptions are impulsive events related to the flashing of the deep hydrothermal system. Differently from smaller phreatic explosions involving only the shallow hydrothermal system, phreatic eruptions may be accompanied by convective columns, ballistic ejection or by PDCs. We assume the Caruggi formation (aka Breccia di Commenda eruption) as a potential reference for Type 0, regardless of the absolute age of the eruption (AD 1000-1200 or VIII century AD, see discussion in Section 2.2). The hypothetical timeline suggests that the main eruptive activity was preceded by weak phreatic/hydrothermal explosions, followed by the phase of emission of ballistic blocks and turbulent PDCs. These were followed by other phases of more concentrated and less dispersed PDCs.

The final stages were represented by ash emission, whose duration could last from weeks to months.

Given their limited preservation potential in the stratigraphic record, especially for the oldest events, the period of completeness for Type 0 eruptions is necessarily limited to the historical period (last 1 ka), in which at least three events are certainly identified. This latter number is a minimum, given the difficulty of discriminating on the basis of the historical chronicles between small hydrothermal explosions and actual phreatic events. The events identified on the basis of eruptive deposits and attributed to events described in historical sources occurred in 1444 AD and 1727 AD (Forgia 1 and Forgia 2), together with the explosive event of Caruggi (Unit of the Breccia of Succession of Commenda, ca1 in De Astis et al., 2013b or Breccia di Commenda in Gurioli et al., 2012 and Rosi et al., 2018).

Type 1 includes eruptions with limited impact area, which we divided into effusive (Type 1a) and Strombolian activity (Type 1b).

Effusive activity (Type 1a) includes flows of modest volume, with a variable composition from shoshonite to rhyolite. In the last 5 ka, there were five lava flows from La Fossa and three from Vulcanello (Vulcanello 1 and 3), and one underwater event associated with the activity of Vulcanello 2 responsible for the formation of an extensive field of submarine pillows to the east of Vulcanello. Given that most of the effusive events occur within complex eruptive periods, it is difficult to define a reference event and a possible timeline.

Strombolian activity (Type 1b) has been concentrated in Vulcanello, with moderate intensity, associated with the emission of scoriaceous material which mostly built Vulcanello's cones. The affected area was limited to Vulcanello surroundings. Strombolian activity occurred in all the three main clusters of Vulcanello activity (1, 2 and 3, see Section 2.2).

Type 2 includes Vulcanian eruptions. Two sub-categories can be distinguished within Type 2 based on the presence of PDCs associated with Vulcanian activity: (i) Type 2a, i.e. Vulcanian eruptions characterized by PDC absence or PDCs with runouts limited to the slopes of La Fossa cone; (ii) Type 2b, Vulcanian activity characterized by significant PDCs, many passing the limit of the LFC. The Vulcanian activity of the last 5 ka of the La Fossa cone were characterized by eruptive periods lasting for years with many explosions associated with repetitive weak, non-sustained eruptive columns (hereinafter, Vulcanian cycles). They were accompanied by strong detonations and launch of ballistic bombs and blocks, as well as by the formation of PDCs. In the last 5 ka, four Type 2a eruptive cycles (all included in the last 2 ka), and five Type 2b cycles were identified (of which three occurred in the last 2 ka; Di Traglia, 2011; De Astis et al., 2013a, 2013b; Biass et al., 2016b).

The reference event for the eruptive scenario of Type 2a can be considered that of 1888-90 AD. Although pre-1888 cycles may have been characterized by slightly higher magnitude and intensity (e.g., Pietre Cotte cycle), longer durations, and height of the eruptive columns, stratigraphic data suggest this event is fully comparable respect to older Vulcanian eruptions at La Fossa, but it is better exposed and preserved. It is by far the best described Vulcanian event by the work by Mercalli and Silvestri (1891), a milestone that provides information about dynamics, timing, products, and hazard. This 1888-90 AD cycle has been characterized by intermittent activity with convective columns with height up to 10 km, significant ballistics, abundant gas and steam emissions, and repose time for single explosions from 4 to 72 hours (see Section 2.2 and Table 4). The reference event of Type 2b is the volcanic eruptive period of Palizzi (Grotta dei Palizzi 2 and 3 formation, gp2a and gp3a member; De Astis et al., 2013b), dominated by the generation of diluted PDCs, minor fall beds and two lava flows. The deposits associated with PDCs are more than 1 meter thick at La Fossa cone base, and indicate transport capacities and runouts that suggest the possibility of reaching and overpass the walls of the current caldera (LFC, Dellino et al., 2011).

Type 3 includes short-lived, explosive sustained eruptions of high intensity. In the 2 ka time window, two events of unequivocally sustained nature occurred within the Palizzi cycle (with a possible younger third event during the Pietre Cotte activity), with different compositions and dispersion axes, but similar size (volumes of 3-4x10^6 m^3 and column heights between 5 and 12 km; Di Traglia, 2011). Even if no PDC deposits linked to the two events were found, the occurrence of possible phenomena of partial collapse of the eruption column cannot be excluded. Although the volumes of the single event may be comparable with the total volumes of a Vulcanian cycle, the accumulations of tephra occurred in a shorter time.

Type 4 includes phreatomagmatic eruptions associated with PDCs able to cross not only the limits of the LFC, but also to affect large areas of the archipelago up to the coast of Sicily (Dellino et al., 2011). Even if this eruption type is not represented in the reference period of 5 ka, we consider its inclusion to provide a reference for extreme (but unlikely) large scale eruptions. The reference eruptive event is TGR (Tuffs of Grotta dei Rossi; De Astis et al., 2013a), which represents the proximal expression of the deposits of the Upper Brown Tuffs (24-8 ka; Lucchi et al., 2008). Although it is not possible to exclude its occurrence in the future, based on the current state of the system the possibility of the occurrence of a Type 4 event appears rather remote, with the past record showing no Type 4 events in the reference period and one eruption in the last 10 ka.

The known eruptions in the last 5 ka of all the types are reported in Table 5, taking into account also the uncertainty in eruption dates. In Table 5 the observed frequencies (the number of observations and the frequency observed for different observation windows) is estimated. A diagram of relative frequencies in the last 2 ka is reported in Fig. 7B. The observed frequencies do not necessarily have to be identified with the probability of occurrence of the different sizes given one eruption. Probability estimates require a deeper analysis of completeness, the possible addition of data from different volcanoes considered analogous, and the definition of a generating process (e.g., Poisson). From these data, it emerges that the most frequent eruptions are of Type 1a, with annual frequencies of the order of 10^{-2}-10^{-3} /year, corresponding to average recurrence times of 0.1-1 ka. Less frequent are Type 0 eruptions, with average recurrence intervals of the order of 1 ka. For the remaining eruptive types (Type 1b, 2a, 2b and Type 3), the range of variability of the frequencies observed is in the order of 10^{-3}-10^{-4}/year, corresponding to recurrence intervals >1 ka. Type 4 eruptions are not considered in the table since no events have been reported in the last 5 ka.

We note that, even in presence of slightly divergent interpretations of the chronostratigraphy and relations among La Fossa and Vulcanello activity (see Section 2.2), the general architecture of the recent, post 5 ka stratigraphy is consistent enough and allows a solid discussion on eruptive styles and mean recurrence rates. Indeed, the different interpretations do not diverge in the type of eruptive style (and thus in the definition of eruption type). They diverge only on the specific dates of single eruptions that, in all cases, remain within the reference period of 5 ka, thus impacting the statistics of inter-event times, but not their overall rates in the reference period. For the observed rates, more critical appears the evaluation of the completeness of the record for all eruption types. We suggest that, for future quantifications of probability of eruption and eruption types, the completeness of the record for all eruption types is carefully evaluated.

The record of the eruptive phenomena for each of the defined eruptive type appears sufficient to characterize the source variability beyond the observed one, at least for ordinary hazard quantifications. This variability can be also carefully benchmarked in the future, for example making use of the records in analogue volcanoes (Tierz et al., 2019, and references therein). This type of comparisons, at the moment largely missing in literature, will enable to better constrain the potential variability of the source to explore the natural variability of the phenomena in hazard quantifications, providing important information especially in the tails of the distributions.

Table 5

Number of observed eruptions for the different types of activity and for the variable time windows. Values of maximum and minimum frequencies for each type are in red and green, respectively. For each type, a reference eruption is defined reporting the eruptive parameters. In brackets, number of multiple events is reported. Question marks refer to a possible discrepancy in dating of some events.

		Time window [a]			
		500	1000	2000	5000
Type 0 Phreatic		Eruption 1727 AD	Eruption 1727 AD, Eruption 1444 AD, Caruggi/ Commenda(?)	Eruption 1727 AD, Eruption 1444 AD, Caruggi/ Commenda	-
	#	1	2/3	3	-
	Freq. [1/year]	2.0×10^{-3}	$2.0/3.0 \times 10^{-3}$	1.5×10^{-3}	-
	Reference eruption	Commenda: Volume > 0.002 km^3			
Type 1a Effusive activity		Pietre Cotte, Vulcanello 3 (2)	Pietre Cotte, Palizzi, Commenda, Vulcanello 3 (2), Vulcanello 1(?), Vulcanello 2(?), Punte Nere(?), Campo Sportivo(?)	Pietre Cotte, Palizzi, Commenda, Vulcanello 3 (2), Vulcanello 2, Vulcanello 1, Punte Nere(?), Campo Sportivo(?)	Vulcanello 3, Punte Nere Pietre Cotte, Palizzi, Campo Sportivo, Commenda, Vulcanello 3 (2), Vulcanello 2, Vulcanello 1, Punte Nere
	#	3	6/9	8/9	9
	Freq. [1/year]	6.0×10^{-3}	$6 / 9 \times 10^{-3}$	$4 / 4.5 \times 10^{-3}$	1.8×10^{-3}
	Reference eruption	Vulcanello 3 lava flow: Volume 0.003 km^3			
Type 1b Strombolian activity		Vulcanello 3	Vulcanello 3, Vulcanello 2(?), Vulcanello 1(?)	Vulcanello 3, Vulcanello 2, Vulcanello 1	Vulcanello 3, Vulcanello 2, Vulcanello 1, Punte Nere
	#	1	1/3	3	4
	Freq. [1/year]	5.0×10^{-3}	$1.0 /3.0 \times 10^{-3}$	1.5×10^{-3}	8.0×10^{-4}
	Reference eruption	Vulcanello Activity: Volume 0.9 km^3			
Type 2a Vulcanian (no PDCs)		1888-90 AD, Pietre Cotte (3)	1888-90 AD, Pietre Cotte (3)	1888-90 AD, Pietre Cotte (3)	1888-90 AD, Pietre Cotte (3)
	#	4	4	4	4
	Freq. [1/year]	8×10^{-3}	4.0×10^{-3}	2.0×10^{-3}	8.0×10^{-4}
	Reference eruption	1888-90 AD eruption: H column 1-10 km Single Explosion 10^4-10^9 kg Duration 30-1095 days Repose time for single explosions 4-72 ore			
Type 2b Vulcanian (with PDCs)			Palizzi (1)	Palizzi (3)	Palizzi (3), Punte Nere, Faraglione
	#	0	1	3	4
	Freq. [1/year]	-	1.0×10^{-3}	1.5×10^{-3}	1.0×10^{-3}
	Reference eruption	Palizzi			
Type 3 Sustained eruptions		Event in Pietre Cotte	Event in Pietre Cotte, Palizzi rhyolitic (?), Palizzi trachitic (?)	Event in Pietre Cotte, Palizzi rhyolitic, Palizzi trachitic	Event in Pietre Cotte, Palizzi rhyolitic, Palizzi trachitic
	#	1	1/3	3	3
	Freq. [1/year]	2.0×10^{-3}	$1.0/3.0 \times 10^{-3}$	1.5×10^{-3}	6.0×10^{-4}
	Reference eruption	PalB/PalD: Mass 0.6-6x10^9 kg Column Height 5-12 km			

3. STEP 2: State-of-the-art on hazard assessments

The main goal of STEP 2 is to provide a review of the state of the art on hazard assessment at Vulcano. The review is extended to all potential hazards, including the non-eruptive ones and independently from their frequency in Vulcano. We considered the guidelines of the International Atomic Energy Agency (IAEA) to classify the volcanic hazards (IAEA, 2012, IAEA, 2016), slightly adapted to the Vulcano case. More specifically, we organized eruptive phenomena in 6 sections (opening of new vents; atmospheric phenomena and shock waves; tephra fallout; volcanic ballistic blocks; pyroclastic density currents, lava flows) and non-eruptive phenomena in 7 sections (hydrothermal and groundwater anomalies; volcanic gases and aerosol; volcanoclastic flows and floods, landslides; tsunami; ground deformation; seismicity).

To systematize the analysis, we defined 5 common criteria for the review, as well as a common reference verbal scale for probabilities and a set of reference locations for the spatial information.

The 5 criteria are: 1) the definition of the phenomenon (and its intensity measures); 2) a discussion about past observations in the reference period (with attention to the most recent observations and those associated with the most intense phenomena); 3) the quantification of the probability of occurrence of the phenomenon in the different states of the volcano (quiescence / unrest / eruption); 4) the analysis of hazard curves or, when not available, of the range of potential intensities in the different areas; 5) the description of potential triggering / cascading events. For each hazard, we discussed also the main limitations of the present state of knowledge.

As in Selva et al. (2019), probability values have been systematized adopting a common verbal scale, modified from IPCC (2013) and ACS-CCS (2015), as reported in Table 6. As reference locations, we considered the areas of Vulcanello, Porto, Lentia in the northern part of the island, and Piano and Gelso in the southern part (Fig. 1C), due to their high exposure and/or for their potential use in case of potential evacuation of the island.

The results of the reviews are discussed in the following subsections and summarized in the comparative Tables 7 and 8.

3.1. Eruptive hazards

3.1.1. Opening of new vents

Vent opening is associated with all magmatic and phreatic eruptions and will occur as the reactivation of previous vents (e.g. La Fossa, Vulcanello) or as the activation of a new structure.

Existing vents associated with a Holocene activity include La Fossa craters, inside the caldera, and Mt. Saraceno, Mt. Lentia, and Vulcanello, along or in the proximity of the caldera rim (Sections 2.1 and 2.2; Figs. 1, 2 and 3). However, during the last 5 ka, activity was concentrated at La Fossa volcano and Vulcanello. The most recent event of reactivation was associated with the 1888-90 AD eruption of La Fossa volcano and the most recent vent opening was associated with Vulcanello 3 in 1600 AD (Fusillo et al., 2015). During this time, La Fossa and Vulcanello have also erupted simultaneously.

Currently, no probabilistic or structural study of possible vent opening exists in the literature. Given that most of the activity within the reference period concentrated in La Fossa and Vulcanello vents, future eruptions are expected to occur mostly around these vents. However, vent opening is possible also in newly formed vents, as already happened in the past.

A NS and NW-SE preferential axis for vent opening associated with magmatic eruptions (Eruption Types ≥ 1, hereinafter indicated with Type 1+) has been hypothesized by several authors (e.g., Ruch et al., 2016), based upon the lineament of La Fossa crater, Vulcanello and other eruptive centers. These local structures seem to have a stronger impact with respect to regional tectonics structures (Fig. 2A; see discussion in Section 2.1). All the activity in the reference period, as well as the older activity in the last 10 ka, is concentrated within the LFC (Section 2.2) and thus this may represent an outer limit for the present volcanic system. It is important to note that the LFC caldera is mostly subaerial, with only its NE part at present under the sea (e.g., Casalbore et al., 2018).

Vent opening associated with phreatic eruptions (Eruption Type 0) is thought to be related to the location of the deep hydrothermal system, mostly close to Vulcano Porto and Baia Levante areas that are highly altered (Section 2.5).

From a multi-hazard perspective, vent opening is the starting phase of all eruptions; it may generate landslides and tsunami, and it is usually accompanied by ground deformations and earthquakes (as described also in some chronicles, Section 2.2.2). Generally speaking, it has been suggested in literature that vent opening may be triggered by pressurization/depressurization of the magmatic system due to phreatic activity (as probably occurred in 1888 AD, see Sections 2.2.2) and/or gravitational collapses, as well as favoured by large regional earthquakes.

The lack of quantifications of the spatial probability of vent opening largely limits the hazard assessment of eruptive phenomena, especially of those that have a strong topographic control (e.g. PDCs and lava flows). Therefore, a quantitative analysis to quantify the spatial probability of vent opening will be of primary importance for future hazard quantifications.

3.1.2. Atmospheric phenomena

The main atmospheric phenomenon associated with eruptions on Vulcano are shock waves, high-energy acoustic waves associated with loud detonations. Detonations associated with La Fossa volcano activity have been heard as far as the north coast of Sicily during the XVII and XIX centuries, as reported by historic chronicles. During the 1888-90 AD eruptions, shock waves broke glass windows on Lipari, up to 40 km from the vent (Mercalli and Silvestri, 1891); loud detonations have also been associated with lightning inside the eruptive plumes.

Shock waves and smaller-scale atmospheric phenomena (such as lightning) are generally very likely during eruptive phases. More specifically, they are rare for Type 0 and 1 eruptions, possible for Types 3 and 4 and almost certain during Vulcanian cycles (Type 2). They are usually triggered by the explosive phases of eruptions, while smaller atmospheric phenomena may be induced by phenomena associated with the dynamics of the eruptive columns. At present, no specific studies quantify the hazard associated with shockwaves at Vulcano.

3.1.3. Tephra fallout

Tephra sedimentation includes fallout of ash (< 2 mm), lapilli (2-64 mm), and bombs and blocks (>64 mm). In particular, ash an lapilli mostly fall from the convective plume and the horizontally-spreading cloud, while bombs and blocks are mostly ejected from the eruptive vent and follow ballistic trajectories.

For the last Vulcanian cycle (1888-90 AD, Type 2a), Di Traglia (2011) reports an accumulation of 100-500 kg/m² (i.e. 10-50 cm thickness) in the Porto area and < 300 kg/m² (i.e. < 30 cm thickness)

Table 6
Common verbal scale to express probability values.

Verbal scale	Probability ranges
Certain	Probability = 1
Almost certain / Very frequent	0.9 ≤ Probability < 1
Likely / Frequent	0.5 ≤ Probability < 0.9
Possible	0.1 ≤ Probability < 0.5
Rare	0.01 ≤ Probability < 0.1
Very rare	Probability < 0.01

Table 7

Synthetic state-of-the-art regarding hazard quantifications, reporting in rows the different hazards and in columns the 5 criteria adopted to characterize their potential impact.

Phenomenon	Past observations	Probability in phases	Intensity & hazard curves	Linked phenomena
Opening of new vents Section 3.1.1 Intensity Measure: Occurrence (YES/NO)	**Last observations:** Reactivation: La Fossa, 1888-90 AD Formation of a new crater: Vulcanello 3 (1600)	**Rest/Unrest:** Not applicable **Eruption:** Certain For reactivation: Possible / Likely For formation of new crater: Rare / Possible	Quantitative studies are not available. **Spatial distribution:** [qualitative, based on expert opinion] The most probable area seems to be included within (or close to) La Fossa crater and Vulcanello, and in general along the N-S / NE-SW lineament within the La Fossa caldera.	**Trigger:** - Earthquakes, - Large landslides and Debris avalanches **Cascade:** - All eruptive phenomena - Large deformations - Tsunami (if offshore) - Landslides and debris avalanches
Atmosphere phenomena and Shock waves Section 3.1.2 Intensity Measure: Not defined	**Last observations:** During 1888-1890 AD: - shaking of glasses in houses of Lipari, - volcanic roars hearable up to 40 km - detonations produced by electric shocks in the eruptive plume. **Largest observation:** During the eruptive activity of XVIII and XIX centuries, volcanic roars hearable up to the Northern coast of Sicily.	**Rest/Unrest:** Not applicable **Eruption:** Types 0 and 1: Very rare; Type 2: Very likely Types 3 and 4: possible	Quantitative studies are not available	**Trigger:** - new vents
Tephra fallout Section 3.1.3 Intensity Measure: Loading at ground (kg/m²)	**Last observation:** 1888-1890 AD eruption, with 100-500 kg/m² In Vulcano Porto, <300 kg/m² for Piano, with maxima in the island up to 1000 kg/m² around the crater **Largest observations:** Eruptions Palizzi B and D (VEI 2), with 20-1200 kg/m² in Porto, <800 kg/m² in Piano, with maxima in the island up to 2000 kg/m² around the crater	**Rest/Unrest:** Not applicable **Eruption:** Certain for all Types (0-4)	**For eruptions of Type 0 - 1:** Quantitative studies are not available **For eruption of Type 2:** [probabilistic hazard, vent in La Fossa] Porto: 1-300 kg/m² (10% probability; location: Medical center) Piano: 1-600 kg/m² (10% probability; location: Scuola; 100% of accumulating 10 kg/m² after 2 months, 80% of accumulating 100 kg/m² after 9 months, and 40% of accumulating 300 kg/m² after 20 months. Maxima in island: 50% probability for accumulating >300 kg/m² in the largest part of the southern part of the island (Piano), and 100-200 kg/m² in the northern part and northwestern part of the islands (Lentia, Porto and Vulcanello) **For eruption of Type 3:** [probabilistic hazard, vent in La Fossa] Porto: 10% probability for accumulating 50-300 kg/m² (VEI 2-3), location: centro medico Piano: 10% probability of accumulating 100-1000 kg/m², location Scuola Maxima in island: for VEI 2, 50% probability of accumulating > 100 kg/m² in the whole island; for VEI 3 : 50% probability of accumulating >300 kg/m² in SE part of the island (northern part of Piano), between 100-300 kg/m² in the	**Trigger:** - New vents **Cascade:** - Ballistics - acid rains - gas - lahar (in case of rain after significant accumulation) - possible PDC in case of column collapse - shock waves associated to Type 2 (Vulcanian) eruptions - atmospheric phenomena (lightening)

Table 7 (*continued*)

Phenomenon	Past observations	Probability in phases	Intensity & hazard curves	Linked phenomena
			southern part of Piano, and <50 kg/m² in the area of Porto, Lentia and Vulcanello Note: All these probabilities should be increased by 3-10% in case of 20-50 mm of rain (medium and large rains). The vent is assumed at La Fossa.	
Ballistics Section 3.1.4 Intensity Measure: Impact Energy (J)	**Last observation:** 1888-1890 AD eruption: The maxima observations are in the range $0.06-4 \times 10^6$ J for ballistics observed on the South rim of the La Fossa caldera. Observations in Porto are not available, since rocks have been removed, but are likely for symmetry.	**Rest/Unrest:** Not applicable. **Eruption:** They may occur in all types; Type 0: certain Type 1: almost certain Types 2,3,4: certain	**For eruptions of Type 0 - 1:** Quantitative studies are not available. **For eruption of Type 2:** [probabilistic hazard, vent in La Fossa] Porto: 10^4-10^7 J Piano: 10^4-10^7 J Maxima in island: 10^4-10^7 J	**Trigger:** - new vents **Cascade:** - shock waves - tephra - gas - wild fires due to hot blocks fall
Pyroclastic flows and Pyroclastic Density Currents (PDCs) Section 3.1.5 Intensity Measures: Dynamic Pressure (kPa) Concentration	**Last observation:** Small PDC associated to the 1888-90 AD eruption (testified, but deposits not preserved) **Largest observations:** For Type 2b, Palizzi cycle: Porto: Dynamic Pressure 1.5 kPa, concentration 1.5 x 10⁻³ (modelled 1-2 x 10⁻³) Piano: Dynamic Pressure 0.5-1.5 kP, concentrations 1-2 x 10⁻³ Maxima in island: Dynamic Pressure 5 kPa, concentrations 2-3 x 10⁻³ For Type 4, TGR (Upper Brown Tuff) eruption: Porto: not observed (modelled Dynamic pressure 1-4 kPa; concentration 1-2 x 10⁻³); Piano: Dynamic pressure 5 kPa (modelled 1-2 kPa; concentration1,5-2,5 x 10⁻³ (modelled 1-2 x 10⁻³) Maxima in island: Dynamic pressure 5 kPa (modelled 1-4 kPa); Concentration 3 x 10⁻³ (modelled 2-3 x 10⁻³)	**Rest/Unrest:** Not applicable. **Eruption:** Type 0: possible Type 1: very rarely Types 2 and 3: frequent Types 4: almost certain	Quantitative studies are not available. Based on expert opinion, since observations cover a very large range, it can be through that phenomena with larger intensity are rather unlikely.	**Trigger:** - New vents **Cascade:** - Lahars (rain after pyroclastic deposit) - Tsunami (in case of dense pyroclastic flows reaching the sea) - wild fire
Lava flows Section 3.1.6 Intensity Measure: Invasion (YES/NO)	**Last observation:** Pietre Cotte eruption (1739 AD)	**Rest/Unrest:** Not applicable. **Eruption:** Type 1: almost certain Type 2: possible within the cycle Types 3 and 4: rare	Quantitative studies are not available.	**Trigger:** - New vent **Cascade:** - Small slides on lava flow tip and side, causing small PDC and tsunami - wild fire
Hydrothermal activity and anomalies in aquifers Section 3.2.1 - Development and expansion of the fields of fumaroles, release of toxic hydrothermal	**Last observation:**	**Rest:**	Quantitative hazard not available.	**Trigger:**

Table 7 (*continued*)

Phenomenon	Past observations	Probability in phases	Intensity & hazard curves	Linked phenomena
gases, acidification and chemical contamination of phreatic groundwater	Extension of the crater fumarole fields during 1987-1993 unrest (Bukumirovic et al., 1997). **Largest observation:** Development of fumarole degassing field at the foot of the La Fossa cone (Sicardi, 1940).	Possible, if triggered by other phenomena (seismicity, gravitational phenomena) **Unrest:** Frequent **Eruption** Certain in <u>all types</u>	**Spatial distribution:** [qualitative, based on past observations] Porto: certain during all eruption types, frequent during unrest, with preferential areas located on NW and NE flanks of the La Fossa cone, as well as in Baia di Levante. Piano: very rare in unrest and during eruption Types 0 and 1, rare in eruption Types 2, 3 and 4. Quantitative hazard not available.	- Magmatic degassing, seismicity, gravitational phenomena **Cascade:** - Phreatic eruption, landslides, gas hazard
- Vaporization of aquifers, hydrothermal explosions and geyser.	Never reported	Possible, if triggered by other phenomena (seismicity, gravitational phenomena) **Unrest:** Possible **Eruptions:** Certain for <u>all types</u>	**Spatial distribution:** [qualitative, based on past observations] Porto: certain during all eruption types, possible during unrest, with preferential areas located on NE flank of the La Fossa cone and in Baia di Levante. Piano: very rare in unrest and Eruption Types 0 and 1, rare in Eruption Types 2, 3 and 4.	**Trigger:** - Magmatic degassing, seismicity, gravitational phenomena **Cascade:** - Phreatic eruption, landslides, gas hazard
Volcanic gases Section 3.2.2 Intensity measures: CO_2 concentration in air ($[CO_2]$ Vol. %) H_2S concentration in air ($[H_2S]$ ppm) SO_2 concentration in air ($[SO_2]$ ppm)	**Last observation:** $[CO_2]$ Vol. %: <u>Porto</u>: 2; <u>Piano</u>: -; <u>La Fossa</u>: <0.1; <u>Maxima in island</u>: 2 $[H_2S]$ ppm: <u>Porto</u>: 270; <u>Piano</u>: -; <u>La Fossa</u>: 179; <u>Maxima in island</u>: 270. $[SO_2]$ ppm: <u>Porto</u>: 0.05; <u>Piano</u>: 0.05; <u>La Fossa</u>: 179; <u>Maxima in island</u>: 179. **Largest observation:** $[CO_2]$ Vol. %: <u>Porto</u>: 100; <u>Piano</u>: -; <u>La Fossa</u>:15; <u>Maxima in island</u>: 100. $[H_2S]$ ppm: <u>Porto</u>: 4500; <u>Piano</u>: -; <u>La Fossa</u>: 450; <u>Maxima in island</u>: 4500. $[SO_2]$ ppm: <u>Porto</u>: 0.05; <u>Piano</u>: 0.05; <u>La Fossa</u>: 250; <u>Maxima in island</u>: 250. These data refer to discrete observations, averaged or of short duration (max. 48h) made during quiescence phases and not necessarily in the locations with highest concentrations	Certain in <u>all phases</u> Significant gradual increase in case of magmatic input, increase of seismicity, and for meteorological factors (e.g., atmospheric pressure and precipitations). Significant more rapid (seconds to minutes) increase may be triggered by phreatic explosions, phreatic eruptions, and gravitational phenomena.	Quantitative hazard not available **Rest:** [qualitative, maxima from observations and some simulation] $[CO_2]$ Vol. %: <u>Porto</u>: 0-100; <u>Piano</u>: no data; <u>Maxima in island</u>: 0-100 $[H_2S]$ ppm: <u>Porto</u>: 0-270 ppm (up to hundreds /thousands ppm); <u>Piano</u>: no data; <u>Maxima in island</u>: 0-270 ppm (up to hundreds of ppm) $[SO_2]$ ppm: <u>Porto</u>: 0-30 ppm (up to hundreds /thousands ppm); <u>Piano</u>: no data; <u>Maxima in island</u>: 0-179 ppm (up to hundreds /thousands ppm) **Unrest / Eruption:** Not accessible	**Trigger:** - Earthquakes - Magmatic fluids release - Magmatic movements - Meteorological factors - New vents - Phreatic explosions and eruptions - Gravitational phenomena **Cascade:** - Acid rain (SO_2)
Volcanic debris flows, lahars and floods Section 3.2.3 Intensity measure: Invasion (YES/NO)	**Last observation:** 2015 **Largest observation:** Invaded down to Vulcano Porto (Porto Ponente) with a <u>maximum</u> thickness of approximately 1 m	**Rest and Unrest:** Frequent **Eruption:** Almost certain, in presence of tephra deposits	Quantitative hazard not available **Spatial distribution:** [qualitative based on observations] Invasion: La Fossa flanks, including Palizzi	**Trigger:** - Heavy rain - Eruption with PDCs or tephra fall (new material) - Debris avalanche (new material)

Table 7 (*continued*)

Phenomenon	Past observations	Probability in phases	Intensity & hazard curves	Linked phenomena
Volume (Vol) (m³) Invasion Area (km²)			valley, the area of Porto di Levante, Porto di Ponente and Vulcano Porto.	**Cascade:** - small tsunami
Landslides Section 3.2.4				
Debris avalanches and sector collapses	**Last/Largest observation:** post-100 ka, in the SW area of the island (Casa Grotta dell'Abate).	**Rest/Unrest/Eruption:** Very rare	Quantitative hazard not available.	**Trigger:** - Earthquakes - Eruptions - Large deformations - Alteration of the edifice - Significant increase of degassing
Intensity Measure: Volume (V) (km/h) Invasion Area (km²)	Events within the reference period are not known.		**Spatial distribution:** [qualitative, based on expert opinion] Costal area or close to sub-vertical slopes	**Cascade:** - Tsunami - Eruptions - Pyroclastic flows (rain after avalanche)
Rockfalls	**Last observations:** 31/08/2009 landslide, at Spiaggia dell'Asino (Gelso) with unknown intensity 16/08/2010 landslide at Spiaggia di Vulcanello with unknown intensity **Largest observation:** 20 April 1988, landslide along the NE flank of the La Fossa cone $V = \sim 2 \times 10^5$ m³.	**Rest/Unrest** Possible **Eruption** Types 0.1: possible Types 2.3.4: likely	Quantitative hazard not available. Spatial distribution (of the impact) is not available. Volumes: [expert qualitative evaluation, based on known sources in literature] From small volumes (0.8×10^6 m³) up to larger volumes are possible. The smaller volumes are more likely in quiescence periods, while larger volumes in unrest period.	**Trigger:** - Earthquakes - Eruptions - Large deformations - Significant increase of degassing or groundwater variations - erosion or argillifications **Cascade:** - Tsunami - Pyroclastic flows (rain after avalanche)
Intensity Measure: - Volume of the source [m³] - Invasion				
Tsunami Section 3.2.5	**Last and largest observation:** 20/04/1988: Porto: 1 m Piano: 0 Maxima in island: 1 m	**Rest:** Rare **Unrest:** Rare / possible **Eruption:** Rare / possible	Quantitative hazard not available. Detailed simulations of 1988 event are available in Tinti et al. (1999). **Rest:** Not evaluable; **Unrest/Eruption:** [qualitative, based on known landslide sources and expert opinion] Based on potential sources (landslides and eruptions), the area of Vulcano Porto seems to be the one with relatively largest tsunami. As superior limits for the intensity, it can be speculated that the maxima may be localized in the Porto area, with moderate intensity (ca 1 m) during quiescence, and up to 10 m during unrest (since larger landslides are considered possible).	**Trigger:** - Debris avalanche and landslides - dense pyroclastic flows and PDCs - New vent - Large shallow earthquakes
Intensity Measure: Wave height close to coastline [m]				
Ground deformations Section 3.2.6	**Last observation:** Period 1990-1996: 5-6 cm at La Fossa cone	**Unrest:** Very frequent	**Unrest:** [qualitative, based on past observations] From several cm up to tens of cm, localized in the	**Trigger:** - aquifers overpressure

25

Table 7 (*continued*)

Phenomenon	Past observations	Probability in phases	Intensity & hazard curves	Linked phenomena
Intensity Measures: Horizontal and Vertical displacements [cm]	**Largest observation:** Period 1987-1993: ca 10-15 cm along the N rim of the La Fossa cone	**Eruption:** Very frequent for all types	La Fossa cone **Eruption:** [qualitative, based on analogues] No data for Vulcano. From global data, the largest deformations occur in case of eruptions of Type 1 and 3.	- dykes - new vent **Cascade:** - Landslides and debris avalanches - Fractures/eruptions
Seismicity Section 3.2.7 Intensity Measures: PGA [g] Macroseismic intensity (MCS)	**Last observation:** Regional earthquake in 16/08/2016, with PGA = 0.05g at Piano **Largest observation:** MCS 6 at Porto and 7-8 at Piano, 15/04/1978 (regional Mw = 5.5 event)	**Rest:** Certain, but with low energies **Unrest/Eruption:** Certain	**Rest/unrest:** [regional PSHA (MPS04)] PGA of 0.175 - 0.200 g for 10% in 50 years hazard level. **Eruption:** Quantitative studies are not available	**Trigger:** - Magmatic movements and dykes **Cascade:** - Eruptions - Phreatic explosions - Landslides

in the Piano area. Mercalli and Silvestri (1891) also report sedimentation in the southern part of the Italian peninsula (Calabria region) and in the northern coast of Sicily (between Palermo on the west and Catania/Siracusa on the east). For sustained eruptions (Type 3, i.e. Palizzi B and D), Di Traglia (2011) reported an accumulation of 20-1200 kg/m^2 (i.e. 3-150 cm thickness) in the Porto area, while in the Piano area values < 800 kg/m^2 (i.e. < 100 cm thickness) can be extrapolated based on the compiled isopach maps (as no outcrops were found in the area). Palizzi B and D are included within the Palizzi 2 sequence of Dellino et al. (2011) and within the Grotta dei Palizzi formation of De Astis et al. (2013b).

So far, only tephra fallout associated with Vulcanian eruptions of Type 2a (based on the 1888-90 AD eruption) and sustained eruptions (Type 3: VEI 2 and 3) as well as ballistic fallout associated with Vulcanian eruptions (Type 2a) have been modelled (Biass et al., 2016a, 2016b; Fig. 8). The associated hazard assessments have only been considered for a vent location at La Fossa.

For the Type 2a scenario, plume height of 1-10 km, individual explosions with masses of 10^4-10^9 kg, durations of 30-1095 days and repose intervals of 4-72 hours have been considered ("V-LLERS: *Eruption Range Scenario of Long-Lasting Vulcanian eruptions*" in Biass et al., 2016a). In the Type 3 scenario (VEI 2, based on Palizzi B and D eruptions), plume heights of 5-12 km and masses of 0.6-6 x 10^9 kg have been considered ("*ERS scenario: Eruption Range Scenario VEI 2*" in Biass et al., 2016a). In the Type 3 scenario (VEI 3), plume heights of 8-17 km and masses of 6-60 x 10^9 kg have been considered ("*ERS scenario: Eruption Range Scenario VEI 3*" in Biass et al., 2016a). Finally, a Type 3 scenario specific for the Palizzi B and D eruptions has also been analysed, with plume heights of 7-8 km and masses of 2.1-2.4 x 10^9 kg ("*OES scenario: One Eruption Scenario*" in Biass et al., 2016a).

Given the direction of prevailing winds (Biass et al., 2016a), the south and southeast of the island are the most impacted by all scenarios. Conditional hazard curves have been compiled for two reference localities (school in Piano and medical center in Porto, Fig. 8A) for all scenarios. Cumulative hazard curves for the same locations have also been compiled to assess the variation of tephra accumulation in time (Fig. 8B). Maps that show the probability of reaching 10 kg/m^2 (damage to vegetation and traffic disruption), 100 kg/m^2 (reference for collapse of weak roofs) and 300 kg/m^2 (collapse of strong roofs) have also been compiled together with probabilistic isomass maps for a probability of 50% for 3 scenarios (Eruption Type 2a, Type 3 VEI 2 and Type 3 VEI 3; Fig. 8C). These probabilities are conditional to the scenario considered. The effect of increase of density due to infiltration of rain water within tephra deposits has also been evaluated, showing an increase of probability between 3-10% for rain between 20-50 mm (i.e. medium and torrential rains).

In detail, Piano has a probability of 35-60% of reaching a 300 kg/m^2 accumulation for Type 3 VEI 2 and 3 eruptions. Probabilistic isomass maps of 50% probability show accumulation between 100-300 kg/m^2 at Piano for both Type 2a and Type 3 VEI 3 eruptions, even though the accumulation associated with a Type 2a eruption is more widespread. As an example, hazard curves show how the probability of reaching 200 kg/m^2 in Porto is 50% for a Type 2a eruption and 20% for a Type 3 VEI 3 eruption. To sum up, Type 2a eruptions have a 10% probability of accumulating 1-300 kg/m^2 in Porto and 1-600 kg/m^2 in Piano. There is a 100% probability of accumulating 10 kg/m^2 of tephra at the school in Piano after 2 months, 80% probability of accumulating 100 kg/m^2 after 9 months and 40% probability of accumulating 300 kg/m^2 after 20 months. For an eruption Type 3 VEI 3, there is a 10% probability of reaching 50-300 kg/m^2 in Porto and 100-1000 kg/m^2 in Piano.

From a multi-hazard perspective, tephra fallout can be associated with other primary and secondary eruptive phenomena such as acid rains, gas emissions (in particular SO_2), ash remobilization, lahars, PDCs, lightning and shock waves mostly associated with Vulcanian explosions. Specifically, tephra fall is associated with any vent opening and this opening may trigger various potential cascading phenomena,

Table 8
Extraction of the information about the probability of the different hazardous phenomena from Table 7. Values are expressed in terms of the common verbal scale of Table 6.

	Quiescence	Unrest	Eruption Type 0 Phreatic	Eruption Type 1 Strombolian and effusive	Eruption Type 2 Vulcanian	Eruption Type 3 Sustained	Eruption Type 4 Phreato-magmatic
Opening of new vents	-	-	Certain	Certain	Certain	Certain	Certain
Atmospheric phenomena and shock waves	-	-	Very rare	Very rare	Almost certain	Possible	Possible
Tephra fallout	-	-	Certain	Certain	Certain	Certain	Certain
Ballistics	-	-	Certain	Almost certain	Certain	Certain	Certain
Pyroclastic density currents (PDCs)	-	-	Possible	Very rare	Likely	Likely	Almost certain
Lava flows	-	-	-	Almost certain	Possible	Rare	Rare
Hydrothermal activity and anomalies in aquifers	Likely	Likely	Certain	Certain	Certain	Certain	Certain
Volcanic gases	Certain	Certain	Certain	Certain	Certain	Certain	Certain
Volcanoclastic debris flows, lahars and floods	Likely	Likely	Almost certain	Almost certain	Almost certain	Almost certain	Almost certain
Landslides (Debris avalanches and sector collapses)	Very rare	Very rare	Very rare	Very rare	Very rare	Very rare	Very rare
Landslides (rockfalls)	Possible	Possible	Possible	Possible	Likely	Likely	Likely
Tsunami	Rare	Rare	Rare	Rare	Rare	Rare	Rare
Ground deformations	Rare	Almost certain	Likely	Likely	Likely	Likely	Likely
Seismicity	Certain	Certain	Certain	Certain	Certain	Certain	Certain

such as lahars and ash remobilisation by wind (co-eruptive, but also long after eruptions), PDCs (for collapse of the column), and atmospheric phenomena (e.g. lightning). Secondary hazards on Vulcano have only been studied with respect to lahars (e.g., Ferrucci et al., 2005; Baumann et al., 2019).

The main limitations of the available tephra fallout hazard quantifications are related to the fact that not all eruptions types potentially producing tephra have been studied and, that simulations are limited to eruptions from La Fossa crater (Section 3.1.1).

3.1.4. Ballistic blocks and bombs

Sedimentation of tephra from eruptive plumes can also be associated with ejection of ballistic bombs and blocks for all eruptive activity considered (Type 0 - phreatic, Type 2 - Vulcanian and Type 3 - sustained).

Dellino et al. (2011) report the occurrence of ballistic blocks from La Fossa associated with an impact energy between 10^5 and 10^6 J at a distance of < 300 m from vent and of 1.4×10^5 J up to Vulcanello in the north of the island and down to the southern caldera rim in the southern part of the island (at a distance up to 2.5 km; Fig. 9A). These observations are related to the successions of Punte Nere (Type 1b), Caruggi (Type 0) and Cratere Attuale that includes the 1888-90 AD Vulcanian eruption. Biass et al. (2016b) report impact energies associated with the 1888-90 AD Vulcanian eruption between 0.06-4×10^6 J at distances between 1000-1500 m from the vent along the southern caldera rim. Historical chronicles (Mongitore, 1743) also report large blocks (reported of about 8 kg, see Table 4) along the northern coast of Sicily (at Brolo, 25 km from Vulcano) associated with the 1739 eruption; however, considering the large distance from the vent, we hypothesize that these blocks did not follow ballistic trajectories. Specific observations of not remobilized ballistic blocks are rare, with the most

reliable being those on the southern caldera rim, which could explain the discrepancy between Dellino et al. (2011) and Biass et al. (2016b) observations. The main characteristics of these blocks are described in Table 9.

Biass et al. (2016b) have compiled probabilistic maps based on the 1888-90 AD Vulcanian eruption (Fig. 9B). As an example, probabilistic isomass maps of 90% of occurrence show that most of the island would be affected by impact energy > 60 J (associated with the perforation of weak tile roofs) with impact energies up to 8000 J (associated with perforation of strong armoured roofs) in the areas of Porto, Piano, Lentia and Vulcanello.

Due to the elevated temperatures, secondary phenomena associated with the sedimentation of ballistic bombs and blocks include wildfires. Ballistics may also be accompanied by tephra fallout, shockwaves, and significant gas emissions. Specific studies for Vulcano on these issues are not available.

As in the case of tephra fallout, the main limitations of the available hazard models are related to the fact that not all eruptions types have been studied and that the analyses are limited to eruption from La Fossa crater, even though similar activity at different vents cannot be excluded.

3.1.5. Pyroclastic Density Currents (PDCs)

PDCs are mixtures of pyroclastic particles and gas that move across the landscape under the effect of gravity. They macroscopically behave as dense, multiphase gravity currents (flowing pyroclastic mixtures of particles and gas) immersed in a less dense, almost isotropic fluid (the atmosphere; Sulpizio et al., 2014).l

The main PDCs observed on Vulcano are associated with the Palizzi eruption (Vulcanian eruption Type 2b; Dellino et al., 2011) and those associated with the Brown Tuff (TGR, Type 4; Dellino et al., 2011;
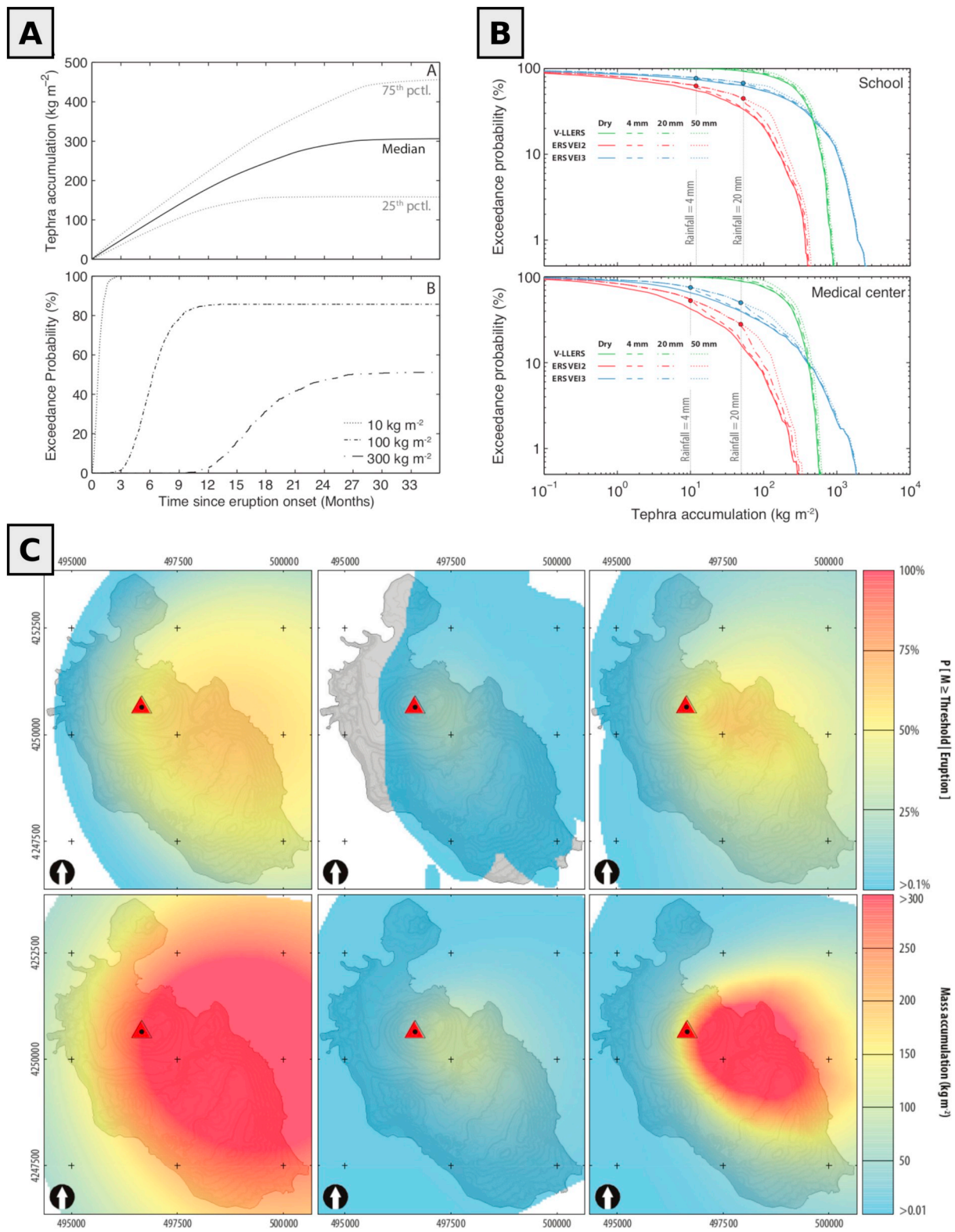
Fig. 8. Tephra hazard at Vulcano: A) Cumulative curves computed for the School of Piano in case of Eruption Type 2a: (above) variation in time through median, 25th and 75th percentiles, (below) variations in probability to reach a given accumulation (10, 100, and 300 kg/m²), from Biass et al. (2016b). B) Effect of rain: hazard curves for School at Piano and Medical Center in Porto for Eruption Type 2a (V-ELLERS) and 2 scenarios of Eruption Type 3 (ERS VEI2 and VEI3) considering light, moderate and torrential rains (corresponding to 4, 20 and 50 mm), from Biass et al. (2016b). C) probability maps to reach 300 kg/m² (top row) and conditional hazard maps (or probabilistic isomass) (bottom row), considering a probability threshold of 50% for 3 scenarios (Eruption Type 2a, Type 3 - VEI2; Type 3 - VEI 3), from Biass et al. (2016b).
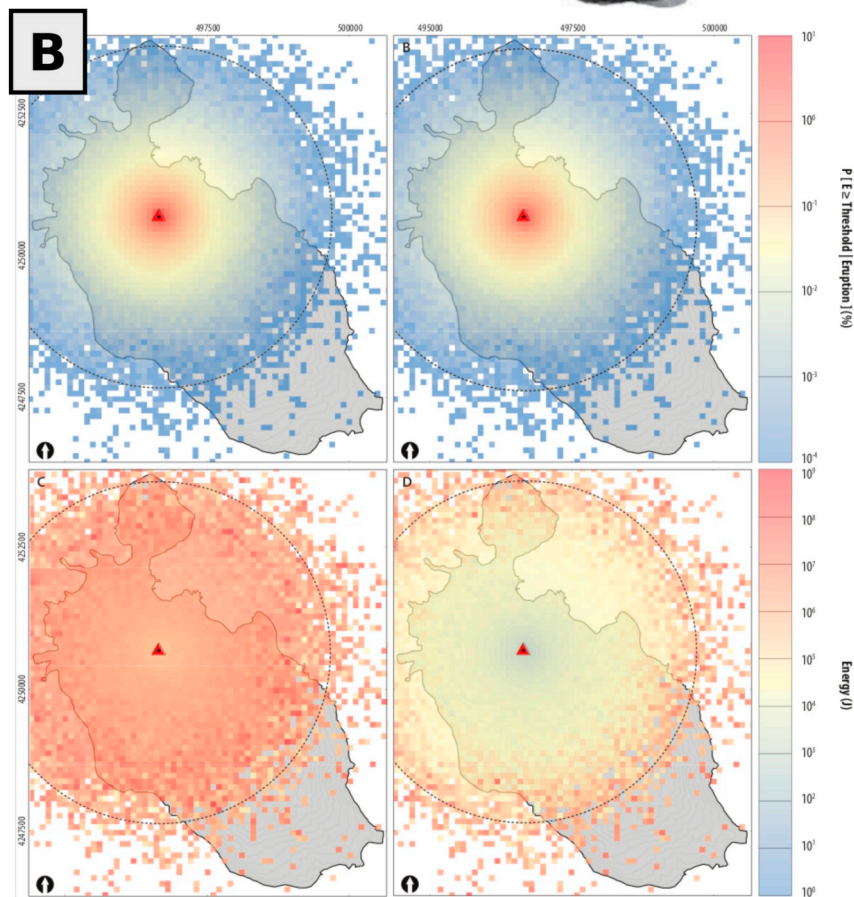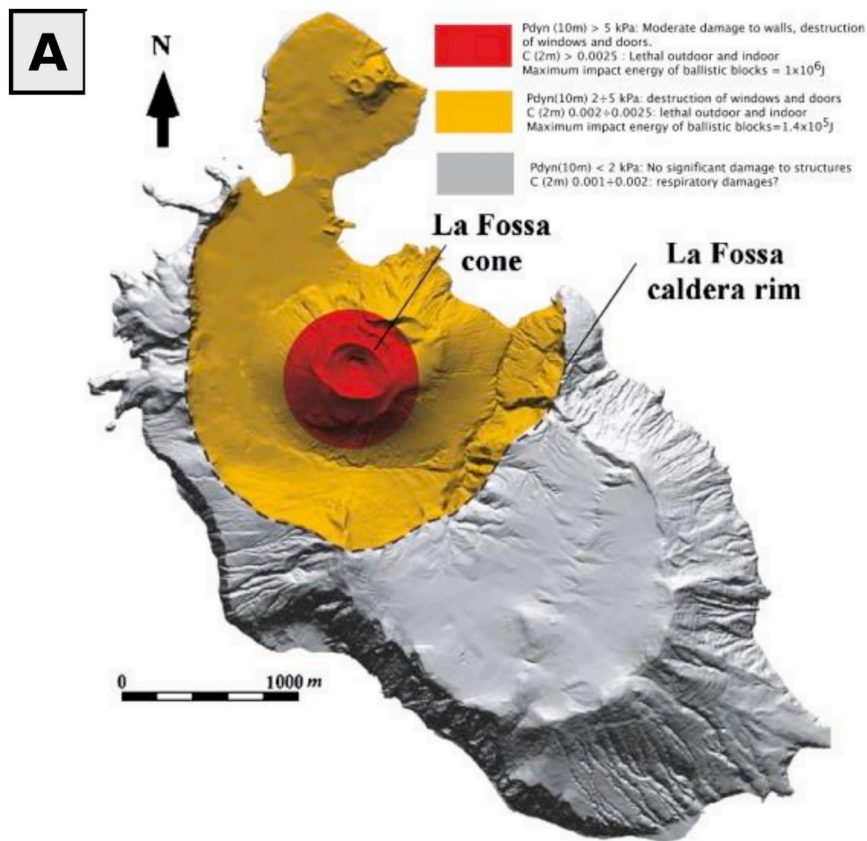
Fig. 9. Ballistics hazard at Vulcano: A) Map of distribution of ballistics based on field observations. Red zone: energy of impact 10^6 J; yellow zone: energy of impact 1.4×10^5 J (from Dellino et al., 2011). B) Map of distribution of impact energy for an occurrence probability of 90% (Biass et al., 2016c). The dashed circle line shows the credibility limit for the model based on the distance from the vent.

Table 9

Characteristics of ballistic blocks observed by Biass et al. (2016b), related to the last Vulcanian eruption (1888-90 AD) in SE rim of LFC (La Fossa Caldera).

Distance from eruptive vent (m)	Diameter (cm)	Density (kg/m3)	Velocity of impact (m/s)	Energy of impact (J)
1560	25	1600	350	8.02E + 05
960	68	2300	150	4.26E + 06
960	31	2300	150	4.04E + 05
960	24	800	150	6.51E + 04
960	27	1600	150	1.86E + 05
1000	56	1600	150	1.66E + 06

Fig. 10A). Dynamic pressure of the PDCs associated with the Palizzi eruption is 0.5-1.5 kPa in Piano with a particle concentration of 1-2 x 10^{-3} and 1.5 kPa in Porto with a particle concentration of 1.5 x 10^{-3}, as simulated by Doronzo et al. (2016; Fig. 10B and C). The maximum value of dynamic pressure was derived for the Brown Tuff (TGR) with a value of 5 kPa in Piano and 1.5-2.5 x 10^{-3} particle concentration (TGR does not crop out in Porto). This value of the dynamic pressure is derived from the integrated average of the first ten meters of the PDC in downcurrent direction (Dellino et al., 2011). Most PDCs at Vulcano are dilute, even though a few examples of dense PDCs have been found in the stratigraphic record (e.g., Caruggi, 1000-1200 AD or VIII century AD, see discussion in Section 2.2).

PDCs are almost certain for Eruption Type 4, frequent for Eruption Types 2 and 3, possible for Type 0, and very rare for Type 1 eruptions. Probabilistic hazard quantifications are not available for PDCs at Vulcano. All the available scenarios have the La Fossa crater as the vent. Given that PDCs are strongly controlled by the topography, a part for source parameter variability, future hazard quantifications should account also for the potential of vent opening also in other positions of the La Fossa caldera, to better cover the potential natural variability. In addition, PDCs can be quite directional, even without topography, and position of the vent within the crater will control the runout direction.

PDCs can trigger wildfires, provide material for the generation of lahars and ash remobilisation by wind and may produce small tsunami if they reach the sea.

3.1.6. Lava flows

No direct observations of lava flows on Vulcano exist (Barbano et al., 2017), even though many lava flows occur within the stratigraphy of both La Fossa volcano and Vulcanello (Section 2.2). The most recent lava flow is that of Pietre Cotte that has been attributed to the eruption of 1739 AD, which is testified in historical chronicles but not directly observed (De Fiore, 1922; Barbano et al., 2017). Other lava flows include those inside Palizzi 2 succession and Punte Nere (Dellino et al., 2011). The only lava flows that went beyond the base of La Fossa cone are those of Campo Sportivo and Punte Nere (see Fig. 1C).

Lava flows are related to Type 1 eruptions (by definition), for which they are almost certain. Effusive phases are located both within Vulcanian cycles (Type 2, essentially at LFC) and during Strombolian construction phases (mainly Vulcanello). Therefore, they should be considered as possible during Type 2 events, while they are rare for Type 3 and 4 eruptions. Lava flows are not possible for Type 0 eruptions since they can be generated only by newly erupted magma.

No probabilistic studies of lava inundation in Vulcano exist in the literature. Magmas have been associated with medium-high viscosity resulting in short lava-flow runouts. With the exception of the pillow lava field associated with Vulcanello 2 (whose volume is estimated at 0.2 km^3), the volumes of the lavas are small. Even if no observational

data are available at LFC, low effusion rates ($<< 10$ m^3/s) can be assumed due to the high viscosity and the low mobility of lava bodies.

Dedicated multi-hazard studies including lava flows on Vulcano do not exist. Generally speaking, lava flows could trigger small PDCs due to frontal collapse and landslides, as well as cause wild-fires and very small tsunami.

3.2. Non-eruptive hazards

3.2.1. Hydrothermal activity and anomalies in aquifers

Hydrothermal systems can give rise to a wide range of dangerous phenomena (e.g. explosions, geysers, mud volcanism, contamination of water, steam flows), all linked to the presence of the hydrothermal system itself and related to the disruption of the equilibrium conditions caused by volcanic events.

At Vulcano, as discussed in Section 2.5, we have evidence from well data of a shallow thermal aquifer in Vulcano Porto (Carapezza et al., 1983), two boiling aquifers at depths of about 90 and 230 m below sea level, at Baia di Levante (Sommaruga, 1984), as well as of the existence of a deep fossil hydrothermal system (~400 °C, 25 wt% NaCl; Faraone et al., 1986; Cavarretta et al., 1988). In the recent past, the chronicles of Sicardi (1940) reported the appearance of fumaroles at the base of the La Fossa cone during unrest, and their subsequent disappearance in quiescence, as well as widespread thermal anomalies of wells in the area of Vulcano Porto, similar to what observed during the monitored unrest of the last 20-30 years (Section 2.7.1). Chiodini et al. (1991) have shown that, during events linked to the contribution of deep high-enthalpy fluids, the geotemperatures and geopressures estimated in the hydrothermal system of the Baia di Levante are higher, thus increasing the probability of hydrothermal explosions.

The hazards linked to the hydrothermal system are significant in all the phases (quiescence, unrest, eruptions of all types). Several phenomena (expansion / appearance of steam and gas exhalant areas, acidification and pollution of surface aquifers, mixing between deep and superficial bodies of water with variation of the chemical-physical characteristics) are highly probable to near-certain in all the levels of activity (unrest, Type 0 eruptions up to 4), as well as other phenomena like the pressurization of the boiling aquifers present under the Baia di Levante or at the foot of the La Fossa cone. Hydrothermal explosions may also occur due to sudden decompression of hot aquifers, and therefore be triggered by earthquakes (also regional) and landslides in all phases, including quiescence.

Specific quantifications regarding these hazards are still missing. Geochemical studies suggest that a deep hydrothermal system contributes to the present fumarolic degassing at La Fossa (Nuccio et al., 1999). Italiano et al. (1984) estimated that aquifers with a volume around 0.1 km^3 or higher, located within the first 2 km of depth, may give rise to hydrothermal explosions (up to actual phreatic events, classifiable as eruptions of Type 0). Such potential involves the whole area investigated (La Fossa caldera). From a spatial point of view, the NE and NW flanks of the La Fossa cone and the Faraglione, Baia di Levante and Isthmus areas are the most likely sites, due to the observable thermal anomalies.

From a multi-hazard perspective, the triggering of hydrothermal phenomena is mainly linked to the increase in the contribution of hot fluids from the deep magmatic system towards more superficial aquifers, but permeability changes related to landslides or seismic events can equally disrupt the hydrothermal system (e.g. NE side of La Fossa facing Punte Nere). On the other hand, hydrothermal alterations of the rocks may trigger slope instability (e.g. downhill and unstable zones of the Forgia Vecchia), ground deformations, and lahars.

The main problem in quantifying these hazards in Vulcano, as for most of volcanoes worldwide, is that there is no detailed historical information to constrain the statistics on occurrence and magnitude of hazardous events. In particular, there are no measurements during either eruptive phases or unrest preceding eruptive phases. Physical-
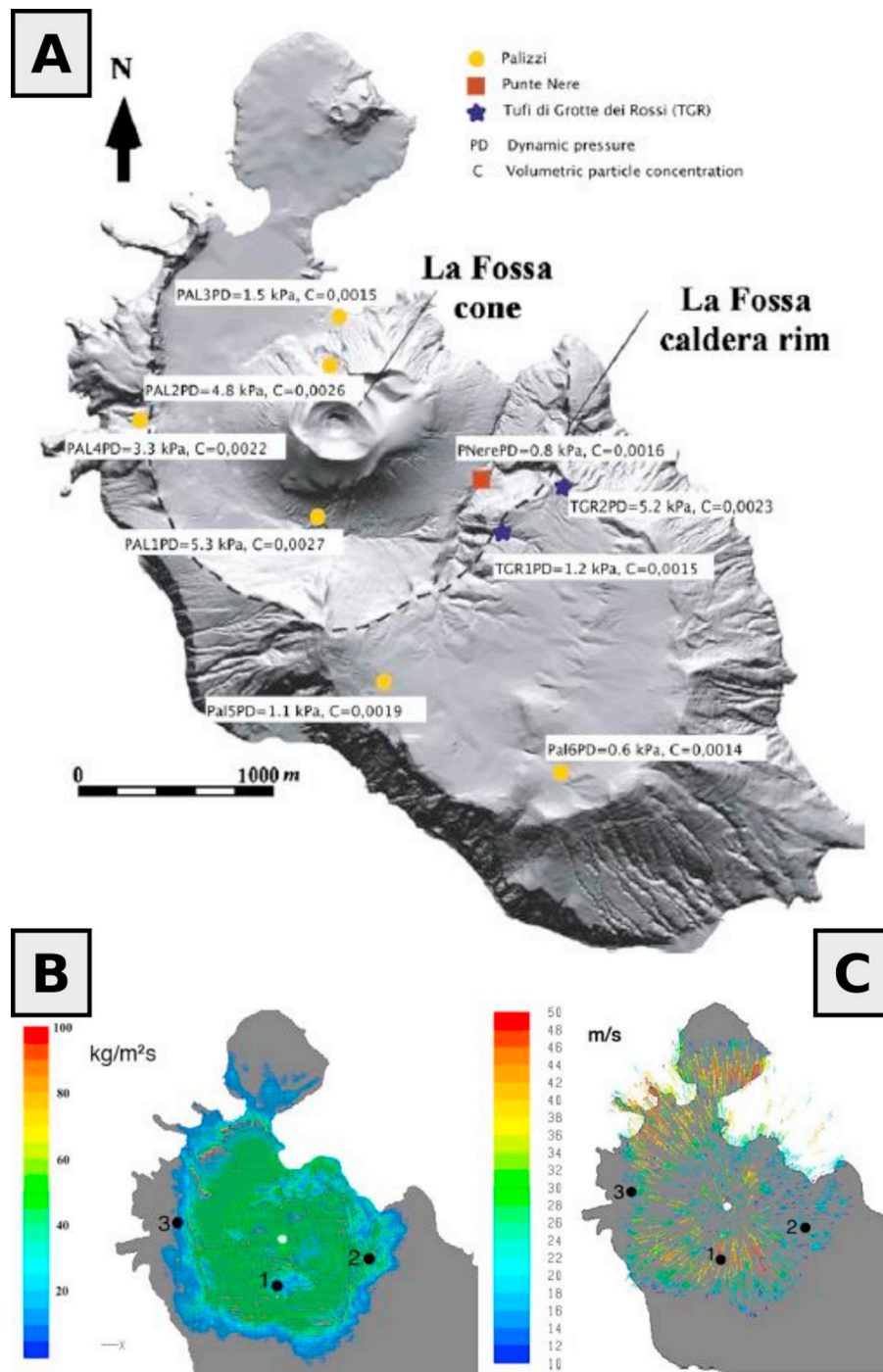
Fig. 10. PDC hazard at Vulcano: A) Distribution map of dynamic pressure and concentration of particles for Palizzi and Punte Nere – Eruption Type 3, and the TGR – Eruption Type 4 (from Dellino et al., 2011). B) Map of the sedimentation rate of PDC for the Palizzi – Eruption Type 3. C) Map of PDC velocity for the Palizzi – Eruption Type 3 (from Doronzo et al., 2016).

numerical simulators of geothermal reservoirs have also been used to model the hydrothermal circulation at Vulcano (Todesco, 1997), but their applicability for the purpose of an evaluation in space and in the short term of the evolution of the hydrothermal system is seriously hindered from the limited geological characterization of the substrate, a necessary input for the models.

3.2.2. Volcanic gases

Gas hazard is related to the toxicity and/or asphyxiating properties of the endogenous gas species emitted and to their concentration and dispersion in the atmosphere. In the short term, the gas hazard at

Vulcano is mainly related to the reaching of dangerous concentration levels of CO_2, H_2S and SO_2 in the air, or a mixture of them. Long-term exposure to volcanic gas, aerosol and particulate matter can also be harmful but the effects are poorly understood and will not be taken into account here. More details on the potential impact can be found in IVHHN (2005).

At Vulcano, gas emission occurs both from fumarolic fields and from soil characterized by diffuse degassing. In the first case, hazardous levels of gas (mainly SO_2 and H_2S and, secondarily, CO_2) can be reached in the plume while dangerous concentrations of endogenous gas emitted by diffuse degassing (mainly CO_2 and, secondarily, H_2S) can
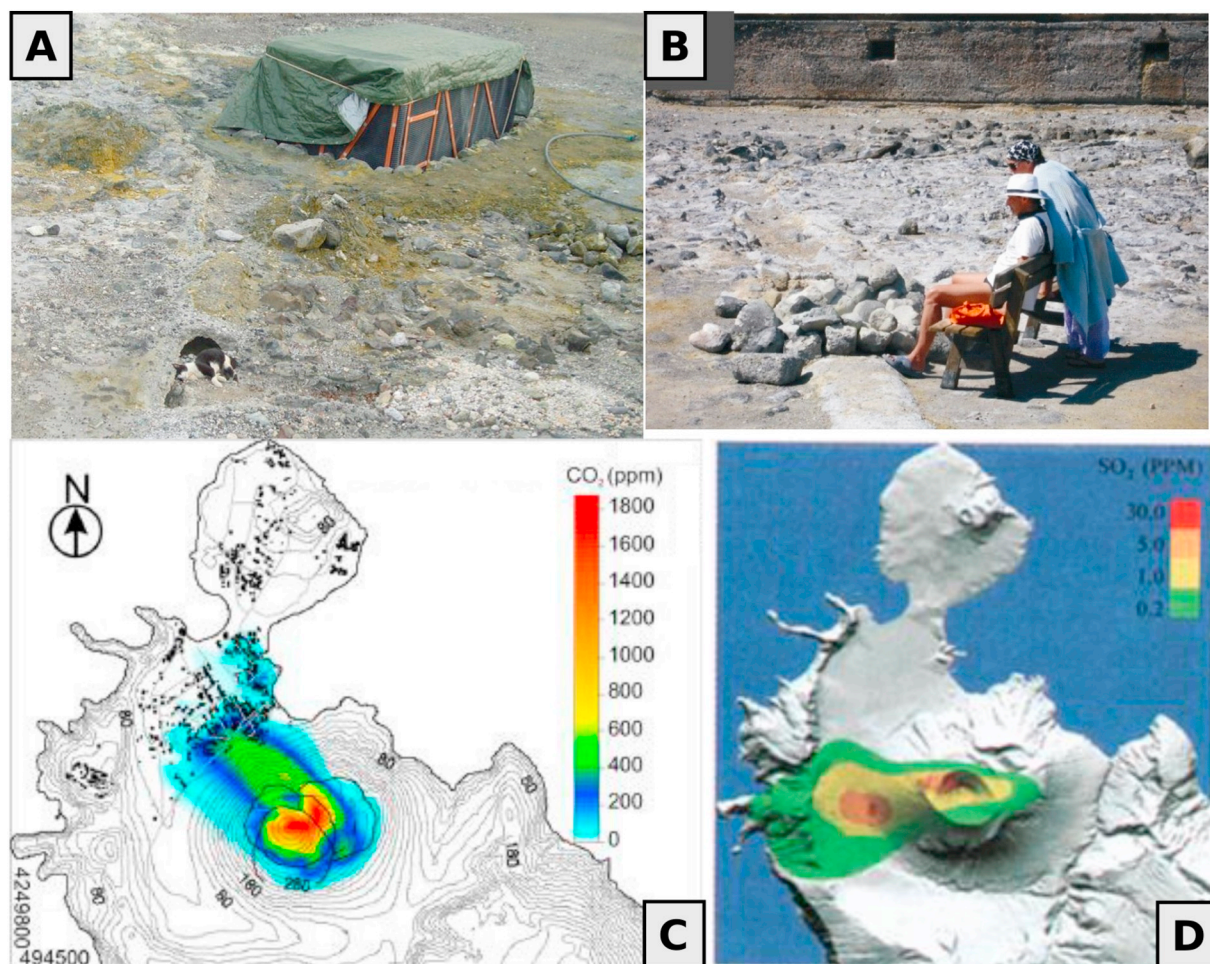
Fig. 11. Gas hazards at Vulcano: A) Cat killed by lethal concentration of gases (Photo: A. Gattuso, April 2009). B) Tourists doing "aerosol therapy" with fumarolic emissions in the same location of 10A (Carapezza et al., 2011). C) Simulation of CO_2 concentration in air with contributions from crater area, Forgia Vecchia, Vulcano Porto and Levante Beach (from Granieri et al., 2014). D) Numerical model of SO_2 dispersion (from Pareschi et al., 1999).

affect low-lying areas and confined spaces. In the latter case, CO_2 is usually the most hazardous endogenous gas while, more in general, H_2S is the gas that more easily reaches an outdoor concentration potentially hazardous for human health (Fig. 11A,B).

At Vulcano the diffuse degassing of CO_2 is comparable to that emitted from the plume of open-conduit volcanoes. During unrest episodes, soil degassing can increase up to nearly one order of magnitude in the crater area and up to a factor 3-4 at Levante Beach and Palizzi, as happened during the 2005 unrest phase (Carapezza et al., 2011).

Past concentrations of dry fumarolic gas ranged from 95 to 97.72% and from 1.57 to 2.47% for CO_2 and H_2S, respectively (Chiodini et al., 1991, 1995; Capaccioni et al., 2001) while concentrations of SO_2 up to 3% were observed at the crater-rim fumaroles (Badalamenti et al., 1984).

In Vulcano Porto, for CO_2, the maximum air concentration values were observed during the 2005 unrest phase and reached levels of 9.8 and 100% for indoor and outdoor measurements, respectively (Carapezza et al., 2011). In the same period, a total diffuse degassing of 92 tons/day was recorded at Vulcano Porto while 14 tons/day were emitted at Levante Beach (Granieri et al., 2014). Numerical simulations of CO_2 dispersion in the atmosphere, taking into account the diffuse degassing contributions of La Fossa cone, Vulcano Porto and Levante Beach for the 2005 unrest phase for a total of 1714 tons/day (Granieri et al., 2014, Fig. 11C), show that excess CO_2 air concentration never exceeds 300 ppm, mainly due to local soil degassing more than from the crater. For H_2S, the maximum air concentration levels were observed in

1991 (quiescence) a few tens of meters N of the thermal pool (4500 ppm; Annen, 1992). In 2015 (quiescence), 270 ppm and 65 ppm of H_2S were recorded at fumaroles located 20 m off-shore Levante Beach and at the thermal pool, respectively (Carapezza et al., 2016a, 2016b). The total amount of H_2S emitted by viscous degassing in these areas was measured on 2009 (quiescence) for a total of 20.3 kg/day, while the H_2S released in 2007 (quiescence) by diffuse degassing was 93.5 kg/day (Carapezza et al., 2011). A maximum concentration value of 19.8 ppm was recorded at Levante beach in 2007 (quiescence; Carapezza et al., 2011) along a 20 m-long profile (20 cm height for 33'). For SO_2, the maximum air concentration levels were observed in 2005 (quiescence) at Ponente Beach (0.05 ppm; D'Alessandro et al., 2013). Numerical simulations of SO_2 dispersion, based on a fumarolic SO_2 flux of 30 tons/day (quiescence), have shown values just above 10 ppm in the easternmost sector of Levante Bay (Graziani et al., 1997) and more than 30 ppm at the western foot of La Fossa cone (Pareschi and Ranci, 1997; Pareschi et al., 1999, Fig. 11D).

In Vulcano Piano, no air concentration data are available for CO_2 and H_2S at Vulcano Piano while the maximum air concentration level of SO_2 was 0.05 ppm observed in 2005 (quiescence; D'Alessandro et al., 2013). A total CO_2 soil diffuse degassing of 4 tons/day was measured at Vulcano Piano and 1 ton/day in the Gelso area (quiescence; Inguaggiato et al., 2012).

Within La Fossa cone, the maximum air concentration of CO_2 (15%) was observed in 1984 (quiescence) in a channel on the NW slope of the cone (Badalamenti et al., 1984). A peak of 600 tons/day of CO_2 flux

from the crater fumaroles was recorded in 1988 (unrest; Italiano and Nuccio, 1992), while 362 tons/day was observed in 2007 (quiescence; Inguaggiato et al., 2012). A total soil diffuse degassing of 180 tons/day from the crater area was observed in July 2005 (quiescence; Granieri et al., 2006) while 1579 tons/day from the same area, plus 29 tons/day from the Forgia Vecchia, were observed on December 2005 (unrest; Granieri et al., 2014). Numerical simulations of CO_2 dispersion in the atmosphere realized for La Fossa cone (Granieri et al., 2014) show concentration values just above 0.5% with an input of 300 tons/day for the fumarolic contribution (quiescence). For H_2S, the maximum air concentration observed on the crater rim is 179 ppm (quiescence, maximum concentration value along a 30-m-long profile at 1.5 m; Carapezza et al., 2011). The total amount of H_2S emitted from the crater fumaroles was 6 tons/day in 2005 (quiescence; Aiuppa et al., 2005). For SO_2, the concentration in the air up to hundreds of ppm were measured on at least two occasions on the crater rim: 250 ppm on 1991 (quiescence; Annen, 1992) and 179 ppm on 2005 (quiescence; Aiuppa et al., 2005). More recently, 0.85 ppm were measured 100 m downwind of crater rim fumaroles (quiescence, average value calculated over a 2-day measurement period, the maximum concentration value is evidently much higher; D'Alessandro et al., 2013). Peaks of SO_2 plume flux of 120 and 100 tons/day were observed in 1988 (unrest; Bukumirivic et al., 1997) and in 2009 (unrest; Vita et al., 2012), respectively. An SO_2 plume flux of 15 tons/day was measured in 2005 from the crater fumaroles (quiescence; Aiuppa et al., 2005). Numerical simulations of SO_2 dispersion in the atmosphere resulting in over 30 ppm were realized using an input of 30 tons/day (quiescence; Pareschi and Ranci, 1997).

The emission of volcanic gas at Vulcano occurs in all the levels of volcanic activity (quiescence, unrest, eruptions of Type 0, 1, 2, 3 and 4). Note that all known deaths due to the emission of endogenous gas at Vulcano occurred in the inter-eruptive period post-1890 AD (during the last eruption, the island was almost uninhabited).

Probabilistic hazard quantifications are not available for Vulcano. A health risk assessment, through a fuzzy-logic procedure, has been carried out for SO_2 by Klose (2007). However, the model is affected by the inexact assumption that, in addition to the SO_2 released by the high-temperature fumarole located on the NE sector of the rim of Gran Cratere, SO_2 clouds are emitted also by the degassing areas of Vulcano Porto.

More in general, past studies of gas dispersion show that, in quiescence and unrest, the areas more exposed to the gases are La Fossa cone, Levante Beach, Vulcano Porto village, and Palizzi. In these areas, diffuse and/or fumarolic degassing occur permanently and dangerous concentrations can be reached. Potentially, all the areas located on the bottom of the Fossa caldera, including offshore, are highly exposed. During unrest and eruptions, significant increases of both fumarolic and diffuse emissions (also with variations in the composition) are expected to occur, with an increase of their areal distribution and the possible appearance of new emission sites (as "Lentia fumaroles" of Sicardi (1940); see Section 3.2.1).

From a multi-hazard perspective, gradual increases of gas release may occur in cases of new magmatic input, local and/or regional seismicity, meteorological factors (atmospheric pressure, wind and rainfall), while significant and sudden increases (from seconds to minutes) of gas air concentrations could be due to phreatic, phreatomagmatic and magmatic eruptions as well as to landslides. The sudden increase of gas emissions to the hazardous levels in the air can also be triggered by human activities (e.g. excavations and borehole drillings).

The main concerns in the state of knowledge and risk mitigation measures are: lack of an indoor and outdoor surveillance network in the areas more exposed to short-term gas hazard; lack of delimitation of the most hazardous areas to interdict people' access (e.g. Vasca degli Ippopotami); lack of an epidemiological study on the exposure effects to gas and aerosols in the long term; lack of an efficient and constant work of awareness raising to the gas hazard and to volcanic hazards (Nave

et al., 2015; Carapezza et al., 2016a, 2016b). About this latter point, the INGV Operational Center "Marcello Carapezza" (D'Addezio et al., 2008; INGV-DPC, 2013) is the only structure to date that explains gas hazards to tourists that spontaneously go to visit the exhibition area.

3.2.3. Volcanoclastic flows and floods

The term volcaniclastic flows includes the whole spectra of gravity driven mixture of volcanic material and water. The term lahar is usually used as synonymous of volcaniclastic flow, although it best applies to flows occurring on the slope of a volcano (Smith and Lowe, 1991). Both volcaniclastic flows and lahars may vary their characteristics downstream over time and may include a variety of flow types including debris flow, transitional or hyperconcentrated flows, or floods.

The occurrence of lahars at Vulcano is widely documented in the literature (Frazzetta et al., 1984; Dellino and La Volpe, 1997; Di Traglia, 2011; De Astis et al., 2013a, 2013b; Di Traglia et al., 2013). In particular, during the reference period (5 ka), the occurrence of lahars is associated both with intra-eruptive phenomena during the cycles of Vulcanian activity and during periods of volcanic quiescence. In both cases, lahars occurred as remobilization of the material emplaced during the phases of activity of La Fossa and accumulated on the slopes of the cone. Such phenomena are always triggered by heavy rain events. In particular, the triggering conditions are linked to the accumulation of ash, slope, characteristics of the material (e.g. grain-size) and the amount of provided water (Ferrucci et al., 2005). Both types (syn- and post-eruptive lahars) have contributed over the years to progressive denudation of La Fossa, where the ash products of recent Vulcanian cycles (post-1000 years) have been removed from the slopes and accumulated at the foot of the volcano.

During quiescence or unrest, lahars are related to the remobilization of the material from past eruptions due to the rain. The frequency in the reference period is high, with periods of nearly annual occurrence for small-volume lahars linked to the seasonality of the rains. During the eruptive phases, lahars can occur both during intra-eruptive periods within periods of Vulcanian activity (Eruption Type 2), and during or immediately after sustained column eruptions (Eruption Type 3). The frequency of occurrence, even in these cases, is linked to rain events, and is higher during the Type 2 activity due to their longer duration and to the associated deposits (ash) for this type of activity, which are more suitable (in grain-size and thickness) to the initiation of the lahar phenomena.

Observed deposit volumes in Vulcano are variable; in the intra-eruptive events, a reworking of ash is largely visible within the eruptive sequences and rarely affects large areas. The variability of the volumes associated with the inter-eruptive events is larger, essentially due to longer periods in which the probability of the occurrence of torrential rains increases. The deposit volumes are from low (20-50 m^3), with only local effects at the scale of the cone and formation of small lobes (Ferrucci et al., 2005), to large events that remobilize significant volumes of material (10^3-10^4 m^3), with events affecting the road system and the Porto di Levante area. All the ash remobilized in the last 1 ka has led to an accumulation of material in the area of Vulcano Porto and Porto di Ponente, where the ground level has progressively risen by 2-3 m.

Probabilistic hazard quantifications for lahars in Vulcano are still missing. Literature and observational data suggest that the lahar scale is linked to the intensity of the rains. It is, however, possible that the highest intensity values can occur immediately after a new eruptive activity when the availability of grain-size material and ash thicknesses is higher. Indeed, observational data suggest that the potentially invaded areas during the most important phenomena include the area of Vulcano Porto and Porto di Ponente, where the maximum observed lahar deposit thickness reaches one meter for single events.

3.2.4. Landslides

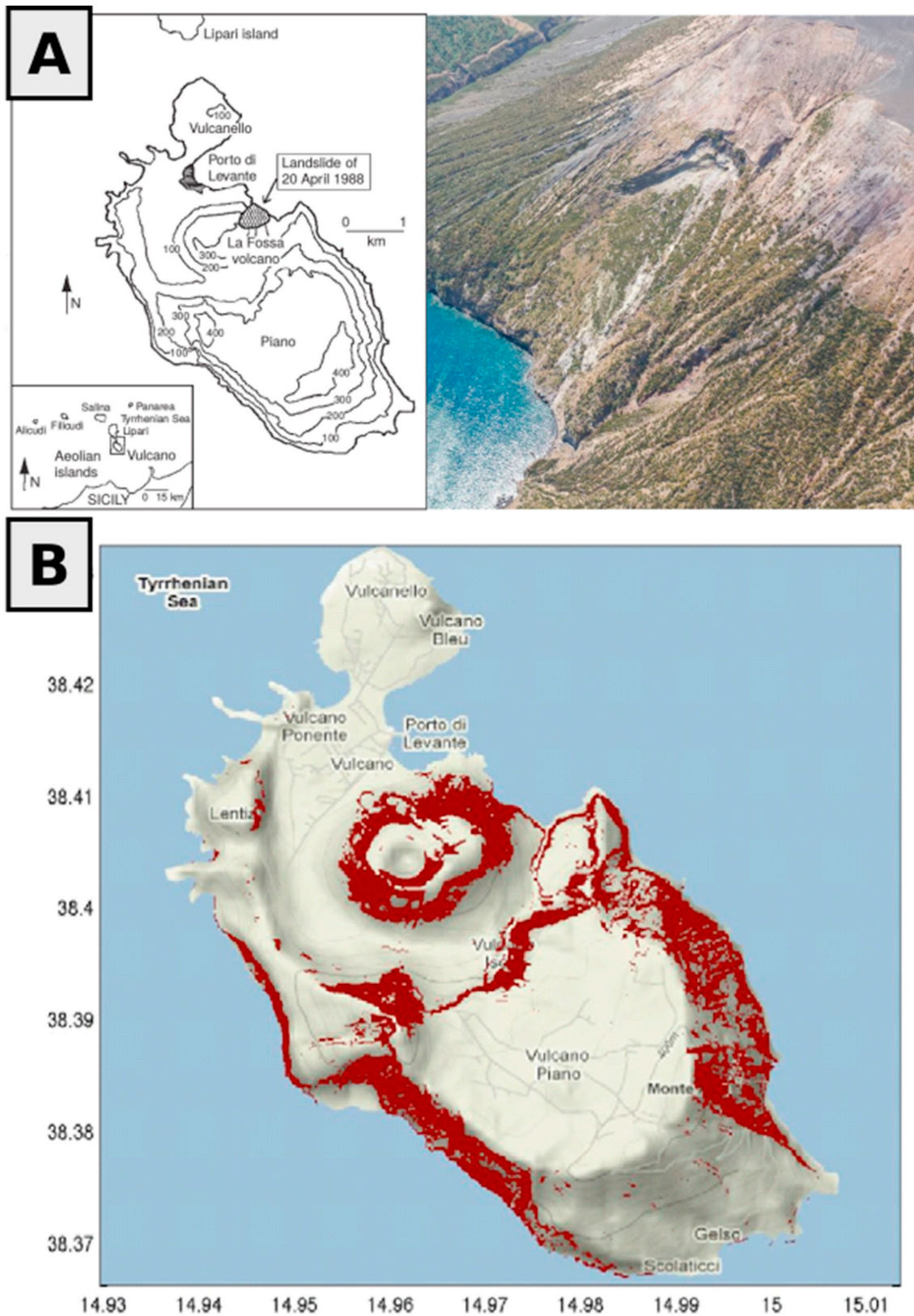At Vulcano, two main types of slope processes have occurred in the

Fig. 12. A) Simplified sketch map of Vulcano island (from Tinti et al., 1999) with position and picture of the 1988 landslide (picture of T. Ricci). B) Zones of slope instability at Vulcano calculated by Galderisi et al. (2013) with a Mohr-Coulomb failure criterion on water-saturated deposits.

past: i) shallow landslides (e.g., rotational and drift landslides), and ii) deep-seated slope deformation (e.g. debris avalanches and sector failures).

Based on morphological evidence, around the La Fossa cone,

Tommasi et al. (2007) documented shallow landslides along pyroclastic strata with volume up to 200,000 m³, and local rock slides were recognized at Lentia by Marsella et al. (2015). Frazzetta et al. (1980) found a landslide of 24,000 m³ at Forgia Vecchia slope, whereas the

youngest shallow landslide occurred on April 1988 along the NE slope of La Fossa (Fig. 12A and B), with a volume between 193,000 m³ (Achilli et al., 1998) and 201,000 m³ (Tinti et al., 1999). This latter event was likely triggered by seismic shaking during the earthquake swarm of March-June 1988, which reached a maximum Magnitude of 4 (Neri et al., 1991). Other predisposing factors may have included regional seismic activity, hydrothermal alteration of the involved deposits, and repetition of cycles of fluid inflation/deflation that might decrease the geotechnical characteristics of rock masses (Rasà and Villari, 1991); the landslide occurred during a period of low rainfall (Tommasi, pers. comm.).

Past deep-seated failures occurred prior to 10 ka and were linked to the growth and collapse of the ancestral volcano (De Astis et al., 2013a, 2013b). A sector collapse developed along the southwestern flank of the island, producing a debris avalanche deposit documented at 5-10 km offshore (Bosman et al., 2013; Romagnoli et al., 2013).

Landslides are possible in all the phases of the volcano, with an increase of probability in case of unrest and eruption. Probabilistic hazard analyses for the different types of landslides are still lacking. Only a few specific quantitative studies are available. Modelling by the Bishop method (Bishop, 1955) showed that general failure of the La Fossa cone is very difficult, being characterized by a Factor of safety (Fs) ≥ 1.34, whereas minor shallow landslides are possible in the upper part of the crater with Fs = 0.95 (Pesci et al., 2013). Tommasi et al. (2016) showed the possibility of flank failure of the NE part of the La Fossa cone, only in the case of important external forces, such as a shallow magma intrusion producing a vertical gradient of at least 10 kN/m applied for a height of 100 m, and if there are horizons in the potentially unstable rock mass that are completely altered into clays.

Geodetic measurements of active deformation of the topographic surface of the slopes of the La Fossa cone support the presence of an unstable rock volume of about 0.8×10^6 m³ that affects the slope facing the harbour and the village (Bonaccorso et al., 2010). Other analyses found other potential instabilities in the area of La Forgia Vecchia (Marsella et al., 2011; INGV-DCP-V3, 2016) and in the area NW and SE of the 1988 landslides (Madonia et al., 2019), with a potential volume up to several hundred thousand cubic metres.

Apart from the La Fossa cone, other zones of slope instability have been located along the western and southern island coast by the "Piano Stralcio dell'Assetto Idrogeologico" (Regione Sicilia, 2004; Galderisi et al., 2013; Fig. 12C). Here, landslides of "rock slide" and "rock toppling" type have been identified. Coastal instability can also be enhanced by submarine erosion processes, as those observed NE of the La Fossa cone (Romagnoli et al., 2012).

We lack quantitative multi-hazard quantifications related to landslides. However, landslides may cause tsunami, as happened in 1988 (Tinti et al., 1999; see Section 3.2.5). Larger tsunami may be generated by larger landslides and/or submarine landslides. Landslides may also provide material for lahars and induce important changes to hydrothermal and degassing systems that, in the worst cases, may trigger explosions and even eruptions. In general terms, landslides may be triggered by deformations, earthquakes, soil alterations due to the hydrothermal and degassing systems, erosion and argillification, as well as other meteorologically induced changes.

An important step forward toward the realization of probabilistic hazard analyses would be a systematic collection of past data, including distribution of past events, and of instability analyses (static conditions, geophysical surveys, detailed analyses of past large scale debris analyses in land and at sea, etc.), which are still missing for Vulcano.

3.2.5. Tsunami

Vulcano may produce tsunami, as all volcanic islands (Paris et al., 2014; Paris, 2015). Tsunami may reach Vulcano from other regional events (earthquakes, landslides in other areas, etc.), but these events are not considered here.

In the historical record, only one tsunami related to Vulcano is known to have occurred, on 20 April 1988 (Maramai et al., 2005, 2014), and originated in the bay between Punte Nere and Punta Luccia by a landslide of approximately 2x10⁵ m³ (Tinti et al., 1999) during an unrest phase started in 1987 (see Section 3.2.4). A fisherman observed a positive wave of approximately 1-2 m, the wave was clearly observed in the Porto di Levante, and it reached Lipari with waves up to 0.5 m (Maramai et al., 2005, 2014).

Tsunami are theoretically possible in all the phases of Vulcano. In quiescent periods, tsunami are rare and may be caused by large gravitational collapses ($> 10^5$ m³), which are mainly possible on the slopes of La Fossa cone (see Section 3.2.4), as well as by submarine landslides. During unrest, tsunami may be triggered also by large earthquakes (M > 6), even if local earthquakes with these magnitudes are unlikely (Section 3.2.7). Collapses in the area of La Fossa cone may be triggered by ground deformation and/or structural weakening due to the interaction with the hydrothermal system (Section 3.2.4). Overall, tsunami during unrest may be considered rare to possible. During eruptions, tsunami may be additionally caused by submarine explosions (possible for all types, Section 3.1.1) or dense pyroclastic flows (more likely for an eruption of Type 0, Sections 3.1.5), but they may be still considered rare to possible.

Probabilistic hazard quantifications regarding tsunami generated by volcanoes are rare in literature, and for Vulcano they are not available. Qualitatively, the most exposed area is Vulcano Porto and tsunami intensity probably do not exceed a few meters during quiescence, while larger tsunami (up to around ten meters, as locally in Stromboli in 2002, Maramai et al., 2014) may be generated during unrest and eruptions.

There are no quantitative multi-hazard or multi-source studies for tsunami at Vulcano. Qualitatively, the most likely cause of tsunami seems to be gravitational collapses in the area of La Fossa and near-to-coast or submarine landslides, potentially affecting Vulcano Porto and its surroundings.

3.2.6. Ground deformation

Vulcano ground deformation is associated with tectonic and magmatic/hydrothermal processes. Regional tectonics usually cause slight ground deformations (several millimetres per year; e.g. Bonaccorso, 2002; Esposito et al., 2015; see Section 2.4), while the shallow hydrothermal system may cause ground deformation on La Fossa cone, as the rim subsidence of 0.055 m and the horizontal changes up to 0.06-0.07 m recorded during 1990-96 (Gambino and Guglielmino, 2008; Alparone et al., 2019). Moreover, between 1987 and 1993, significant deformations (ca. 0.10-0.15 m) affected a narrow zone of the northern edge of the cone close to a fumarolic area. These deformations have been correlated to the temperature changes of the fumaroles (Italiano et al., 1998; Bonaccorso et al., 2010).

Overall, ground deformations are constantly present at Vulcano, with low deformation rates. The ground deformation may become significant during unrest and eruptions. However, specific quantification of the hazard, as well as systematic multi-hazard studies involving deformation, do not exist in the literature. Tinti et al. (1999) suggested cone inflation/deflation as a possible trigger of the April 20, 1988, landslide and consequent tsunami (Sections 3.2.4 and 3.2.5).

3.2.7. Seismicity

Vulcano is characterized by occurrence of Volcano-Tectonic events (VT) and a more widespread seismicity at La Fossa area of very low energy (see Section 2.4). VT events, recorded in recent decades, represent a modest seismicity both in terms of events number (few per year) and intensity ($M_d \leq 2.5$).

Vulcano could also be significantly affected by strong regional earthquakes of medium/high intensity. In the last 50 years, two main events have been recorded within an area with a radius of 20 km centered on Vulcano: $M_w = 5.5$ (April 15, 1978) and $M_w = 4.8$ (August 16, 2010). Macroseismic observations (INGV database, https://emidius.

mi.ingv.it/CPTI15-DBMI15) report for the 1978 event an MCS (Mercalli-Cancani-Sieberg scale) of 7-8 at Vulcano Piano and 6 at Porto di Levante.

Seismic activity is certain during all the states of the volcano, with potentially different energetic bounds. Specific quantifications are still lacking. Qualitatively, seismicity during quiescence is expected to be similar to that observed in recent decades, with a few low-energy events per year. During an unrest episode, sequences of events may occur, probably with medium-low energy, as occurred in the 1980s and 1990s. During eruptive phases, however, there is a larger probability that higher energy VT swarms may occur.

Local quantitative seismic hazard assessments do not exist. The Italian Probabilistic Seismic Hazard Analysis includes Vulcano without any specific treatment for volcanic areas; in the Vulcano area, the quantified reference intensity for the Italian building code (intensity with an exceedance probability of 10% in 50 years) corresponds to values between 0.175 and 0.200 g of PGA (Peak Ground Acceleration; GdL_MPS, 2004).

Systematic multi-hazard studies involving earthquakes in Vulcano are also not available. Apart from the 1988 landslide (see Sections 3.2.4 and 3.2.5), it has been reported that the 2010 earthquake triggered some landslides at Lipari and rock falls on the flanks of Vulcano, Lipari and Salina (Gambino et al., 2014).

4. STEP 3: the conceptual model

STEP 3 includes the development of a reference conceptual model of the volcanic system, with the main goal of producing a comprehensive interpretative framework that distils the information derived from STEPs 1 and 2. In particular, the main target of the developed conceptual model is to investigate the processes that could lead to the onset of an eruption, based on the different phenomena that may characterize unrest episodes. STEP 3 is an important part of the review that outlines the subjective interpretative framework that eventually emerged from the review of the objective observations and the past studies discussed in STEPs 1 and 2. STEP 3 also provides a general framework interconnecting the different phenomena, representing a very first step toward the analysis of interdependencies among hazards, in a multi-hazard perspective (Selva et al., 2019).

In the state-of-the-art best practice of volcanic surveillance, it is crucial to define a conceptual model of the monitored volcano that i) addresses the dynamics of the system, and, ii) assigns each monitored parameter an interpretative physical meaning. When modern monitoring data linked to eruptive unrest are absent (as in the case of Vulcano), it may be practical to use as a benchmark what happened in monitored modern volcanic unrest episodes. In the case of Vulcano a benchmarking unrest and eruption may be that of Monserrat (1995-2005; Druitt and Kokelaar, 2002), which witnessed the renewal of activity at a calc-alkaline volcano erupting dacitic magma (Barclay et al., 1998).

A conceptual model also allows that any changes in observable features yield immediate implications, at least qualitatively, for the purpose of assessing the state of activity of the system. The ultimate goal of this conceptual model is then to provide the basis on which to establish future improvements in single- and multi-hazard quantifications at Vulcano, both for long-term hazard quantifications (e.g., IAEA, 2012, IAEA, 2016) and for the development of quantitative short-term eruption forecasting (e.g., Marzocchi et al., 2008; Hincks et al., 2014) and hazard quantifications (e.g., Selva et al., 2014).

4.1. Formulation of the model

For Vulcano, as anticipated in Section 2.7.1, the challenge of the conceptual model has historically been to explain the sudden and intense variations observed periodically in the set of monitored geophysical and geochemical parameters, well known in literature by the term "crisis". This term, generally adopted in the scientific community, assumes that these episodes represent a trend of the system toward hazardous conditions, due to the increase in emissive activity, sometimes evident through simple visual observation of the fumarolic field. On this ground, the word "crisis" can be considered synonymous of unrest (and this use has been indeed done through the text). Even if it is a natural starting point to define the "crisis" as an anomaly and what is not a crisis as the background, it will be clear below that there is not a simple relation between "crisis" and changes in the state of volcanic activity.

As shown by Paonita et al. (2013), the analysis of the periods of volcanic unrest highlights a discrepancy that arises from the covariation of some parameters during a crisis: geophysical data indicate in fact the absence of magmatic movements, while geochemical data indicate a magmatic degassing by decompression, due to ascent of magma batch at lower pressures. The interpretative framework resulting from a multidisciplinary and integrated approach, which models fluid geochemistry data within the constraints given by the petrology of the magmatic products (Paonita et al., 2013), envisages at the origin of this observation the polybaric nature of the plumbing system (Section 2.3), with several magmatic ponding zones. The shallowest part, directly involved in the fumarole degassing of La Fossa, consists of at least two poorly connected magmatic storage bodies of latitic composition, located at a depth of 3-4 km (Paonita et al., 2013; Mandarano et al., 2016; Fig. 13A). The available data (see Clocchiatti et al., 1994; Peccerillo et al., 2006; Mandarano et al., 2016 and references therein) indicate for the shallow part ofthe upper crust below Vulcano (between 5 and 2 km) a system of small-volume reservoirs having different compositions, which can connect to each other during pre-eruptive and eruptive
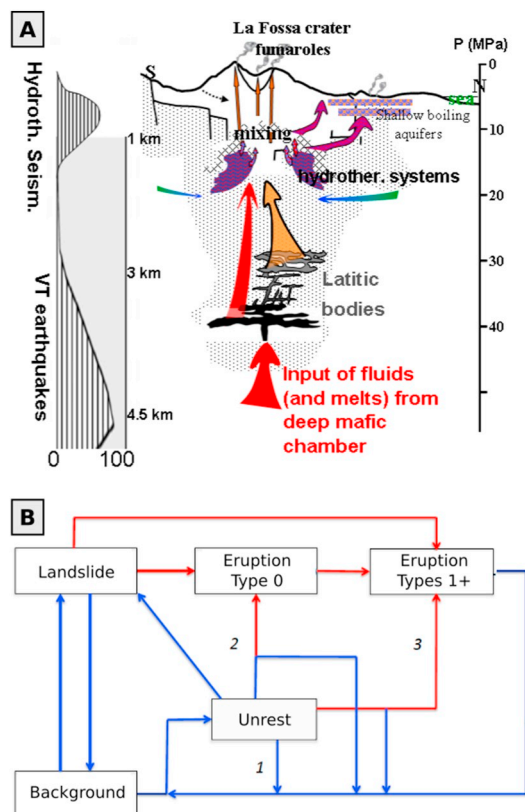

Fig. 13. A) Shallow portion of the magmatic feeding system below Vulcano (based on the view of Paonita et al., 2013). Pressure-depth relation has been computed by assuming hydrostatic load down to the top of the latitic body, given the presence of deep hydrothermal circulation. B) Hazardous events and possible scenarios, indicated by the numbers visible near the paths. In blue the non-eruptive paths, in red the eruptive ones.

phases, as testified by mixing/mingling textures found in the deposits (Section 2.3). These reservoirs undoubtedly include the aforementioned bodies of latitic magma.

In Fig. 13A, we graphically represent the link between the polybaric plumbing system (Section 2.3) and the main characteristics of the crisis periods of Vulcano (Section 2.7.1). Data on basalt-shoshonite lavas from Vulcanello (Zanon et al., 2003; Fusillo et al., 2015) and on compositional and textural record preserved in plagioclase crystals (Nicotra et al., 2018) highlight the possibility that the mafic magma has a main level of accumulation at the limit between the lower crust and the mantle (>18 km), and duration (some years) and transient ponding levels in more superficial reservoirs (<11 km). The decompression of the (mafic) magma from 18-21 km up to 5 km would provide most of the magmatic fluids released on the island (Paonita et al., 2013). This is consistent with the current rate of degassing at Vulcano (Inguaggiato et al., 2012) that could not be sustained only by the small shallow bodies of latitic composition and requires a strong contribution from a more primitive magma. The deeply sourced fluids would periodically feed the gaseous fraction of the latite bodies (Paonita et al., 2013).

The 2004 crisis was probably linked to the massive degassing of the shallowest latite body, while fluids from the deeper latite level were those previously dominant. Therefore, it is probable that the recurrence of these abnormal degassing events is linked to the progressive accumulation of volatiles at the top of an accumulation zone (e.g., a foam), followed by their massive release (Paonita et al., 2013).

It should be noted that the large geochemical variations of the 2004 crisis were preceded in 1998-1999 by some variations with similar qualitative significance, but having a much smaller extent (e.g. the observed changes of He/CO_2 ratio). In the same period, a modest but significant increase in seismicity was observed under the La Fossa cone (Alparone et al., 2010). These variations, especially if accompanied by events of volcano-tectonic seismicity in time periods far from crises, could suggest important reorganization in the magmatic feeding system (e.g., activation of new degassing levels), whose effects at the surface are delayed over time (Paonita et al., 2013). Thus, the origin of the crises subsequent to that of 1996 seems linked to the episodic increase in the degassing from the shallow latitic bodies, which had previously accumulated volatiles at the top of the reservoir.

It is worthy of note that, although all crises show very similar variation patterns for many parameters, some peculiar differences could have a deep impact on the evaluation of the activity. The data show that crises since 1996 have not been accompanied by significant variations in CO_2 flow from soils in the Vulcano Porto area and from changes in the chemical and physical characteristics of thermal aquifers in the same area (Capasso et al., 2001). Taking into account that these peripheral systems are certainly pathways for deep fluid ascent less effective than the crater zone, the presence or not of geochemical variations in such systems during a crisis can be considered as a qualitative indicator of the involved mass of magmatic fluids and therefore, in some way, of the amount of degassing magma. This obviously has implications on the type and extent of expected unrest events. From this point of view, the 2004 crisis was smaller than previous crises (e.g. 1988), which caused significant changes in gas flows from soils and in aquifers (Capasso et al., 1999; Diliberto et al., 2002).

Given their modest volumes, the shallow latitic bodies are sensibly degassed melts, capable of inducing only modest perturbations, which are "disposable" through the crater system or, at most, through the involvement of some peripheral systems. Under these conditions, it could be deduced that they are not able to determine magmatic eruptions (Eruption Type 1+) without a connection with deeper sources, and it is not likely that they will cause even phreatic events that involve the deep hydrothermal system (Eruption Type 0). This can be true unless significant inputs of fluids come from the deeper mafic melts (Fig. 13A). The eruptive potential of Vulcano seems therefore linked to the possibility that the eruptive system reopens through an explosion of

the hydrothermal system (as it probably happened in the past, see Section 2.2.2) or the sudden migration of a deep magmatic body to levels closer to the surface.

The presented conceptual model provides reasonable paths-to-eruptions for this volcanic system and is the base for the development of the possible scenarios of unrest. These types of unrest link together different hazards, providing a first order tool for integrating in a multi-hazard perspective. The model arises from a combined analysis of the petrological knowledge of the magmatic feeding system with data from the geochemistry of the fumaroles and from seismical and geodetical monitoring. It is therefore an integrated functioning scheme largely compatible with the whole body of knowledge acquired on the volcano. It should be noted that, as the geochemical and geophysical data refer to the present state of the system, it implies a degree of extrapolation for their coupling to the information from petrology of past eruptions. Moreover, it does not mean that other models cannot explain the available information, or that in the future, other models will be developed, potentially distinct from the one discussed here. On the contrary, the model explicited here can facilitate the development of alternative models challenging its main assumptions.

4.2. Unrest scenarios

The conceptual model provides a framework that allows us to hypothesize three possible unrest scenarios based on:

1) the potential involvement of the surface hydrothermal system,
2) the involvement of the deep hydrothermal system,
3) the potential trigger of migration of magmatic bodies coming from the deepest sources.

In analogy with eruptions (Section 2.7.2), we refer to these different scenarios also as unrest types. Note that even in Unrest Types 1 and 2 concerning the hydrothermal systems, it is clear that the true engine of anomalies is an increase in the contribution of deep magmatic fluids, but its contribution is limited to the excitement of the system and not to magma movement.

In the following, we discuss the unrest types in the framework of our conceptual model, linking them to the eruptive types defined in Section 2.7.2. As discussed in Section 3 (STEP 2), each unrest and eruption phase is then linked to various dangerous phenomena, regardless of the causes of the unrest itself.

In Fig. 13B, we report a logical flow chart that summarizes the unrest types. It should be noted that the paths on the left side of the figure indicate that even an eruptive scenario that does not provide unrest is considered in the scheme, linked to the occurrence of a landslide that directly triggers a magmatic eruption by decompression.

Before entering the details of the flow chart (next sections), we must highlight some important limits: i) it is useful to remember that the scheme follows the chosen conceptual model, but we cannot exclude the development of other conceptual models that may alter significantly the interpretation provided here; ii) the described unrest scenarios are not necessarily identifiable by means of the present monitoring system (Section 2.6); iii) we did not define any time scale for the passage between the different states defined in the flowchart, which may occur simultaneously or be somehow jumped, meaning that the different passages will not necessarily be followed step by step in the event of a future unrest, with their precise temporal order; iv) there is not distinction between Eruption Types 1+ (that is magmatic eruptions), since to date it is impossible to determine the type of volcanic eruption and its duration only based on the monitoring data of the unrest.

It should finally be noted that the presented conceptual model can represent a starting point for the quantification of short-term eruption forecasting and hazard quantification, adopting statistical strategies like Event Trees (e.g., Newhall and Hoblitt, 2002; Marzocchi et al.,

2008; Newhall and Pallister, 2015) or Bayesian Belief Networks (e.g., Aspinall et al., 2003; Hinks et al., 2014), or other similar techniques. However, this quantification will require future work for the definition of the probability of the different paths identified in Fig. 13B, on the basis of past unrest episodes and monitoring data of Vulcano or analogue volcanoes.

4.2.1. Shallow hydrothermal unrest (Unrest Type 1)

Crises similar to those of 2004 are events that involve only the shallow hydrothermal system, and its connected hazards. In these episodes, the increase of the gas/water ratio, the CO_2 (e.g., >10 mole%) and He concentration, the $^3He/^4He$ isotopic ratio and the $\delta^{13}C_{CO2}$ of the fumarolic gases at the crater, together with a modest increase of the frequencies of occurrence of the volcano-seismic events (e.g., >15 events per day), are indicative of degassing anomalies (the "crisis"). These events are accompanied by modest increases in emission temperature and flow of fumarolic fluids at the crater, homogenization of the chemical and isotopic composition throughout the fumarolic field, and its areal extension.

In this case, the observable variations are mainly evident in the crater area of La Fossa, and do not extend significantly into the peripheral systems of degassing. More in detail, anomalies in the chemical-physical parameters of the thermal waters are not observed, and the release of CO_2 from soils increases only at Faraglione and Grotte Palizzi sites, but not in the low-flux sites of the Vulcano Porto area. Moreover, these variations do not match any significant ground deformation or intense volcano-tectonic seismicity.

Within our conceptual model, as indicated by the paths around "1" in Fig. 13B, this type of unrest indicates a modest increase in the total contribution of magmatic fluids to the volcanic system, linked to variations in permeability or local overpressures in the latite magmatic reservoirs. Such crises are therefore to be considered as episodes of increased activity of the system, although they are not necessarily linked to magmatic dynamics *sensu stricto*. In this view, specific geochemical variations in fumaroles (i.e. He/CO_2), although smaller than those during crises, can be indicative of the involvement of new magma in the volcanic degassing, and therefore can actually anticipate an episode of increase of gas emissions even by a few years, as happened in the case of the 2004 crisis. These phases are accompanied by modest or no increases in superficial microseismicity. Although they do not indicate any increases in volcanic activity in the short term, they can have a profound significance for assessing the possible evolution of the system in the medium and long term.

4.2.2. Deep hydrothermal unrest (Unrest Type 2)

Crises similar to those of 1988 could lead to more significant and possibly more dangerous phenomena. In addition to the variations observed to the crater and discussed for Unrest Type 1 (Section 4.2.1), the occurrence of variations in the physical-chemical parameters of the thermal aquifer (variations in pH, Eh, temperature and phreatic level, simultaneously in different measurement sites), the increase in CO_2 flux from soils in peripheral areas (e.g., the soils of Vulcano Porto area, with average values >80 g m^{-2} d^{-1}), and the evident expansion of exhalative areas, or the reappearance of mofette (low-temperature fumaroles) and steam emissions (e.g., in the Camping Sicilia and Centrale Telecom areas), can be related to a large contribution of deep fluids, which cannot be disposed exclusively via the crater.

This has qualitative implications on the degassing of magma amounts that, in this case, may imply an evolution of the deep hydrothermal system towards critical conditions. The geochemical anomalies in the peripheral systems would indeed indicate a significant increase in the contribution of fluids and energy from the magmatic system, which would cause an important perturbation of the deep hydrothermal system (as well as the superficial ones). In this condition, as highlighted by the paths around "2" in Fig. 13B, the geothermal system is considered more susceptible to being decapitated by a significant phreatic

event (Eruption Type 0, see Section 2.7.2), which could trigger successive magmatic and eruptive activity (Eruption Type 1 +, see Section 2.7.2).

The instability of the deep hydrothermal system that characterizes the Unrest Type 2 may be caused by deep magma sources, as well as by the occurrence of large landslides that could disrupt the deep hydrothermal system through a quick and massive depressurization and/or the occurrence of a "cap" effect that could inhibit the normal degassing dynamics.

Rapid and widespread variations in peripheral systems could be considered anomalies connected to the approach of eruptive phenomena, even in the absence of crater crises. It is not known whether rapid escalation to volcanic events could overturn the temporal relations between the anomalies in the crater area (including the volcano-seismic sequences under La Fossa) and those in the peripheral systems. During these phases, the probable pressurization of the boiling aquifers under Baia di Levante can dangerously approach phreatic explosion conditions. If, on one hand, the concentrations of reactive species (CO, H_2, partly CH_4) in the fumaroles of Baia di Levante can theoretically record this evolution, two critical issues emerge from the perspective of forecasting explosive episodes. First, the overpressure threshold is not known with respect to the hydrostatic value for which the aquifer in question becomes truly unstable. Second, the evolution of the geothermal system toward flashing could be extremely rapid, with shorter time scales both with respect to those of the migration of the gaseous signals to the surface and with respect to the available observing and processing systems.

4.2.3. Magmatic unrest (Unrest Type 3)

The migration of magma bodies toward the surface determines the conditions for volcanic eruptions with the involvement of magma. Crises linked to eruptive events of this type have never been monitored at Vulcano with a modern system.

The detection of fracturing seismicity at depths of 2-5 km and/or medium- to short-term ground deformations, accompanied by the geochemical anomalies to the crater and peripheral systems (as in Unrest Types 1 and 2), characterizes Unrest Type 3, being indicative- of changes in the dynamics of the magmatic system and magma migrations toward the surface.

As for Unrest Type 2, Unrest Type 3 may have a deep origin, as well as may be triggered by the occurrence of phreatic events (Eruption Type 0, Section 2.7.2) that could trigger a depressurization of the magmatic system inducing consequent magmatic migrations and therefore lead to magmatic eruptive episodes (Eruption Type 1 +, Section 2.7.2). These paths are indicated around "3" in Fig. 13B.

5. Conclusions and final remarks

The adopted three steps review scheme allowed evaluating the strengths and the weakness of the present day state of knowledge about hazard quantifications for Vulcano and for its main input information.

These steps led to several important results, such as i) the definition of the reference period for Vulcano (5 ka), ii) the definition of 5 possible eruption types and their frequency in Vulcano eruptive record in the reference period, iii) the review of all available hazard quantification for practically all possible eruptive and non-eruptive hazardous phenomena, iv) the identification of the potential paths to eruptions and the consequent definition of 3 different unrest types. More specifically:

- A reference period of 5 ka is considered to represent the present day volcanic system. We consider the variability of the volcanic activity in this period representative for future activity, at least for ordinary mean return periods (> 10^{-4} -10^{-5} yr^{-1}, Connor, 2011). Eruptive styles not represented in this period, but that occurred in the same tectonic context (that is, in the period 10 to 5 ka), cannot be completely ruled out. Thus, we included in the discussions also those

events that occurred in this longer period, even if not represented in the 5 ka. It is also worth noting that existing discrepancies among stratigraphic successions of La Fossa and Vulcanello activity do not prevent a solid discussion on eruptive styles and recurrence rates in the reference period of 5 ka. Consequently, they have only a limited impact on hazards quantifications.

- Based on present knowledge, volcanic phases (quiescence, unrest, eruption) may be characterized as it follows:
  o Quiescence periods are characterized by diffuse degassing at and around La Fossa cone, and evident activity of the hydrothermal system, with almost absent seismicity and deformations and episodic landslides and lahars mainly triggered by rain.
  o Recent unrest episodes mainly show anomalies in the hydrothermal system, with an increase in concentration of magmatic gases, larger fluxes and higher temperatures, mainly concentrated in the crater area, but sometimes extended to more peripheral areas. Unrest episodes leading to eruptions have never been observed through a modern monitoring system. On the one side, this lack prevents an objective investigation of the possible paths to eruptions, that are here discussed only in terms of an interpretative conceptual model. On the other side, this lack does not allow for a characterization of the non-eruptive hazards in periods of intense activity. In future studies, this may be partially compensated by considering unrest in analogue volcanoes.
  o Eruptions can by classified into 5 Eruption Types: Type 0 - Phreatic, Type 1 - Effusive and Strombolian, Type 2 – Vulcanian, Type 3- Explosive sustained, Type 4 – Phreatomagmatic. Phreatic eruptions are phreatic explosions involving the deep hydrothermal system and thus causing eruptive phenomena as ashfall, ballistic clasts or PDCs. From the known eruptive record, all types have mean annual frequencies in range 10^{-2} - 10^{-3} /year, with a relative prevalence of Type 1 and 2 eruptions (almost 50% and 30% in the last 2 ka, respectively). Rarer are Type 0 and 3 eruptions (about 10% in the last 2 ka). Type 4 eruptions are not represented in the reference period (there is one event in 10 ka). While uncertainty in the stratigraphic succession has a limited impact in these counts, some important analyses are missing, like a solid evaluation of the completeness of the eruptive record through time. The record of the eruptive phenoma at Vulcano appears sufficient to enable the characterization of source variability beyond the observed one, at least for ordinary mean annual frequencies. This variability, and in particular extreme values, may be potentially benchmarked making use of analogue volcanoes.
- Quantitative probabilistic hazard studies are few, limited to tephra and ballistic clasts (2 out of the 13 considered hazards), and these studies include a limited exploration of natural variability (for eruptive size and vent position). More common are the analyses of specific scenarios, as for PDCs, gases, large landslides, and tsunami. For other hazards, quantifications are completely absent, apart from susceptibility studies (slope instability), past data (vent opening, lava flows, shock waves, lahars), regional studies (seismic hazard) or qualitative analyses (deformations). The most frequent and potentially dangerous hazards are volcanic gases, anomalies in the aquifers and the hydrothermal system, as well as seismic activity and lahars, which may occur in all the phases of the volcano. For eruptive hazards, apart from vent opening, tephra fallout and ballistic clasts are the most common, for which more advanced studies exist. PDCs are instead common only for rarer Type 2b and Type 4 eruptions, and lava flows only for Eruption Types 1 and 2.
- The developed qualitative conceptual model allows for a characterization of unrest episodes linking their potential evolution toward eruption to the deep and superficial structure of the volcanic feeding system. We defined 3 types of unrest (shallow hydrothermal, deep hydrothermal, and magmatic unrest episodes) that may be

potentially distinguished by the monitoring signals. Phreatic eruptions (Type 0) are expected only during deep hydrothermal or magmatic unrest that involve the deepest part of the hydrothermal system. Magmatic eruptions (Type 1+) are mainly expected in magmatic unrest episodes, when new magma ascends from the deepest reservoirs. Path to eruptions in this conceptual model have been organized into a flow chart that links quiet periods to the different eruption types through different phenomenological escalations. The main paths to eruptions identified include either rapid depressurization of the magmatic system (due to large-scale landslides and/or hydrothermal explosions and/or the onset of an unrest involving the deeper hydrothermal system) or movements of magma from the deep plumbing system.

The overall level of knowledge that emerges from this review appears adequate for a satisfactory quantification, on a statistical basis, only of the conditional hazards for tephra fall and ballistic blocks, even if the available hazard studies present some significant gaps. These gaps are mainly due to the lack of some important input information, like the lack of quantification of the spatial probability of vent opening, of the unconditional probability of eruption, and of the conditional probability of eruption types, preventing the possibility of developing full unconditional hazard quantifications. Moreover, only the most frequent types of eruptions are considered, and part of the natural variability in terms of eruptive size is neglected. For the other eruptive hazards, probabilistic hazard studies quantifying the impact of source variability do not exist, while quantitative studies exist only for single past events. An extension toward probabilistic (conditional and unconditional) hazard quantifications is therefore required in the future, to allow a quantitative evaluation of the range of potential intensity and their probability of occurrence in the future in all the areas of Vulcano. For non-eruptive hazards, quantitative hazard assessments are not available, and this gap should be overcome in the future. Noteworthy, the lack of monitored unrest leading to eruptions reduces the possibility to quantify their potential in periods of higher activity. For all these reasons, at present, the characterization of the multiple hazards of the island of Vulcano is largely incomplete.

This review identified the main potential hazards characterizing Vulcano and may provide the ground for future improvements for single and multi-hazard long to short-term hazard quantifications. More specifically, it highlighted important gaps in both hazard models and monitoring system. To fill these gaps, different activity may be put in place. Among these possible activities, in the followings we try to list the ones that we judge potentially more impacting, grouping them for type of activity:

- Analyses to improve the knowledge at the base of hazard quantifications:
  o A better definition of the regional tectonics and the local structures, to overcome the alternative interpretations available in the literature.
  o New samplings at La Fossa and Vulcanello, to overcome the existing discrepancies in chronostratigraphic interpretations.
  o New multi-disciplinary analyses of the historical documents for the last 2500 years, to fill the important gaps for ancient Greco-Roman and, especially, Medieval epochs.
  o Detailed reconstruction of the eruptive units and careful evaluation of the completeness of the eruptive records for all eruption types in the reference period.
- Analyses at the base of hazard quantifications:
  o Quantification of the spatial probability of vent opening, potentially as a function of eruption types and local structures.
  o Quantification of the probability of the different eruption types, conditional upon the occurrence of an eruption in the next future.
  o Quantification of the unconditional probability of eruption.

o Joint inversion of existing and new data to constrain the sub-surface structure of the La Fossa cone, to constrain the potential for future collapses.

- Hazard analyses:

o Probabilistic hazard analyses are very limited and, when they exist, are focused on specific types of eruptions occurring at La Fossa. This limits the ability to evaluate the range of potential intensity and their probability of occurrence in the future in all the areas of Vulcano. Thus, hazard quantifications should progressively consider all potential phenomena, starting from the most frequent. For example, there is the need of detailed characterization of gas hazards, including in houses and touristic areas, aerosol of species with long-term impacts, also increasing the awareness on these hazards and the potential associated risks.

o Analysis of the potential remobilization of volcanic ashes due to the wind, which may drastically modify volcanic ash hazard maps in windy and arid areas like Vulcano.

o Re-evaluation of exposure and vulnerability, in order to refine the areas in which it is required to detail more hazard quantification, to improve the quantification of risk.

- Monitoring system:

o Deployment of instrumentations in the area of Vasca degli Ippopotami and Isthmus, where potential toxic gases and phreatic activity are possible.

We note that these analyses are strictly finalized to those studies that may directly impact in the short term the quantification and the characterization of hazards in Vulcano. Therefore, we did not report the many potential studies that may lead to important improvements of the basic scientific knowledge on which to ground long-term improvements.

Declaration of Competing Interest

The authors declare that they have no known competing financial interests or personal relationships that could have appeared to influence the work reported in this paper.

Acknowledgements

References

Achilli, V., Baldi, P., Baratin, L., Bonin, C., Ercolani, E., Gandolfi, S., Anzidei, M., Riguzzi, F., 1998. Digital photogrammetric survey on the island of Vulcano. Acta Vulcanol. 10, 1–5.

ACS-CCS (American Chemical Society – Committee on Chemical Safety), 2015. Identifying and Evaluating Hazards in Research Laboratories - Guidelines developed by the Hazard Identification and Evaluation Task Force of the American Chemical Society's Committee on Chemical Safety. American Chemecial Society, Washington, D.C.

Agnello, G.M., 1992. Terremoti ed eruzioni vulcaniche nella Sicilia medievale. Quaderni medievali 34, 73–111.

Aiuppa, A., Dongarrà, G., Capasso, G., Allard, P., 2000. Trace elements in the thermal groundwaters of Vulcano Islands (Sicily). J. Volcanol. Geotherm. Res. 98, 189–207.

Aiuppa, A., Inguaggiato, S., McGonigle, A.J.S., O'Dwyer, M., Oppenheimer, C., Padgett,

M.J., Rouwet, D., Valenza, M., 2005. H2S fluxes from Mt. Etna, Stromboli and Vulcano (Italy) and implications for the global volcanic sulfur budget. Geochim. Cosmochim. Acta 69, 1861–1871.

Alparone, S., Cannata, A., Gambino, S., Gresta, S., Milluzzo, V., Montalto, P., 2010. Time-space variation of volcano-seismic events at La Fossa (Vulcano, Aeolian Islands, Italy): new insights into seismic sources in a hydrothermal system. Bull Volcanol 72, 803–816.

Alparone, S., Bonforte, A., Gambino, S., Guglielmino, F., Obrizzo, F., Velardita, R., 2019. Dynamics of Vulcano Island (Tyrrhenian Sea, Italy) investigated by long-term (40 years) geophysical data. Earth Sci. Rev. 190, 521–535.

Annen, C., 1992. Fumerolles et champs fumerolliens de L'ile de Vulcano, iles eoliennes. Institute of Earth Sciences, University of Geneva, Switzerland, Italie Master Thesis.

Argnani A, Serpelloni E, Bonazzi C (2007). Pattern of deformation around the central Aeolian Islands: evidence from multichannel seismics and GPS data. Terra Nova, 19, 317–323, 2007.

Arrighi, S., Tanguy, J., Rosi, M., 2006. Eruptions of the last 2200 years at Vulcano and Vulcanello (Aeolian Islands, Italy) dated by high accuracy archeomagnetism. Phys. Earth Planet. Interiors 159, 225–233.

Aspinall, W.P., Woo, G., Voight, B., Baxter, P., 2003. Evidence-based volcanology: application to eruption crises. J Volcanol Geotherm Res 128 (1–3), 273–285.

Badalamenti, B., Gurrieri, S., Hauser, S., Tonani, F., Valenza, M., 1984. Considerazioni sulla concentrazione e sulla composizione isotopica della CO2 presente nelle manifestazioni naturali e nella atmosfera dell'isola di Vulcano. Miner. Petrogr. Acta 39, 367–378.

Barbano, S., Castelli, V., Pirrotta, C., 2017. Materiali per un catalogo di eruzioni di Vulcano e di terremoti delle isole Eolie e della Sicilia nordorientale (secc. XV-XIX). Quaderni di Geofisica, 142, ISSN 1590-2595.

Barberi, F., Gandino, A., Gioncada, A., La Torre, P., Sbrana, A., Zenucchini, C., 1994. The deep structure of the Eolian Arc (Filicudi –Panarea –Vulcano sector) in light of gravimetric, magnetic and volcanological data. J. Volcanol. Geotherm. Res. 61, 189–206.

Barclay, J., Rutherford, M.J., Carroll, M.R., Murphy, M.D., Devine, J.D., Gardner, J., Sparks, R.S.J., 1998. Experimental phase equilibria constraints on preeruptive storage conditions of the Soufrière Hills magma. Geophys. Res. Lett. 25, 3437–3440.

Barde-Cabusson, S., Finizola, A., Revil, A., Ricci, T., Piscitelli, S., Rizzo, E., et al., 2009. New geological insights and structural control on fluid circulation in La Fossa cone (Vulcano, Aeolian Islands, Italy). J. Volcanol. Geothermal Res. 185 (3), 231–245.

Barreca, G., Bruno, V., Cultrera, F., Mattia, M., Monaco, C., Scarfì, L., 2014. New insights in the geodynamics of the Lipari–Vulcano area (Aeolian Archipelago, southern Italy) from geological, geodeticand seismological data. J. Geodyn. 82, 150–167.

Baumann, V., Bonadonna, C., Cuomo, S., Moscariello, M., Biass, S., Pistolesi, M., Gattuso, A., 2019. Mapping the susceptibility of rain-triggered lahars at Vulcano island (Italy) combining field characterization, geotechnical analysis, and numerical modelling. Natural Hazards and Earth System Science.

Bergeat, A., 1899. Die aeolischen Inseln Stromboli, Panaria, Salina, Lipari, Vulcano, Filicudi und Alicudi geologisch beschrieben. Abhandlungen bayer. Akad Wissenschaften 20 (1899/1900) I Abt. 1-274, München.

Biass, S., Bonadonna, C., 2012. A fast GIS-based risk assessment for tephra fallout: the example of Cotopaxi volcano, Ecuador - Part I: Probabilistic hazard assessment. Nat. Haz. https://doi.org/10.1007/s11069-012-0378-z.

Biass, S., Bonadonna, C., Connor, L., Connor, C., 2016a. TephraProb: a Matlab package for probabilistic hazard assessments of tephra fallout. J. Appl. Volcanol. 5, 10. https://doi.org/10.1186/s13617-016-0050-5.

Biass, S., Bonadonna, C., Di Traglia, F., Pistolesi, M., Rosi, M., Lestuzzi, P., 2016b. Probabilistic evaluation of the physical impact of future tephra fallout events for the Island of Vulcano, Italy. Bull Volcanol 78, 37. https://doi.org/10.1007/s00445-016-1028-1.

Biass, S., Falcone, J.L., Bonadonna, C., Di Traglia, F., Pistolesi, M., Rosi, M., Lestuzzi, P., 2016c. Great Balls of Fire: A probabilistic approach to quantify the hazard related to ballistics — A case study at La Fossa volcano, Vulcano Island, Italy. J. Volcanol. Geotherm. Res. 325, 1–14.

Billi, A., Barberi, G., Faccenna, C., Neri, G., Pepe, F., Sulli, A., 2006. Tectonics and seismicity of the Tindari Fault System, southern Italy: crustal deformations at the transition between ongoing contractional and extensional domains located above the edge of a subducting slab. Tectonics 25 (2).

Bishop, A.W., 1955. The use of the slip circle in the stability analysis of slopes. Geotechnique 5 (1), 7–17.

Blanco-Montenegro, I., De Ritis, R., Chiappini, M., 2007. Imaging and modelling the subsurface structure of volcanic calderas with high-resolution aeromagnetic data at Vulcano (Aeolian Islands, Italy). Bull. Volcanol. 69, 643–659. https://doi.org/10.1007/s00445-006-0100-7.

Bolognesi, L., D'Amore, F., 1993. Isotopic variation of the hydrothermal system on Vulcano Island, Italy. Geochim. Cosmochim. Acta 9, 2069–2082. https://doi.org/10.1016/0016-7037(93)90094-D.

Bonaccorso, A., 2002. Ground deformation of the southern sector of the Aeolian islands volcanic arc from geodetic data. Tectonophysics 351, 181–192.

Bonaccorso, A., Bonforte, A., Gambino, S., 2010. Thermal expansion– contraction and slope instability of a fumarole field inferred from geodetic measurements at Vulcano. Bull Volcanol. https://doi.org/10.1007/s00445-010-0366-7.

Bonafede, M., 1995. Interaction between seismic and volcanic deformation: A possible interpretation of ground deformation observed at Vulcano Island (1976-84), Terra Research. Terra Nova 7 (1), 80–86.

Bonforte, A., Guglielmino, F., 2008. Transpressive strain on the Lipari–Vulcano volcanic complex and dynamics of the "La Fossa" cone (Aeolian Islands, Sicily) revealed by GPS surveys on a dense network. Tectonophysics 457, 64–70. https://doi.org/10.1016/j.tecto.2008.05.016.

Bosman, A., Casalbore, D., Chiocci, F.L., Romagnoli, C., 2013. Bathymorphological map. Central Aeolian Sector (Scale 1: 50,000). In: Lucchi, F., Peccerillo, A., Keller, J., Tranne, C.A., Rossi, P.L. (Eds.), Geology of the Aeolian Islands (Italy). Geological Society, London Memoirs, 37, enclosed DVD.

Boyce, A.J., Fulignati, P., Sbrana, A., Fallick, A.E., 2007. Fluids in early stage hydrothermal alteration of high-sulfidation epithermal systems: A view from the Vulcano active hydrothermal system (Aeolian Island, Italy). J. Volcanol. Geotherm. Res. 166, 76–90.

Bruno, P.P.G., Castiello, A., 2009. High-resolution onshore seismic imaging of complex volcanic structures: An example from Vulcano Island, Italy. J. Geophys. Res. 114, B12303. https://doi.org/10.1029/2008JB005998.

Bukumirovic, T., Italiano, F., Nuccio, P.M., 1997. The evolution of a dynamic geological system: The support of a GIS for geochemical measurements at the fumarole field of Vulcano, Italy. Volcanol. Geotherm. Res. 79, 253–263. https://doi.org/10.1016/S0377-0273(97)00032-2.

Bullock, L.A., Gertisser, R., O'Driscoll, B., Harland, S., 2019. Magmatic evolution and textural development of the 1739 CE Pietre Cotte lava flow, Vulcano, Italy. J. Volcanol. Geotherm. Res. 372, 1–23. https://doi.org/10.1016/j.jvolgeores.2019.01.017.

Cannata, A., Diliberto, S., Alparone, S., Gambino, S., Gresta, S., Liotta, M., Madonia, P., Milluzzo, V., Aliotta, M., Montalto, P., 2012. Multiparametric approach in investigating volcano-hydrothermal systems: the case study of Vulcano (Aeolian Islands, Italy). Pure Appl. Geophy 169, 167–182. https://doi.org/10.1007/s00024-011-0297-z.

Capaccioni, B., Tassi, F., Vaselli, O., 2001. Organic and inorganic geochemistry of low temperature gas discharges at the Levante beach, Vulcano Island, Italy. J. Volcanol. Geotherm. Res. 108 (1–4), 173–185. https://doi.org/10.1016/S0377-0273(00)00284-5.

Capasso, G., Federico, C., Madonia, P., Paonita, A., 2014. *Response of the shallow aquifer of the volcano-hydrothermal system during the recent crises at Vulcano Island (Aeolian Archipelago, Italy)*. J. Volcanol. Geotherm. Res. 273, 70–80.

Capasso, G., Inguaggiato, S., 1998. A simple method for the determination of dissolved gases in natural waters.An application to thermal waters from Vulcano Island. Appl. Geochem. 13, 631–642.

Capasso, G., Dongarrà, G., Haiser, S., Favara, R., Valenza, M., 1992. Isotope composition of rain water, well water and fumarolic steam on the island of Vulcano, and their implications for volcanic surveillance. J. Volcanol. Geotherm. Res. 49, 147–155. https://doi.org/10.1016/0377-0273(92)90010-B.

Capasso, G., Favara, R., Inguaggiato, S., 1997a. Chemical features and isotopic gaseous manifestation on Vulcano Island (Aeolian Island): An interpretative model of fluid circulation. Geochim. Cosmochim. Acta 61, 3425–3442. https://doi.org/10.1016/S0016-7037(97)00163-4.

Capasso, G., Inguaggiato, S., Nuccio, P.M., Pecoraino, G., Sortino, F., 1997b. *Variazioni composizionali dei fluidi fumarolici di Vulcano*. In: La Volpe, L., Dellino, P., Nuccio, P.M., Privitera, E., Sbrana, A. (Eds.), Progetto Vulcano: Risultati dell'Attività di Ricerca 1993-95. Felici, Pisa, pp. 86–92.

Capasso, G., Favara, R., Francofonte, S., Inguaggiato, S., 1999. Chemical and isotopic variations in fumarolic discharge and thermal waters at Vulcano Island (Aeolian Island, Italy) during 1996: Evidence of resumed volcanic activity. J. Volcanol. Geotherm. Res. 88, 167–175. https://doi.org/10.1016/S0377-0273(98)00111-5.

Capasso, G., Favara, R., Inguaggiato, S., 2000. Interaction between fumarolic gases and thermal groundwaters at Vulcano Island (Italy): evidences from chemical composition of dissolved gases in waters. J. Volcanol. Geotherm. Res. 102, 309–318.

Capasso, G., D'Alessandro, W., Favara, R., Inguaggiato, S., Parello, F., 2001. Interaction between the deep fluids and the shallow groundwaters on Vulcano Island (Italy). J. Volcanol. Geotherm. Res. 108, 187–198. https://doi.org/10.1016/S0377-0273(00)00285-7.

Carapezza, M., Nuccio, P.M., Valenza, M., 1981. *Genesis and evolution of the fumaroles of Vulcano (Aeolian Islands, Italy): A geochemical model*. Bull. Volcanol. 44, 547–563.

Carapezza, M., Dongarrà, G., Hauser, S., Longinelli, A., 1983. *Preliminary isotopic investigations on thermal waters from Vulcano Island, Italy*. Miner. Petrogr. Acta 27, 221–232.

Carapezza, M.L., Barberi, F., Ranaldi, M., Ricci, T., Tarchini, L., Barrancos, J., Fischer, C., Perez, N., Weber, K., Di Piazza, A., Gattuso, A., 2011. Diffuse CO2 soil degassing and CO2 and H2S air concentration and related hazard at Vulcano Island (Aeolian arc, Italy). J. Volcanol. Geotherm. Res. https://doi.org/10.1016/j.jvolgeores.2011.06.010.

Carapezza, M.L., Di Piazza, A., Gattuso, A., Ranaldi, M., Sortino, F., Tarchini, L., 2016a. Gas hazard assessment in the touristic area of Levante Beach (Vulcano island, Italy). EGU General Assembly, Vienna.

Carapezza, M.L., Di Piazza, A., Gattuso, A., Ranaldi, M., Sortino, F., Tarchini, L., 2016b. Hazardous emission of volcanic gases in the touristic site of Levante Beach (Vulcano island, Italy). Cities on Volcanoes, Chile.

Casalbore, D., Romagnoli, C., Bosman, A., De Astis, G., Lucchi, F., Tranne, C.A., 2018. Chiocci FL (2018), Multi-stage formation of La Fossa Caldera (Vulcano Island, Italy) from an integrated subaerial and submarine analysis. Mar Geophys Res. https://doi.org/10.1007/s11001-018-9358-3.

Cavarretta, G., Tecce, F., Serracino, M., De Vivo, B., 1988. Fluid inclusion, sulphur and strontium isotopes in hydrothermal anhydrite from the Isola di Vulcano-1 deep well, Aeolian Islands, Italy. Rend. Soc. Ital. Mineral. Petrol. 43, 975–985.

Chiarabba, C., Pino, N.A., Ventura, G., Vilardo, G., 2004. Structural features of the shallow plumbing system of Vulcano Island Italy. Bull. Volcanol. 66 (6), 477–484.

Chiodini, G., Cioni, R., Raco, B., Taddeucci, G., 1991. Gas geobarometry applied to evaluate phreatic explosion hazard at Vulcano Island. Acta Vulcanol. 1, 193–198.

Chiodini, G., Cioni, R., Marini, L., 1993. Reactions governing the chemistry of crater fumaroles from Vulcano Island, Italy, and implications for volcanic surveillance.

Appl. Geochem. 8, 357–371. https://doi.org/10.1016/0883-2927(93)90004-Z.

Chiodini, G., Cioni, R., Marini, L., Panichi, C., 1995. Origin of fumarolic fluids of Vulcano Island, Italy and implications for volcanic surveillance. Bull. Volcanol. 57, 99–110. https://doi.org/10.1007/BF00301400.

Chiodini, G., Cioni, R., Guidi, M., Marini, L., Panichi, C., Raco, B., Taddeucci, G., 1996. Geochemical surveillance at Vulcano island from 1993 to 1995. Acta Vulcanol. 8, 193–197.

Chiodini, G., Allard, P., Caliro, S., Parello, F., 2000. 18O exchange between steam and carbon dioxide in volcanic and hydrothermal gases: Implications for the source of water. Geochim. Cosmochim. Acta 64, 2479–2488. https://doi.org/10.1016/S0016-7037(99)00445-7.

Cioni, R., D'Amore, F., 1984. A genetic model for the crater fumaroles of Vulcano Island (Sicily, Italy). Geothermics 13, 375–384. https://doi.org/10.1016/0375-6505(84)90051-8.

Clocchiatti, R., Gioncada, A., Mosbah, M., Sbrana, A., 1994. Possibile deep origin of sulfur output at Vulcano (Southern Italy) in the light of melt inclusion studies. Acta Vulcanol. 5, 49–53.

Connor, C.B., 2011. A quantitative literacy view of natural disasters and nuclear facilities. Numeracy 4 (2), 2. https://doi.org/10.5038/1936-4660.4.2.2.

Continisio, R., Ferrucci, F., Gaudiosi, G., 1997. Malta Escarpment and Mt Etna: early stages of an asymmetric rifting process? Evidences from geophysical and geological data. Acta Vulcanologica 9, 45–53.

Cortecci, G., Dinelli, E., Bolognesi, L., Boschetti, T., Ferrara, G., 2001. Chemical and isotopic compositions of water and dissolved sulfate from shallow wells on Vulcano Island, Aeolian Archipelago, Italy. Geothermics 30 (1), 69–91.

Cortese, E., Sabatini, V., 1892. Descrizione geologico-petrografica delle Isole Eolie. Tipografia Nazionale, Roma.

Costa, S., Masotta, M., Gioncada, A., Pistolesi, M., Bosch, D., Scarlato, P., 2020. Magma evolution at La Fossa volcano (Vulcano Island, Italy) in the last 1000 years: evidence from eruptive products and temperature gradient experiments. Contrib Mineral Petrol 175, 31. https://doi.org/10.1007/s00410-020-1669-0.

D'Addezio, G., Carapezza, M.L., Riposati, D., Piccione, C., Ricci, T., Angioni, B., Di Laura, F., Palone, S., 2008. "IlVulcanoInforma": The restyling of the INGV Volcanological Information Centres, Aeolian Islands, Italy. In: AGU Fall meeting, San Francisco (USA), December 15-19, 2008.

D'Alessandro, W., Aiuppa, A., Bellomo, S., Brusca, L., Calabrese, S., Kyriakopoulos, K., Liotta, M., Longo, M., 2013. Sulphur-gas concentrations in volcanic and geothermal areas in Italy and Greece: Characterising potential human exposures and risks. J. Geochem. Expl. 131, 1–13. https://doi.org/10.1016/j.gexplo.2012.08.015.

Davì, M., De Rosa, R., Barca, D., 2009. A LA-ICP-MS study of minerals in the Rocche Rosse magmatic enclaves: Evidence of a mafic input triggering the latest silicic eruption of Lipari Island (Aeolian Arc, Italy). J. Volcanol. Geotherm. Res. 182, 45–56.

De Astis, G., Frazzetta, G., La Volpe, L., 1989. I depositi di riempimento della caldera del Piano ed i depositi della Lentia. BollettinoGNV (Gruppo Nazionale di Vulcanologia) 2, 763–778.

De Astis, G., La Volpe, L., Peccerillo, A., Civetta, L., 1997a. Evoluzione vulcanologica e magmatologica dell'isola di Vulcano. In: La Volpe, L., Dellino, P., Nuccio, P.M., Privitera, E., Sbrana, A. (Eds.), Progetto Vulcano: Risultati dell'attività di Ricerca 1993-95. Felici Editore, Pisa, pp. 155–177.

De Astis, G., La Volpe, L., Peccerillo, A., Civetta, L., 1997b. Volcanological and petrological evolution of Vulcano island (Aeolian Arc, southern Tyrrhenian Sea). J. Geophys. Res. 102 (B4), 8021–8050.

De Astis, G., Ventura, G., Vilardo, G., 2003. Geodynamic significance of the Aeolian volcanism (Southern Tyrrhenian Sea, Italy) in light of structural, seismological, and geochemical data. Tectonics 22 (4).

De Astis, G., Dellino, P., La Volpe, L., Lucchi, F., Tranne, C.A., 2006. Geological map of the island of Vulcano (Aeolian Islands). University of Bari, University of Bologna and INGV.LAC, Firenze.

De Astis, G., Lucchi, F., Dellino, P., La Volpe, L., Tranne, C.A., Frezzotti, M.L., Peccerillo, A., 2013a. Geology, volcanic history and petrology of Vulcano (central Aeolian archipelago). Geol. Soc. Lond. Memoirs 37 (1), 281–349.

De Astis, G., Dellino, P., La Volpe, L., Lucchi, F., Tranne, C.A., 2013b. Geological map of the island of Vulcano, scale 1:10,000 (Aeolian archipelago). In: Lucchi, F., Peccerillo, A., Keller, J., Tranne, C.A., Rossi, P.L. (Eds.), The Aeolian Islands Volcanoes. Geological Society, London Memoirs, 37, enclosed DVD.

De Fino, M., La Volpe, L., Piccarreta, G., 1991. Role of magma mixing during the recent activity of La Fossa di Vulcano (Aeolian Islands, Italy). J. Volcanol. Geotherm. Res. 48, 385–398.

De Fiore, O., 1922. Vulcano (Isole Eolie). Riv. Vulcanologica I. Friedlaender (Suppl. 3). pp. 1–393.

De Fiore, O., 1925a. Sulla geologia di Vulcano (Isole Eolie). Rendiconti della Reale Accademia delle Scienze Fisiche e Matematiche. Napoli 3, 32–42.

De Fiore, O., 1925b. Il massiccio riolitico di Monte Lentia. Rendiconti della Reale Accademia delle Scienze Fisiche e Matematiche. Napoli 3, 178–182.

De Fiore, O., 1926. Le neoformazioni di Monte Saraceno. Rendiconti della Reale Accademia delle Scienze Fisiche e Matematiche. Napoli 3, 207–214.

De Ritis, R., Ventura, G., Chiappini, M., 2007. Aeromagnetic anomalies reveal hidden tectonic and volcanic structures in the central sector of the Aeolian Islands, southern Tyrrhenian Sea Italy. J. Geophys. Res. 112, B10105. https://doi.org/10.1029/2006JB004639.

Del Moro, A., Gioncada, A., Pinarelli, L., Sbrana, A., Joron, J.L., 1998. Sr, Nd, and Pb isotope evidence for open system evolution at Vulcano, Aeolian Arc, Italy. Lithos 43, 81–106.

Dellino, P., La Volpe, L., 1997. Stratigrafia, dinamiche eruttive e deposizionali, scenario eruttivo e valutazioni di pericolosità La Fossa di Vulcano. In: La Volpe, L., Dellino, P., Nuccio, M., Privitera, E., Sbrana, A. (Eds.), Progetto Vulcano: Risultati dell'attività di

ricerca 1993–1995. CNR - Gruppo Nazionale per la Vulcanologia Felici Editore, Pisa, pp. 214–237.

Dellino, P., Astis, G., Volpe, L., Mele, D., Sulpizio, R., 2011. Quantitative hazard assessment of phreatomagmatic eruptions at Vulcano (Aeolian Islands, Southern Italy) as obtained by combining stratigraphy, event statistics and physical modelling. J Volcanol Geotherm Res 201 (1–4), 364–384.

Di Liberto, V., Nuccio, P.M., Paonita, A., 2002. Genesis of chlorine and sulfur in fumarolic emissions at Vulcano Island (Italy): assessment of pH and redox conditions in the hydrothermal system. J. Volcanol. Geotherm. Res. 116, 137–150. https://doi.org/10.1016/S0377-0273(02)00215-9.

Di Maio, R., Berrino, G., 2016. Joint analysis of electric and gravimetric data for volcano monitoring. Application to data acquired at Vulcano Island (southern Italy) from 1993 to 1996. J. Volcanol. Geotherm. Res. 327, 459–468 s00445-001-0198-6.

Di Traglia, F., 2011. The last 1000 years of eruptive activity at the Fossa Cone (Island of Vulcano, Southern Italy). University of Pisa PhD thesis.

Di Traglia, F., Pistolesi, M., Rosi, M., Bonadonna, C., Fusillo, R., Roverato, M., 2013. Growth and erosion: The volcanic geology and morphological evolution of La Fossa (island of Vulcano, Southern Italy) in the last 1000 years. Geomorphology 19, 94–107.

Diliberto, I.S., 2013. Time series analysis of high temperature fumaroles monitored on the island of Vulcano (Aeolian Archipelago, Italy). J. Volcanol. Geotherm. Res. 264, 150–163.

Diliberto, I.S., Gurrieri, S., Valenza, M., 2002. Relationships between diffuse CO2 emissions and volcanic activity on the island of Vulcano (Aeolian Islands, Italy) during the period 1984-1994. Bull. Volcanol. 64, 219–228.

Dongarrà, G., Hauser, S., Capasso, G., Favara, R., 1988. Characteristics of variations in water chemistry of some wells from Vulcano island. Rend Soc It Mineral Petrol 43, 1123–1131.

Doronzo, D.M., Dellino, P., Sulpizio, R., Lucchi, F., 2016. Merging field mapping and numerical simulation to interpret the lithofacies variations from unsteady pyroclastic density currents on uneven terrain: The case of La Fossa di Vulcano (Aeolian Islands, Italy). J. Volcanol. Geotherm. Res. 330, 36–42. https://doi.org/10.1016/j.jvolgeores.2016.11.016.

The Eruption of Soufrière Hills Volcano, Montserrat, from 1995 to 1999. Druitt, T.H., Kokelaar, B.P. (Eds.), Geloficial Society, London, Memoirs 21.

Esposito, A., Pietrantonio, G., Bruno, V., Anzidei, M., Bonforte, A., Guglielmino, F., Mattia, M., Puglisi, G., Sepe, V., Serpelloni, E., 2015. Eighteen years of GPS surveys in the Aeolian Islands (southern Italy): open data archive and velocity field. Ann. Geophys 58, 4.

Faraone, D., Silvano, A., Verdiani, G., 1986. The monzogabbroic intrusion in the island of Vulcano, Aeolian Archipelago, Italy. Bull. Volcanol. 48, 299–307.

Favalli, M., Karátson, D., Mazzuoli, R., Pareschi, M.T., Ventura, G., 2005. Volcanic geomorphology and tectonics of the Aeolian archipelago (Southern Italy) based on integrated DEM data. Bull. Volcanol. 68 (2), 157–170.

Fazello, T., 1558. De rebus Siculis decades duae. Palermo 616.

Federico, C., Capasso, G., Paonita, A., Favara, R., 2010. Effects of steam-heating processes on a stratified volcanic aquifer: Stable isotopes and dissolved gases in thermal waters of Vulcano Island (Aeolian archipelago). J. Volcanol. Geotherm. Res. 192 (3), 178–190.

Ferri, M., Grimaldi, M., Luongo, G., 1988. Vertical Ground Deformation on Vulcano, Aeolian Islands, Southern Italy: Observation and Interpretations 1976 – 1986. JVGR 35, 141–150.

Ferrucci, M., Pertusati, S., Sulpizio, R., Zanchetta, G., Pareschi, M., Santacroce, R., 2005. Volcaniclastic debris flows at La Fossa Volcano (Vulcano Island, southern Italy): Insights for erosion behaviour of loose pyroclastic material on steep slopes. J. Volcanol. Geotherm. Res. 145 (3–4), 173–191. https://doi.org/10.1016/j.jvolgeores.2005.01.013.

Fiorillo, F., Wilson, R., 2004. Rainfall induced debris flows in pyroclastic deposits, Campania (southern Italy). Eng. Geol. 75 (34), 263–289.

Forni, F., Lucchi, F., Peccerillo, A., Tranne, C.A., Rossi, P.L., Frezzotti, M.L., 2013. Stratigraphy and geological evolution of the Lipari volcanic complex (central Aeolian archipelago). Geol Soc Mem 37, 213–279. https://doi.org/10.1144/M37.10.

Frazzetta, G., Lanzafame, G., Villari, L., 1980. Frane e franosità nella Forgia Vecchia di Vulcano (Isole Eolie) Istituto Internazionale di Vulcanologia - Consiglio Nazionale delle Ricerche. Open File Report 1, 80.

Frazzetta, G., La Volpe, L., Sheridan, M.F., 1983. Evolution of the Fossa cone, Vulcano. J. Volcanol. Geotherm. Res. 17, 329–360.

Frazzetta, G., Gillot, P.Y., La Volpe, L., Sheridan, M.F., 1984. Volcanic hazards at Fossa of Vulcano: data from the last 6000 years. Bull. Volcanol. 47, 105–124.

Frazzetta, G., Gillot, P.Y., La Volpe, L., 1985. The Island of Vulcano. In: IAVCEI Scientific Association Excursion Guidebook, pp. 125–140.

Fulignati, P., Gioncada, A., Sbrana, A., 1996. Hydrothermal alteration in the subsoil of Porto di Levante,Vulcano (Aeolian Islands, Italy). Acta Vulcanol. 8 (2), 129–138.

Fulignati, P., Gioncada, A., Sbrana, A., 1998. Geologic model of the magmatic–hydrothermal system of Vulcano (Aeolian islands, Italy). Mineral. Petrol. 62, 195–222.

Fulignati, P., Gioncada, A., Sbrana, A., 1999. Rare-earth element (REE) behaviour in the alteration facies of the active magmatic–hydrothermal system of Vulcano (Aeolian Islands, Italy). J. Volcanol. Geotherm. Res. 88, 325–342.

Fusillo, R., Di Traglia, F., Gioncada, A., Pistolesi, M., Wallace, P.J., Rosi, M., 2015. Deciphering post-caldera volcanism: Insight into the Vulcanello (Island of Vulcano, southern Italy) eruptive activity based on geological and petrological constraints. Bull. Volcanol. 77, 76. https://doi.org/10.1007/s00445-015-0963-6.

Gabbianelli, G., Romagnoli, C., Rossi, P.L., Calanchi, N., Lucchini, F., 1991. Submarine morphology and tectonics of Vulcano (Aeolian islands Southwestern Tyrrhenian sea). Acta Vulcanol. 1, 135–142.

Galderisi, A., Bonadonna, C., Delmonaco, G., Ferrara, F.F., Menoni, S., Ceudech, A., Biass,

S., Frischknecht, C., Manzella, I., Minucci, G., Gregg, C., 2013. Vulnerability Assessment and Risk Mitigation: The Case of Vulcano Island, Italy, Landslide Science and Practice, Volume 7: Social and Economic Impact and Policies. Springer, Berlin Heidelberg, pp. 55–64.

Gamberi, F., Marani, M.P., 1997. Detailed Bathymetric Mapping of the Eastern Offshore Slope of Lipari Island (Tyrrhenian Sea): insight into the Dark Side of an Arc Volcano. Mar. Geophys. Res. 19, 363–377.

Gambino, S., Guglielmino, F., 2008. Ground deformation induced by geothermal processes: a model for La Fossa Crater (Vulcano Island, Italy). J Geophys Res 113, B07402. https://doi.org/10.1029/2007JB005016.

Gambino, S., Campisi, O., Falzone, G., Ferro, A., Guglielmino, F., Laudani, G., Saraceno, B., 2007. Tilt measurements at Vulcano Island. Ann. Geophys. 50, 233–247.

Gambino, S., Milluzzo, V., Scaltrito, A., Scarfì, L., 2012. Relocation and focal mechanisms of earthquakes in the south-central sector of the Aeolian Archipelago: New structural and volcanological insights. Tectonophysics 524–525, 108–115.

Gambino, S., Laudani, A., Mangiagli, S., 2014. Seismicity pattern changes before the M = 4.8 Aeolian Archipelago (Italy) Earthquake of August 16, 2010. Sci. World J. https://doi.org/10.1155/2014/531212. ID531212, 8pp.

GdL_MPS - Gruppo di Lavoro MPS, 2004. Redazione della mappa di pericolosità sismica prevista dall'Ordinanza PCM 3274 del 20 marzo 2003, rapporto conclusivo per il Dipartimento della Protezione Civile, INGV, Milano–Roma, aprile 2004. 65 pp. + 5 appendici.

Ghisetti, F., Vezzani, L., 1982. The recent deformation mechanisms of the Calabrian Arc. Earth Ev. Sc. 3, 197–206.

Gioncada, A., Sbrana, A., 1991. La Fossa Caldera, Vulcano: Inferences from deep drillings. Acta Vulcanol. 1, 115–126.

Gioncada, A., Clocchiatti, R., Sbrana, A., Bottazzi, P., Massare, D., Ottolini, L., 1998. A study of melt inclusions at Vulcano (AeolianIslands, Italy): insights on the primitive magmas and on the volcanic feeding system. Bull. Volcanol. 60, 286–306.

Granieri, D., Carapezza, M.L., Chiodini, G., Avino, R., Caliro, S., Ranaldi, M., Ricci, T., Tarchini, L., 2006. Correlated increase in CO$_2$ fumarolic content and diffuse emission from La Fossa crater (Vulcano, Italy): Evidence of volcanic unrest or increasing gas release from a stationary deep magma body? Geophys. Res. Lett. 33, L13316. https://doi.org/10.1029/2006GL026460.

Granieri, D., Carapezza, M.L., Barberi, F., Ranaldi, M., Ricci, T., Tarchini, L., 2014. Atmospheric dispersion of natural carbon dioxide emissions on Vulcano island, Italy. J. Geophys. Res. https://doi.org/10.1002/2013JB010688.

Graziani, G., Martilli, A., Pareschi, M.T., Valenza, M., 1997. Atmospheric dispersion of natural gases at Vulcano island. J. Volc. Geoth. Res. 75, 283–308.

Gurioli, L., Zanella, E., Gioncada, A., Sbrana, A., 2012. The historic magmatic hydrothermal eruption of the Breccia di Commenda, Vulcano, Italy. Bull. Volcanol. 74 (5), 1235–1254. https://doi.org/10.1007/s00445-012-0590-4.

Harris, A., Alparone, S., Bonforte, A., Dehn, J., Gambino, S., Lodato, L., Spampinato, L., 2012. Vent temperature trends at the Vulcano Fossa fumarole field: the role of permeability. Bull. Volcanol. https://doi.org/10.1007/s00445-012-0593-1.

Hincks, T.K., Komorowski, J.-C., Sparks, S.R., Aspinall, W.P., 2014. Retrospective analysis of uncertain eruption precursors at La Soufrière volcano, Guadeloupe, 1975–77: volcanic hazard assessment using a Bayesian Belief Network approach. J. Appl. Volcanol. 3, 3. https://doi.org/10.1186/2191-5040-3-3.

IAEA – International Atomic Energy Agency, 2012. Volcanic Hazards in site evaluation for nuclear installations – Specific Safety Guide. In: in IAEA Safety Standards Series No. SSG-21, Vienna, 2012.

IAEA – International Atomic Energy Agency, 2016. Volcanic Hazard Assessments for Nuclear Installations: Methods and Examples in Site Evaluation. IAEA Tecdoc Series, IAEA-TECDOC-1795, 2016.

Inguaggiato, S., Mazot, A., Diliberto, I.S., Inguaggiato, C., Madonia, P., Rouwet, D., Vita, F., 2012. Total CO$_2$ output from Vulcano island (Aeolian Islands, Italy). Geochem. Geophys. Geosyst. 13 (2). https://doi.org/10.1029/2011GC003920 (Q02012).

Inguaggiato, S., Diliberto, I.S., Federeico, C., Paonita, A., Vita, F., 2018. Review of the evolution of geochemical monitoring, networks and methodologies applied to the volcanoes of the Aeolian Arc (Italy). Earth Sci. Rev. 176, 241–276.

INGV-BullVulcanoFeb20, 2020. Bollettino mensile sul monitoraggio geochimico dell'isola di Vulcano, Febbraio 2020. Istituto Nazionale di Geofisica e Vulcanologia, Palermo. https://www.pa.ingv.it/index.php/bollettini/#6c95b76kup.

INGV-DPC, 2013. Il Vulcano informa, volcanological centre, Vulcano. Opuscolo informativo rivolto ai turisti e realizzato da INGV-DPC.

INGV-DPC-V3, 2016. Project V3: Multi-disciplinary analysis of the relationships between tectonic structures and volcanic activity (Etna, Vulcano-Lipari system). Final Report, Miscellanea INGV 29. pp. 52–53. https://sites.google.com/a/ingv.it/volcpro2014/.

IPCC - Intergovernmental Panel on Climate Change, 2013. Summary for policymakers. In: Stocker, TF, Qin, D, Plattner, G-K, Tignor, M, Allen, SK, Boschung, J ... Midgley, PM (Eds.), Climate Change 2013: The Physical Science Basis. Contribution of Working Group I to the Fifth Assessment Report of the Intergovernmental Panel on Climate Change. Cambridge University Press, Cambridge, United Kingdom and New York, NY, USA.

Italiano, F., Nuccio, P.M., Valenza, M., 1984. Mass geothermal energy release at Vulcano, Aeolian Islands, Italy. Bull. Mineral. Rend. Soc. Ital. Mineral. Petrol. 39, 379–386.

Italiano, F., Pecoraino, G., Nuccio, P.M., 1998. Steam output from fumaroles of an active volcano: Tectonic and magmatic-hydrothermal controls on the degassing system at Vulcano (Aeolian arc). J. Geophys. Res. 103, 29829–29842. https://doi.org/10.1029/98JB02237.

IVHHN - International Volcano Health Hazard News, 2005. Volcanic Gases and Aerosols Guidelines. http://www.ivhhn.org/images/pdf/gas_guidelines.pdf.

Jenkins, S., Magill, C., McAneney, J., Blong, R., 2012. Regional ash fall hazard I: a probabilistic assessment methodology. Bull Volcanol 74, 1699. https://doi.org/10.1007/s00445-012-0627-8.

Keller, J., 1970. Die historischen Eruptionen von Vulcano und Lipari. Zeitschrift Deutsch. Geologie Geochimie 121, 179–185.

Keller, J., 1980. The Island of Vulcano. Rendiconti della Società Italiana di Mineralogia e Petrologia 36, 369–414.

Klose, 2007. Health risk analysis of volcanic SO2 hazard on Vulcano Island (Italy). Nat. Haz. 43 (3), 303–317. https://doi.org/10.1007/s11069-007-9115-4.

Lanzafame, G., Bousquet, J.C., 1997. The Maltese escarpment and its extension from Mt. Etna to Aeolian islands (Sicily): importance and evolution of a lithospheric discontinuity. Acta Vulcanol. 9, 121–135.

Leeman, W.P., Tonarini, S., Pennisi, M., Ferrara, G., 2005. Boron isotope variations in fumarolic condensates and thermal waters from Vulcano Island, Italy: implications for evolution of volcanic fluids. Geochim. Cosmochim. Acta 69, 143–163. https://doi.org/10.1016/j.gca.2004.04.004.

Liu, Z., Nadim, F., Garcia-Aristizabal, A., Mignan, A., Fleming, K., Luna, B.Q., 2015. A three-level framework for multi-risk assessment. Georisk Assess. Manage. Risk Eng. Syst. Geohazards 9 (2), 59–74. https://doi.org/10.1080/17499518.2015.1041989.

Lucchi, F., Tranne, C.A., De Astis, G., Keller, J., Losito, R., Morche, W., 2008. Stratigraphy and significance of Brown Tuffs on the Aeolian Islands (southern Italy). J. Volcanol. Geotherm. Res. 177, 49–70. https://doi.org/10.1016/j.jvolgeores.2007.11.006.

Madonia, P., Capasso, G., Favara, R., Francofonte, S., Tommasi, P., 2015. Spatial Distribution of Field Physico-Chemical Parameters in the Vulcano Island (Italy) Coastal Aquifer: Volcanological and Hydrogeological Implications. Water 7 (7), 3206–3224.

Madonia, P., Cangemi, M., Olivares, L., Oliveri, Y., Speziale, S., Tommasi, P., 2019. Shallow landslide generation at La Fossa cone, Vulcano island (Italy): a multidisciplinary perspective. Landslides 16 (5), 921–935. https://doi.org/10.1007/s10346-019-01149-z.

Mandarano, M., Paonita, A., Martelli, M., Viccaro, M., Nicotra, E., Millar, I.L., 2016. Revealing magma degassing below closed-conduit active volcanoes: geochemical features of volcanic rocks versus fumarolic fluids at Vulcano (Aeolian Islands, Italy). Lithos 248–251, 272–287.

Maramai, A., Graziani, L., Tinti, S., 2005. Tsunamis in the Aeolian Islands (Southern Italy): a review. Mar. Geol. 215, 11–21.

Maramai, A., Brizuela, B., Graziani, L., 2014. The Euro-Mediterranean Tsunami Catalogue. Ann. Geophys. 57 (4), S0435. https://doi.org/10.4401/ag-6437.

Marsella, M.A., Scifoni, S., Coltelli, M., Proietti, C., 2011. Quantitative analysis of the 1981 and 2001 Etna flank eruptions: a contribution for future hazard evaluation and mitigation Ann Geophys 54 (5), 492–498. https://doi.org/10.4401/ag-5334.

Marsella, M., Salino, A., Scifoni, S., Sonnessa, A., Tommasi, P., 2013. Stability conditions and evaluation of the runout of a potential landslide at the northern flank of La Fossa active volcano, Italy. In Landslide Science and Practice Springer, Berlin Heidelberg, pp. 309–314.

Marsella, M.D., Aranno, P.J.V., Scifoni, S., Sonnessa, A., Corsetti, M., 2015. Terrestrial laser scanning survey in support of unstable slopes analysis: the case of Vulcano Island (Italy). Nat Hazards 78, 443–459. https://doi.org/10.1007/s11069-015-1729-3.

Martini, M., Piccardi, G., 1979. Sorveglianza geochimica di aree interessate da vulcanismo attivo: un modello per Vulcano. Rend. Soc. Ital. Mineral. Petrol. 35 (2), 633–638.

Marzocchi, W., Sandri, L., Selva, J., 2008. BET_EF: a probabilistic tool for long- and short-term eruption forecasting. Bull. Volcan. 70, 623–632. https://doi.org/10.1007/s00445-007-0157-y.

Marzocchi, W., Garcia-Aristizabal, A., Gasparini, P., Mastellone, M., Di Ruocco, A., 2012a. Basic principles of multi-risk assessment: a case study in Italy. Nat Hazards 1–23. https://doi.org/10.1007/s11069-012-0092-x.

Marzocchi, W., Newhall, C., Woo, G., 2012b. The scientific management of volcanic crises. J Volcanol Geotherm Res 2012 (247), 181–189. https://doi.org/10.1016/j.jvolgeores.2012.08.016.

Mattia, M., Palano, M., Bruno, V., Cannavò, F., Bonaccorso, A., Gresta, S., 2008. Tectonic features of the Lipari–Vulcano complex (Aeolian archipelago, Italy) from 10 years (1996–2006) of GPS data. Terra Nova 20 (5), 370–377.

Mazzuoli, R., Tortorici, L., Ventura, G., 1995. Oblique rifting in Salina, Lipari and Vulcano islands (Aeolian islands, southern Italy). Terra Nova 7, 444–452.

Mercalli, G., 1883. Vulcani e fenomeni vulcanici in Italia. Milano, Arnaldo Forni.

Mercalli G (1891). Cenni topografici-geologici dell'isola di Vulcano e storia delle sue eruzioni dai più antichi tempi fino al presente, in Silvestri O. e Mercalli G. (edd.), Le eruzioni dell'isola di Vulcano, incominciate il 3 Agosto 1888 e terminate il 22 Marzo 1890. Relazione scientifica, 1891. Ann. Uff. Cent. Meteor. Geodin., 10 (4), 10-50.

Mercalli, G., Silvestri, O., 1891. Le eruzioni dell'isola di Vulcano, incominciate il 3 Agosto 1888 e terminate il 22 Marzo 1890. Ann. Ufficio Centrale Meteorol. e Geodin. 10 (4), 1–213.

Mignan, A., Wiemer, S., Giardini, D., 2014. The quantification of low probability-high consequences events: part I. Generic Multi Risk Approach. Nat Hazards 73, 1999–2022. https://doi.org/10.1007/s11069-014-1178-4.

Milluzzo, V., Cannata, A., Alparone, S., Gambino, S., Hellweg, M., Montalto, P., Cammarata, L., Diliberto, I.S., Gresta, S., Liotta, M., Paonita, A., 2010. Tornillos at Vulcano: clues to the dynamics of the hydrothermal system. J. Volcanol. Geotherm. Res. 198, 377–393. https://doi.org/10.1016/j.jvolgeores.2010.09.022.

Mongitore, A., 1743. Istoria cronologica de' terremoti di Sicilia, in Id., Della Sicilia ricercata nelle cose più memorabili. tomo 2, 345–445.

Napoli, R., Currenti, G., 2016. Reconstructing the Vulcano Island evolution from 3D modeling of magnetic signatures. J. Volcanol. Geotherm. Res. 320, 40–49.

Neri, G., Montalto, A., Patanè, D., Privitera, E., 1991. Earthquake space-time-magnitude patterns at Aeolian Islands (Southern Italy) and implications for the volcanic surveillance of Vulcano. Acta Vulcanol 1, 163–169.

Newhall, C.G., Hoblitt, R.P., 2002. Constructing event trees for volcanic crises. Bull

Volcanol 64, 3–20.

Newhall, C.G., Pallister, J., 2015. Chapter 8 - Using Multiple Data Sets to Populate Probabilistic Volcanic Event Trees. In: Shroder, John F., Papale, Paolo (Eds.), Volcanic Hazards, Risks, and Disasters, Chapter: 8. Elsevier, Elsevier, Amsterdam. https://doi.org/10.1016/B978-0-12-396453-3.00008-3.

Nicotra, E., Giuffrida, M., Viccaro, M., Donato, P., D'Oriano, C., Paonita, A., De Rosa, R., 2018. Timescales of pre-eruptive magmatic processes at Vulcano (Aeolian Islands, Italy) during the last 1000 years. Lithos 315–317, 347–365. https://doi.org/10.1016/j.lithos.2018.07.028.

Nuccio, P.M., Paonita, A., Sortino, F., 1999. Geochemical modeling of mixing between magmatic and hydrothermal gases: The case of Vulcano, Italy. Earth Planet. Sci. Lett. 167, 321–333. https://doi.org/10.1016/S0012-821X(99)00037-0.

Obrizzo F (2000). Vulcano - Vertical ground movements: precise levelling. May 1995-May 1996. Acta Vulcanologica. Data Related to Eruptive Activity, Unrest Phenomena and other Observations on the Italian Active Volcanoes 1996, Editor L. Villari, Vol 12 (1-2), 115-116.

Okuma, S., Nakatsuka, T., Supper, R., Komazawa, M., 2006. High-resolution aeromagnetic anomaly map of the Vulcano-Lipari volcanic complex, Aeolian Islands, Italy. Bull. Geol. Surv. Jpn. https://doi.org/10.9795/bullgsj.57.177.

Pallister, J., Papale, P., Eichelberger, J., Newhall, C., Mandeville, C., Nakada, S., Marzocchi, W., Loughlin, S., Jolly, G., Ewert, J., Selva, J., 2019. Volcano observatory best practices (VOBP) workshops - a summary of findings and best-practice recommendations. J Appl Volcanol Soc Volcan. 8, 2.

Panessa, G., 1991. Fonti greche e latine per la storia dell'ambiente e del clima nel mondo greco, I, Pisa.

Paonita, A., Favara, R., Nuccio, P.M., Sortino, F., 2002. Genesis of fumarolic emissions as inferred by isotope mass balances: CO2 and water at Vulcano Island, Italy. Geochim. Cosmochim. Acta 66 (5), 759–772. https://doi.org/10.1016/S0016-7037(01)00814-6.

Paonita, A., Federico, C., Bonfanti, P., Capasso, G., Inguaggiato, S., Italiano, F., Madonia, P., Pecoraino, G., Sortino, F., 2013. The Episodic and Abrupt Geochemical Changes at La Fossa Fumaroles (Vulcano Island, Italy) and Related Constraints on the Dynamics, Structure, and Compositions of the Magmatic System. Geochim. Cosmochim. Acta 120, 158–178.

Papale, P., 2017. Rational volcanic hazard forecasts and the use of volcanic alert levels. J. Appl. Volcanol. Soc. Volcan. 20176, 13. https://doi.org/10.1186/s13617-017-0064-7.

Pareschi, M.T., Ranci, M., 1997. Risk evaluation of SO2 emission at Vulcano island (Sicily). Trans. Ecol. Environ. 15 ISSN 1743-3541.

Pareschi, M.T., Ranci, M., Valenza, M., Graziani, G., 1999. The assessment of volcanic gas hazard by means of numerical models: An example from Vulcano Island (Sicily). Geophys. Res. Lett. 26 (10), 1405–1408. https://doi.org/10.1029/1999GL900248.

Paris, R., 2015. Source mechanisms of volcanic tsunamis. Phil. Trans. R. Soc. A 373, 20140380. https://doi.org/10.1098/rsta.2014.0380.

Paris, S., Switzer, A.D., Belousova, M., Belousov, A., Ontowirjo, B., Whelley, P.L., Ulvrova, M., 2014. Volcanic tsunami: a review of source mechanisms, past events and hazards in Southeast Asia (Indonesia, Philippines, Papua New Guinea). Nat Hazards 70, 447–470. https://doi.org/10.1007/s11069-013-0822-8.

Peccerillo, A., Frezzotti, M.L., De Astis, G., Ventura, G., 2006. Modeling the magma plumbing system of Vulcano (Aeolian Islands, Italy) by integrated fluid inclusion geobarometry, petrology and geophysics. Geology 34, 17–20.

Pesci, A., Teza, G., Casula, G., Fabris, M., Bonforte, A., 2013. Remote sensing and geodetic measurements for volcanic slope monitoring: Surface variations measured at northern flank of La Fossa Cone (Vulcano Island, Italy). Remote Sensing 5 (5), 2238–2256.

Piochi, M., De Astis, G., Petrelli, M., Ventura, G., Sulpizio, R., Zanetti, A., 2009. Constraining the recent plumbing system of Vulcano (Aeolian Arc, Italy) by textural, petrological, and fractal analysis: The 1739 A.D. Pietre Cotte lava flow. Geochem. Geophys. Geosys 10 (1). https://doi.org/10.1029/2008GC002176.

Rasà, R., Villari, L., 1991. Geomorphological and morpho-structural investigations on the Fossa cone (Vulcano, Aeolian Islands): a first outline. Acta Vulcanologica 1, 127–133.

Regione Sicilia, 2004. Piano Stralcio di Bacino per l'Assetto Idrogeologico.

Revil, A., Finizola, A., Piscitelli, S., Rizzo, E., Ricci, T., Crespy, A., Angeletti, B., Balasco, M., Barde-Cabusson, S., Bennati, L., Bolève, A., Byrdina, S., Carzaniga, N., Di Gangi, F., Morin, J., Perrone, A., Rossi, M., Roulleau, E., Suski, B., 2008. Inner structure of La Fossa di Vulcano (Vulcano Island, southern Tyrrhenian Sea, Italy) revealed by high resolution electric resistivity tomography coupled with self-potential, temperature, and CO2 diffuse degassing measurements. J. Geophys. Res. 113, B07207. https://doi.org/10.1029/2007JB005394.

Revil, A., Johnson, T.C., Finizola, A., 2010. Three-dimensional resistivity tomography of Vulcan's forge, Vulcano Island, southern Italy. Geophys. Res. Lett. 37, L15308. https://doi.org/10.1029/2010GL043983.

Ricci, T., Finizola, A., Barde-Cabusson, S., Delcher, E., Alparone, S., Gambino, S., Milluzzo, V., 2015. Hydrothermal fluid flow disruptions evidenced by subsurface changes in heat transfer modality: The La Fossa cone of Vulcano (Italy) case study. Geology. https://doi.org/10.1130/G37015.1.

Romagnoli, C., Casalbore, D., Chiocci, F.L., 2012. La Fossa Caldera breaching and submarine erosion (Vulcano island, Italy). Marine Geology 303, 87–98.

Romagnoli, C., Casalbore, D., Bortoluzzi, G., Bosman, A., Chiocci, F.L., D'Oriano, F., Gamberi, F., Ligi, M., Marani, M., 2013. Bathy-morphological setting of the Aeolian islands. In: Lucchi, F., Peccerillo, A., Keller, J., Tranne, C.A., Rossi, P.L. (Eds.), The Aeolian Islands Volcanoes. Geological Society, London Memoirs, this volume, 27–36, doi:10.1144/M37.4.

Rosi, M., Di Traglia, F., Pistolesi, M., Esposti Ongaro, T., de' Michieli Vitturi M, Bonadonna C, 2018. Dynamics of shallow hydrothermal eruptions: new insights from Vulcano's Breccia di Commenda eruption. Bull. Volcanol. 80, 83. https://doi.org/10.

1007/s00445-018-1252-y.

Ruch, J., Vezzoli, L., De Rosa, R., Di Lorenzo, R., Acocella, V., 2016. Magmatic control along a strike-slip volcanic arc: The central Aeolian arc (Italy). Tectonics. https://doi.org/10.1002/2015TC004060.

Schöpa, A., Pantaleo, M., Walter, T.R., 2011. Scale-dependent location of hydrothermal vents: Stress field models and infrared field observations on the Fossa Cone, Vulcano Island, Italy. J. Volcanol. Geotherm. Res. 203 (3), 133–145.

Selva, J., 2013. Long-term multi-risk assessment: statistical treatment of interaction among risks. Nat Hazards 67, 701–722. https://doi.org/10.1007/s11069-013-0599-9.

Selva, J., Costa, A., Marzocchi, W., Sandri, L., 2010. BET_VH: Exploring the influence of natural uncertainties on long-term hazard from tephra fallout at Campi Flegrei (Italy). Bull. Volcanol. 72 (6), 717–733. https://doi.org/10.1007/s00445-010-0358-7.

Selva, J., Costa, A., Sandri, L., Macedonio, G., Marzocchi, W., 2014. Probabilistic short-term volcanic hazard in phases of unrest: A case study for tephra fallout. J. Geophys. Res Solid Earth 119, 8805–8826. https://doi.org/10.1002/2014JB011252.

Selva, J., Costa, A., De Natale, G., Di Vito, M.A., Isaia, R., Macedonio, G., 2018. Sensitivity test and ensemble hazard assessment for tephra fallout at Campi Flegrei, Italy. Volcanol Geotherm Res 351, 1–28. https://doi.org/10.1016/j.jvolgeores.2017.11.024.

Selva, J., Acocella, V., Bisson, M., Caliro, S., Costa, A., Della Seta, M., De Martino, P., de Vita, S., Federico, C., Giordano, G., Martino, S., Cardaci, C., 2019. Multiple natural hazards at volcanic islands: a review for the Ischia volcano (Italy). J. Appl. Volcanol. 8 (1), 5. https://doi.org/10.1186/s13617-019-0086-4.

Sicardi, L., 1940. Il recente ciclo dell'attività fumarolica dell'isola di Vulcano. Bull Volcanol 7, 85–139.

Siebert, L., Simkin, T., Kimberly, P., 2010. Volcanoes of the World, 3a ed. Smithsonian Institution, Berkeley: University of California Press, Washington, DC.

Sommaruga, C., 1984. Le ricerche geotermiche svolte a Vulcano negli anni '50. In: Rendiconti della Società Italiana di Mineralogia e Petrologia. 39. pp. 355–366.

SSHAC - Senior Seismic Hazard Analysis Committe [R.J. Budnitz (Chairman), G. Apostolakis, D.M. Boore, L.S. Cluff, K.J. Coppersmith, C.A. Cornell, P.A. Morris], 1997. Recommendations for probabilistic seismic hazard analysis: Guidance on uncertainty and use of experts. U.S. Nuclear Regulatory Commission Report NUREG/CR-6372.

Stothers, R.B., Rampino, M.R., 1983. Volcanic eruptions in the Mediterranean before A.D. 630 from written and archaeological sources. J. Geophys. Res. 88 (B8), 6357–6371.

Supper, R., Motschka, K., Seiberl, W., Fedi, M., 2001. Geophysical investigations in Southern Italian active volcanic regions. Bull. Geol. Surv. Japan 52 (2/3), 89–99.

Sulpizio, R., Dellino, P., Doronzo, D.M., Sarocchi, D., 2014. Invited review: Pyroclastic density currents: state of the art and perspectives. Journal of Volcanology and Geothermal Research 283, 36–65.

Supper, R., De Ritis, R., Motschka, K., Chiappini, M., 2004. Aeromagnetic anomaly images of Vulcano and Southern Lipari Islands (Aeolian Archipelago, Italy). Ann. Geophys. 47, 6.

Taran, Y., 2011. N2, Ar, and He as a tool for discriminating sources of volcanic fluids with application to Vulcano. Italy. Bull. Volcanol. 73, 395–408. https://doi.org/10.1007/s00445-011-0448-1.

Tedesco, D., 1995. Fluid geochemistry at Vulcano Island: a change in volcanic regime or fluctuations in the mixing of different systems? J. Geophys. Res. 100, 4157–4167. https://doi.org/10.1029/94JB02595.

Tedesco, D., Scarsi, P., 1999. Intensive gas sampling of noble gases and carbon at Vulcano (Southern Italy). J. Geophys. Res. 104, 10499–10510. https://doi.org/10.1029/1998JB900066.

Tierz, P., Loughlin, S.C., Calder, E.S., 2019. VOLCANS: an objective, structured and reproducible method for identifying sets of analogue volcanoes. Bull Volcanol 81, 76. https://doi.org/10.1007/s00445-019-1336-3.

Tierz, P., Woodhouse, M.J., Phillips, J.C., Sandri, L., Selva, J., Marzocchi, W., Odbert, H.M., 2017. A Framework for Probabilistic Multi-Hazard Assessment of Rain-Triggered Lahars Using Bayesian Belief Networks. Front. Earth Sci. 5, 73. https://doi.org/10.3389/feart.2017.00073.

Tinti, S., Bortolucci, E., Armigliato, A., 1999. Numerical simulation of the landslide-induced tsunami of 1988 on Vulcano Island, Italy. Bull. Volcanol. 61 (1), 121–137.

Todesco, M., 1997. Origin of fumarolic fluids at Vulcano (Italy). Insights from isotope data and numerical modeling of hydrothermal circulation. J. Volcanol. Geotherm. Res. 79 (1997), 63–85.

Tommasi, P., Boldini, D., Cignitti, F., Graziani, A., Lombardi, A., Rotonda, T., 2007. Geomechanical analysis of the instability phenomena at Stromboli volcano. In: Eberhardt, E., Stead, D., Morrison, T. (Eds.), Dissertation, Proceedings of the 1st Canada-US Rock Mechanics Symposium - Rock Mechanics Meeting Society's Challenges and Demands. 2. pp. 933–941.

Tommasi, P., Rotonda, T., Verrucci, L., Graziani, A., Boldini, D., 2016. Geotechnical analysis of instability phenomena at active volcanoes: Two case histories in Italy, "Landslides and Engineered Slopes. Experience,Theory and Practice" In: Proceedings of the 12th International Symposium on Landslides (Napoli, Italy, 12-19 June 2016), CRC Press.

Ventura, G., 1994. Tectonics, structural and caldera formation on Vulcano island (Aeolian archipelago, southern Tyrrhenian sea). J. Volcanol. Geotherm. Res. 60, 207–224.

Ventura, G., 2013. Kinematics of the Aeolian volcanism (Southern Tyrrhenian Sea) from geophysical and geological data. In: Lucchi, F., Peccerillo, A., Keller, J., Tranne, C.A., Rossi, P.L. (Eds.), The Aeolian Islands Volcanoes. 37. Geological Society, London, pp. 3–11. https://doi.org/10.1144/M37.2. Memoirs.

Ventura, G., Vilardo, G., Milano, G., Pino, N.A., 1999. Relationships among crustal structure, volcanism and strike–slip tectonics in the Lipari–Vulcano volcanic complex (Aeolian islands, southern Tyrrhenian sea Italy). Phys. Earth Planet. Inter. 116, 31–52.

Vetere, F., Behrens, H., Misiti, V., Ventur, G., Holtz, F., De Rosa, R., Deubener, J., 2007. The viscosity of shoshonitic melts (Vulcanello Peninsula, Aeolian Islands, Italy): Insight on the magma ascent in dikes. Chem. Geol. 245 (1–2), 89–102. https://doi.org/10.1016/j.chemgeo.2007.08.002.

Vita, F., Inguaggiato, S., Bobrowski, N., Calderone, L., Galle, B., Parello, F., 2012. Continuous SO2 flux measurements for Vulcano Island, Italy. Ann. Geophys. 55. https://doi.org/10.4401/ag-5759.

Voltaggio, M., Branca, M., Tuccimei, P., Tecce, F., 1995. Leaching procedure used in dating young potassic volcanic rocks by the 226Ra/230Th method. Earth Planet. Sci. Lett. 136, 123–131.

Winson, A.E.G., Costa, F., Newhall, C.G., Woo, G., 2014. An analysis of the issuance of volcanic alert levels during volcanic crises. J Appl Volcanol 3, 14.

Woo, G., 2015. Chapter 11 - Cost-benefit analysis in volcanic risk. In: Shroder, John F., Papale, Paolo (Eds.), Volcanic Hazards, Risks, and Disasters, Chapter: 8. Elsevier, Amsterdam. https://doi.org/10.1016/B978-0-12-396453-3.00011-3.

Zanella, E., Lanza, R., 1994. Remanent and induced magnetization in the volcanites of Lipari and Vulcano (Aeolian Islands). Ann. Geophys. 37 (5), 1149–1156.

Zanon, V., Frezzotti, M.L., Peccerillo, A., 2003. Magmatic feeding system and crustal magma accumulation beneath Vulcano Island (Italy): Evidence from CO2 fluid inclusions in quartz xenoliths. J. Geophys. Res. 108 (B6), 2298. https://doi.org/10.1029/2002JB002140.

Nave R., T. Ricci, M.S. Davis. Percezione del rischio vulcanico alle Eolie (Vulcano, Lipari, Panarea e Stromboli). Rapporto per il DPC nell'ambito dell'Accordo quadro DPC-INGV 2012-2021, 24 febbraio 2015, 22 pp.

Smith, G.A., Lowe, D.R., 1991. Lahars: volcano-hydrologic events 1461 and deposition in the debris flow-hyperconcentrated flow con- 1462 tinuum. In: Fisher, R.V., Smith, G.A. (Eds.), Sedimentation in 1463 Volcanic Settings. Soc. Econ. Paleontol. Mineral. Spec. Publ., 1464 vol. 45, pp. 59–70.